

INTERACTIVE AXIAL SHORTENING OF COLUMNS AND WALLS IN HIGH RISE BUILDINGS

By

HN Praveen Moragaspiya BSc Eng (Hons)



A THESIS SUBMITTED TO
FACULTY OF BUILT ENVIRONMENT AND ENGINEERING
QUEENSLAND UNIVERSITY OF TECHNOLOGY
IN PARTIAL
FULFILLMENT OF THE REQUIREMENTS FOR THE DEGREE OF
DOCTOR OF PHILOSOPHY

April 2011

Dedication

To my parents, wife and twin sons with love

ACKNOWLEDGEMENTS

I would like to express my sincere gratitude to my principal supervisor, Professor David Thambiratnam for giving me this great opportunity together with his motivation, great support and excellent guidance to carry out my research work successfully. I would also like to thank my associate supervisors, Adjunct Professor Nimal Perera and Associate Professor Tommy Chan for their valuable advices and vast useful suggestions as well as professional guidance.

I must thanks all academic and non academic staff members at QUT for their support given in many ways specially in BEE research portfolio office and HPC unit for their assistance and cooperation during the research and for enthusiastic responses to my numerous requests for assistance.

I would like to express my sincere gratefulness to my parents and wife (Chathurani Moragasipitiya) who are always behind me for the successes.

I gratefully acknowledge the financial support granted by Faculty of Built Environment and Engineering, Queensland University of Technology to succeed my research work for entire period of my candidature. I wish also to gratitude to my colleagues at QUT for sharing knowledge and encouragement at friendly and fruitful atmosphere. Finally, I am thankful to all those who have helped me in many ways to my successes.

HN Praveen Moragasipitiya
School of Urban Development
Faculty of Built Environment and Engineering
Queensland University of Technology
Brisbane, Australia
April 2011

STATEMENT OF ORIGINAL AUTHORSHIP

The work included in this thesis has not been previously submitted for a degree or diploma at any other higher education institution. To the best of my knowledge and belief, the thesis contains no material previously published or written by another person except where due reference is made.

HN Praveen Moragaspitiya

April 2011

ABSTRACT

Concrete is commonly used as a primary construction material for tall building construction. Load bearing components such as columns and walls in concrete buildings are subjected to instantaneous and long term axial shortening caused by the time dependent effects of “shrinkage”, “creep” and “elastic” deformations. Reinforcing steel content, variable concrete modulus, volume to surface area ratio of the elements and environmental conditions govern axial shortening. The impact of differential axial shortening among columns and core shear walls escalate with increasing building height. Differential axial shortening of gravity loaded elements in geometrically complex and irregular buildings result in permanent distortion and deflection of the structural frame which have a significant impact on building envelopes, building services, secondary systems and the life time serviceability and performance of a building. Existing numerical methods commonly used in design to quantify axial shortening are mainly based on elastic analytical techniques and therefore unable to capture the complexity of non-linear time dependent effect. Ambient measurements of axial shortening using vibrating wire, external mechanical strain, and electronic strain gauges are methods that are available to verify pre-estimated values from the design stage. Installing these gauges permanently embedded in or on the surface of concrete components for continuous measurements during and after construction with adequate protection is uneconomical, inconvenient and unreliable. Therefore such methods are rarely if ever used in actual practice of building construction.

This research project has developed a rigorous numerical procedure that encompasses linear and non-linear time dependent phenomena for prediction of axial shortening of reinforced concrete structural components at design stage. This procedure takes into consideration (i) construction sequence, (ii) time varying values of Young’s Modulus of reinforced concrete and (iii) creep and shrinkage models that account for variability resulting from environmental effects. The capabilities of the procedure are illustrated through examples. In order to update previous predictions of axial shortening during the construction and service stages of the building, this research has also developed a vibration based procedure using ambient measurements. This procedure takes into

consideration the changes in vibration characteristic of structure during and after construction. The application of this procedure is illustrated through numerical examples which also highlight the features. The vibration based procedure can also be used as a tool to assess structural health/performance of key structural components in the building during construction and service life.

Keywords: Axial Shortening, Concrete Buildings, Creep, Shrinkage, Elastic Deformation, Vibration Characteristic, Finite Element Method, Dynamic Stiffness Matrix

PUBLICATIONS

Journal Papers:

- Moragasipitiya H.N.P, Thambiratnam D. T. P, Perera N and Chan,T, “***A Numerical Method to Quantify Differential Axial Shortening in Concrete Buildings***”, Journal of Engineering Structures, 2010, Vol. 32, Iss. 8, pp 2310-2317. Journal with Excellence in Research, Australia (ERA) Ranking A+.
- Moragasipitiya H.N.P, Thambiratnam D. T. P, Perera N and Chan,T, “***Quantifying In-plane Deformation of Plate Elements using Vibration Characteristics***”, Journal of Sound and Vibration, (Accepted for the publication) (Journal with ERA Ranking A+)
- Moragasipitiya H.N.P, Thambiratnam D. T. P, Perera N and Chan,T, ” ***Health finita Monitoring of Buildings during Construction and Service Stages using Vibration Characteristics***”, ANSHM Special Issue for Advances in Structural Engineer, An International Journal:, (Under Review) (A journal based on ERA ranking)
- Moragasipitiya H.N.P, Thambiratnam D. T. P, Perera N and Chan,T,” ***Influence of Axial Deformation of Structural Members on their Modal Parameters*** ”, Journal of Finite Element in Analysis and Design (Under Review) (Journal with ERA ranking A)
- Moragasipitiya H.N.P, Thambiratnam D. T. P, Perera N and Chan,T, “***Development of a Vibration Based Method to Update Axial Shortening of Vertical Load Bearing Elements in Reinforced Concrete Buildings***”, Journal of Engineering Structures, (Under Review) (Journal with ERA Ranking A+).

Book Chapter:

- Moragasipitiya H.N.P, Thambiratnam D. T. P, Perera N and Chan,T, “***Infrastructure sustainability: differential axial shortening of concrete structures***”, Rethinking sustainable development planning, designing, engineering and managing urban infrastructure and development- Chapter-14,2010 (<http://www.igi-global.com/Bookstore/TitleDetails.aspx?TitleId=40297>)-ISBN13: 9781616920227

Conference Papers:

- Moragasipitiya H.N.Praveen, Thambiratnam D. T. , Perera N and Chan,T. H. T., “***Quantifying axial deformations of columns using vibration characteristics***”, The First International Postgraduate Conference on Engineering, Designing and Developing the Built Environment for Sustainable Wellbeing, held in 27-30 April 2011, Accepted for the publication

- Moragasipitiya H.N.Praveen, Thambiratnam D. T. , Perera N and Chan,T. H. T., ***“Quantifying axial deformations of Shear walls of cores using modal parameters”***, The First International Postgraduate Conference on Engineering, Designing and Developing the Built Environment for Sustainable Wellbeing, held in 27-30 April 2011, Accepted for the publication
- Moragasipitiya H.N.Praveen, Thambiratnam D. T. , Perera N and Chan,T. H. T., ***“Vibration Characteristics of Plate Elements Subjected to In-Plane Loads (Axial Loads)”***, International Conference on Technological Advancements in Civil Engineering (ICTACE 2011)
- Moragasipitiya H.N.Praveen, Thambiratnam D. T. , Perera N and Chan,T. H. T., ***“A Vibration Based Method to Update Axial Shortening of Load Bearing Elements”***, The 5th Civil Engineering Conference in the Asian Region and Australian Structural Engineering Conference 2010, paper-138
- Moragasipitiya H.N.Praveen, Thambiratnam D. T. , Perera N and Chan,T.H.T, ***“Influence of Axial Deformation of Structural Members on Vibration Characteristics”***, The 5th Civil Engineering Conference in the Asian Region and Australian Structural Engineering Conference 2010, paper-140
- Moragasipitiya H.N.Praveen, Thambiratnam D. T. , Perera N and Chan,T.H.T , ***“Influence of Axial Deformation of Structural Members on Modal Strain Energy”***, The 5th Civil Engineering Conference in the Asian Region and Australian Structural Engineering Conference 2010, paper-127
- Moragasipitiya H.N.Praveen, Thambiratnam D. T. P, Perera N and Chan,T, ***“Numerical Method to Quantify the Axial Shortening of Vertical Elements in Concrete”***, Proceedings -ICREATE International Conference, KL, Malaysia, 2009, 2B-paper iCREATE052
- Moragasipitiya H.N.Praveen, Thambiratnam D. T. P, Perera N and Chan,T, ***“Axial shortening in reinforced concrete members using vibration characteristics Part 1-Theory”***, Smart System Conference, 2009, QUT, Brisbane, Australia, 2009, pp 126-131
- Moragasipitiya H.N.Praveen, Thambiratnam D. T. P, Perera N and Chan,T, ***“Axial shortening in reinforced concrete members using vibration characteristics Part 2-Application”***, Smart System Conference, 2009, QUT, Brisbane, Australia, 2009, ISBN: 978-0-9805827-2-7,pp 132-138
- Moragasipitiya H.N.Praveen, Thambiratnam D. T. P, Perera N and Chan,T, ***“Differential Axial shortening of Concrete Structures”***, the second infrastructure theme postgraduate conference, QUT, Brisbane, Australia, 2009, pp 48-58

TABLE OF CONTENTS

ACKNOWLEDGEMENTS	3
STATEMENT OF ORIGINAL AUTHORSHIP	4
PUBLICATIONS.....	7
TABLE OF CONTENTS.....	9
LIST OF FIGURES	11
1 INTRODUCTION	16
1.1 Background	16
1.2 Prediction and Monitoring Methods	22
1.3 Objectives	24
1.4 Research Problem.....	25
1.5 Significance and Innovation of Research.....	26
1.6 Outline of the Thesis	26
2 LITERATURE REVIEW	28
2.1 Deformation of Concrete.....	30
2.2 Elastic Deformation.....	31
2.2.1 Definition	31
2.2.2 Influencing Factors	31
2.2.3 Elastic Modulus of Concrete.....	32
2.3 Shrinkage Deformation	33
2.3.1 Definition	33
2.3.2 Influencing Factors	33
2.4 Creep Deformation.....	34
2.4.1 Definition	34
2.4.2 Original Mechanism.....	35
2.4.3 Influencing Factors	36
2.5 Axial Shortening	37
2.6 Quantify the Axial shortening using Ambient Measurements	39
2.6.1 Vibrating Wire Gauge.....	40
2.6.2 External Mechanical Strain Gauges.....	44
2.6.3 Electronic Strain Gauge	46
2.7 Vibration Measurements	47
2.8 Structural System	49
2.8.1 Belt and Outrigger Systems	50
2.9 Ambient Measurements of Modal Parameters/Vibration Characteristics.....	53
2.10 Characterization of Structural Phenomena	54
2.11 Time strategies.....	54
2.11.1 Sensor System.....	55
2.11.2 Model Flexibility Method (MFM)	56
2.12 Summary.....	57
3 DEVELOP A RIGOROUS NUMERICAL METHOD TO CALCULATE AXIAL SHORTENING IN HIGH RISE BUILDINGS.....	59
3.1 Introduction	59
3.1.1 Time varying Young's Modulus.....	59
3.1.2 Staged Construction Process.....	61
3.1.3 Compression only Element	63

3.1.4	Sub Models.....	64
3.1.5	Load Application and Analysis	64
3.1.6	Analysis	67
3.1.7	Calculation-Creep, Shrinkage and Elastic Deformation	68
3.1.8	Comparison	69
3.1.9	Application	71
3.1.10	Results and Discussion	73
3.2	Conclusion	78
4	INFLUENCE OF AXIAL DEFORMATIONS OF COLUMNS ON THEIR VIBRATION CHARACTERISTICS.....	80
4.1	Introduction.....	80
4.2	Dynamic Stiffness Matrix of a beam/column element	82
4.3	Validation of the modified FE program and study the capabilities of Stiffness Index (SI)-for column elements	88
4.3.1	Validation of the modified FE program-for column elements	88
4.3.2	Study the Capability of Stiffness Index (SI) applied to column elements ..	90
4.4	Conclusion	101
5	INFLUENCE OF AXIAL DEFORMATIONS ON VIBRATION CHARACTERISTICS OF CORE SHEAR WALLS	103
5.1	Introduction.....	103
5.2	Dynamic Stiffness Matrix of Plate Element	105
5.3	Validation of the modified FE program and study the capabilities of Stiffness Index (SI)-Core shear wall element.....	113
5.3.1	Validation of the modified FE program-Core Shear wall element	114
5.3.2	Study the capabilities of Stiffness Index (SI) applied to core shear walls ..	116
5.4	Conclusion	123
6	DEVELOPMENT OF A VIBRATION BASED METHOD TO UPDATE AXIAL SHORTENING OF VERTICAL LOAD BEARING ELEMENTS IN REINFORCED CONCRETE BUILDINGS	125
6.1	Introduction.....	125
6.2	Load Application	126
6.3	Model Upgrading Methods.....	127
6.4	Vibration characteristics and Axial Shortening.....	128
6.4.1	Vibration characteristics.....	128
6.4.2	Quantification of Elastic shortening.....	132
6.4.3	Quantification of axial shortening.....	133
6.5	Illustrative example	134
6.6	Results and Discussion	137
6.7	Calculation -Elastic and Axial shortening	144
6.8	Conclusion	147
7	CONCLUSION AND FUTURE WORKS.....	148
8	REFERENCE	151

LIST OF FIGURES

Figure 1-1: Burj Tower, Dubai -the tallest building in the world (Burj Dubai official website, 2008)	17
Figure 1-2: The Lagoons -proposed for Dubai (Dubai Future Projects, 2009)	17
Figure 1-3: Failure of wall panel due to differential axial shortening (Fintal & Fazlur,1987)	20
Figure 1-4: A typical view of cross sections of structural elements	21
Figure 1-5: Variation of Young's Modulus with time	23
Figure 1-6: Time variations of stress and strains in concrete	23
Figure 1-7: (a) Construction load time histories and (b) load time histories after the construction, for a typical element.	24
Figure 2-1: Time variations of stress and strains in concrete	31
Figure 2-2: The stress Vs. strain variation of aggregate, cement and concrete (Fintal,Ghosh & Iyengar,1987)	32
Figure 2-3: Representation of the stress-strain relationship for concrete (Liu, 2007)	32
Figure 2-4: Components of axial shortening	38
Figure 2-5: A vibrating wire gauge (Bakoss, Burfitt & Cridland, 1977)	41
Figure 2-6: A briquette for vibrating wire gauge (Bakoss, Burfitt & Cridland, 1977)	42
Figure 2-7: A typical view of the detailed of reinforced column with the location of the Vibrating Wire gauge (Bakoss, Burfitt & Cridland, 1977)	42
Figure 2-8: Vibrating wire gauges prior to installation (Implementation program on high performance concrete,2008)	43
Figure 2-9: A typical view of a mechanical gauge being used to measure transfer length in a pre stressed concrete girder (Implementation program on high performance concrete,2008)	45
Figure 2-10 : Classification of structural systems based on their effectiveness in resisting lateral loads (Buyukozturk & Gunes,2008)	49
Figure 2-11 : A schematic diagram of outriggers located in a building.	50
Figure 2-12: SHM system for a building	54
Figure 2-13: Time monitoring strategies (Atkan et al ,2003)	55
Figure 3-1: Compression only elements and load migration during construction	62
Figure 3-2: A schematic diagram of the compression only element at inactive stage (left) and active stage (right)	63
Figure 3-3: The load –time history of a typical concrete element	65
Figure 3-4: Load application to the structure	67
Figure 3-5: Flow chart of the analytical process	67
Figure 3-6: Variation of the elastic shortenings	70
Figure 3-7: Variation of the Axial shortenings	71
Figure 3-6: The isometric view (left) and the sectional end view (right) of the building.	72
Figure 3-7: A typical plan view of the building	72
Figure 3-8: The axial shortening of the core, Column X and Column Y at 4500 days from commencement of construction	74
Figure 3-9: The elastic shortening of the core, Column X and Column Y at 4500 days from commencement of construction	74

Figure 3-10: Differential axial shortening between Column X and Column Y at 4500 days from commencement of construction	75
Figure 3-11: Differential axial shortening between the core and Column X at 4500 days from commencement of construction.....	76
Figure 3-12: Differential axial shortening between the core and Column Y at 4500 days from commencement of construction.....	76
Figure 3-13: Absolute value of graph of Figure 3-11	77
Figure 3-14: Absolute value graph of Figure 3-12.....	78
Figure 4-1: An element with axial compressive force under free vibration.....	82
Figure 4-2: Cross section of the beam structure.....	88
Figure 4-3: the columns with two different boundary conditions	91
Figure 4-4: Percentage of frequency change (a)-first mode, (b)-second mode and (c)-third mode.....	92
Figure 4-5: variation of stiffness index, SI with the axial deformation for case A	93
Figure 4-6: variation of stiffness index, SI with the axial deformation for case B	94
Figure 4-7: two storey structural framing system	95
Figure 4-8: Percentage of frequency change of the first two modes.....	96
Figure 4-9: variation of SI of the elements (a)- columns L1, R1, (b)- column L2 and (c)-column R2	96
Figure 4-10: Structural framing system with shear walls.....	98
Figure 4-11: variation of SI(s) of the columns, (a)-2 nd level, (b)- 4 th level, (c)-6 th level, (d)-8 th level and (e)-10 th level.....	100
Figure 5-1: The plate element with forces - plan view.....	105
Figure 5-2: A plate element with axial compressive load	106
Figure 5-3: plate elements with different boundary conditions	116
Figure 5-4: percentage of frequency change vs. the axial deformation-(a) Case A and (b)-Case B.....	117
Figure 5-5; Deformation contours of the element (plan views): (a) –(c) first 3 modes for case A and (d) – (e) first three modes for case B	118
Figure 5-6: variation of SI with axial deformation- (a)-Case A and (b)-Case B.....	119
Figure 5-7: Structural framing system (a)- isometric view and (b)- plan view.....	120
Figure 5-8: Mode shapes (a) Mode 1 (Front View) and (b) -Mode 2 (End View) (unit in meter).....	121
Figure 5-9: variation of SI of elements of core with axial deformation-(a)- 5 th level ,(b)- 7 th level and (c)-9 th level.....	122
Figure 6-1: Model upgrading methods defined from the construction to service stages	128
Figure 6-2: lump mass systems for a structure -3(a) - before upper floor construction and 3(b)-during upper floor construction	129
Figure 6-3: (a) typical plan view of the building and (b) locations of the shear walls in the outrigger and belt systems (dotted lines).....	134
Figure 6-4: (a) isometric and (b) end view of the building	135
Figure 6-5: variation of the periods with model number from construction to service stage.....	137
Figure 6-6: Comparison of axial shortening indexes of column B	139
Figure 6-7: Variation of Axial Shortening Index of columns B and C at the different floor levels, (a)-Level 4, (b)-Level 12, (c)-Level 32, (d)-Level 42 and (e)-Level 52	140

Figure 6-8: Variations of Axial Shortening Index of columns F and G at the different floor levels-(a)- level 4, (b)-level 12, (c)-level 32, (d)-level 42 and (e)-level 52	142
Figure 6-9: variations of Axial Shortening Index of the locations of the core at different floor levels-(a)- level 4, (b)-level 12, (c)-level 32, (d)-level 42 and (e)-level 52	143
Figure 6-10: Elastic shortening of the structural elements	145
Figure 6-11: Axial shortening of the structural elements	146
Figure 6-12: the behaviour of slab X	146

LIST OF TABLES

Table 2-1: Examples of structural phenomena, strategies and suitable sensors. T: Time dependent strategies, C: Condition dependent strategies and L: Load dependent strategies (Sohn et al, 2003).....	56
Table 3-1: variation of S with cement type.....	60
Table 3-2: The properties used for the compassion study	70
Table 3-3: Sizes of the columns and thicknesses of the core walls	73
Table 3-4: Thicknesses of the shear walls in the outrigger and belt systems	73
Table 4-1: Material properties and other data used in the vibration analysis	89
Table 4-2: Comparison of natural frequencies without axial load.....	89
Table 4-3: comparison of natural frequencies with compressive axial load.....	90
Table 4-4: comparison of natural frequencies with tensile axial load	90
Table 4-5: material properties of the column.....	91
Table 4-6: the applied axial loads for the columns	95
Table 4-7: the applied axial compressive loads on columns initially	99
Table 5-1; Properties of the plate element	114
Table 5-2: Comparison of the frequencies from the experiment and the present study .	115
Table 5-3: properties of the plate elements	116
Table 5-4: Material properties of elements	120
Table 5-5; Element sizes	121
Table 5-6: Applied loads on slabs.....	121
Table 6-1: Column sizes and core wall thicknesses.....	136
Table 6-2: Thickness of shear walls of the outrigger and belt systems	136

LIST OF SYMBOLS AND ABRIVATION

$\delta_{\text{Creep}}(t, t_0)$ - creep strain at time t after loading at t_0

$\Delta h(t_n)$ -the cumulative elastic, creep and shrinkage shortening of an element at time t_n

$\delta_{\text{total}}(t, t_0)$ - total strain at time t after loading at t_0

(v/s)- the volume to surface area ratio (mm)

$[k]_L, [K]_L$ –dynamic stiffness matrix based on local coordinate system for beam and plate elements respectively

[T]-transformation matrix

A_1, A_2 -constants determined from initial conditions of the vibration

A-Area

ASI- Axial Shortening Index

$H(t_r)$ -axial shortening of an element at the time, t_r

D- flexural rigidity of the plate

$D_1, D_2, D_3, D_4, \overline{D}_1, \overline{D}_2, \overline{D}_3, \overline{D}_4, \overline{A}, \overline{B}, \overline{C}, \overline{D}$ - vector constants

$[\overline{K}]$ -dynamic stiffness matrix of the structure

E - Young's Modulus

$E_C(t)$ - the Young's Modulus of concrete at time t

E_{cm28} - the mean modulus of elasticity at 28 days

E_{cmt} -the mean modulus of elasticity at age t

E_{cmto} - the modulus of elasticity at the time of loading

$\delta_{\text{Elastic}}(t, t_0)$ -elastic strain at time t after loading at t_0

f_{cmt} -the mean concrete strength at age t

F-Force □ □

F_x -Modal Flexibility of element x

G -the global coordinate system

h -the humidity

I-Moment of Inertia

K -the correction term for the effect of cement type

k-Stiffness

L- local coordinate system

L-Length

L-loaded case

M-Moment

N_x, N_y, N_{xy}, N_{yx} -in plane forces

P-Axial compressive force or axial pressure load

s -strength development parameter

$\delta_{\text{Shrinkage}}(t)$ -shrinkage strain at time t

SI-Stiffness Index

ξ -Strain

σ -the axially developed stress

f_{cm28} -the concrete mean compressive strength

Δ -the initial gap opening

t-time

U -the unloaded case

V-Shear Force

x,y,z-distances

Z_x -the axial elastic deformation of element x due to the axial force

β_e – a parameter based on strength development with cement type

β_x - vibration based parameter of element x

μ -the mass of the element

ρ -mass per unit length

ϕ_{28} -the creep coefficient

ω_r -natural frequency at r^{th} mode

Φ_r -modal vector at r^{th} mode

1 INTRODUCTION

1.1 Background

Differential axial shortening of gravity load bearing components in tall buildings is a phenomenon that was first noticed in the 1960's with the use of concrete in combination with reinforcing steel for tall buildings. As buildings increased in height, elastic shortening became apparent during construction, and methods for correcting for instantaneous shortening such as construction of each floor to a corrected level or datum, became common practice. The long term effects of shrinkage and creep did not have a significant impact on buildings in the 30 storey range. However, tall buildings in the 40 to 60 storey range showed the detrimental effects of shrinkage and creep that could not be adequately compensated for by building each floor to a datum level. Engineering the materials, components, size and configuration of 100 to 400 meter buildings during the design process to control the impact of differential axial shortening and deformation is a well established method (Fintel & Fazlur, 1987; Smith & Loull, 1991). Methods such as load balancing and axial stress equalization using elastic analytical procedures are convenient for symmetrical and regular building forms. However, controlling differential axial shortening and deformation becomes increasingly difficult for the new generation of super tall buildings in the 400 to 1000 meter range such as Burj Khalifa Tower, Dubai - Figure 1-1 and those with complex geometric structural framing systems such as the proposed Lagoons, Dubai - Figure 1-2.



Figure 1-1: Burj Tower, Dubai -the tallest building in the world
(Burj Dubai official website, 2008)



Figure 1-2: The Lagoons -proposed for Dubai
(Dubai Future Projects, 2009)

Many high-rise commercial, residential and communication towers around the world have been constructed using reinforced concrete structural frames (Bontempi, 2003). Leading examples are the 828 meter tall Burj Khalifa Tower in the UAE (Baker, Korista & Novak, 2007) and the 533 meter tall CNN tower in Toronto (CNN tower official web site, 2010). Many other high-rise buildings such as the 505 meter tall Taipei 101 building has used hybrid construction of structural steel filled with concrete for its mega columns linked to concrete cores by steel outrigger systems (Shieh, Cang & Jong, 2010).. Importantly the vertical load bearing frames of these super tall buildings use concrete with conventional bar reinforcements, embedded structural steel and steel skins as a primary material. The steel contents are provided as reinforcement to resist load and enhance the performance characteristics of concrete. Many researchers highlighted the importance of concrete used as a primary material for high-rise construction (Elnimeiri & Joglekar, 1989; Smith & Loull, 1991).

The effective use of reinforced concrete, concrete encased steel and steel encased concrete construction in high rise construction has been made possible by the rapid advancement of construction and materials technology during the latter half of the 20th century. The key building components that control axial shortening are the shear cores, internal and perimeter columns that are subjected to axial compression. Although concrete filled steel tubes show superior axial shortening control over conventional reinforced concrete columns, they tend to magnify the problem of differential axial shortening when built in combination with reinforced concrete shear cores and outrigger framing systems. Such effects can complicate the structural design and construction of outriggers that connect perimeter columns to shear cores such as in the 481m tall Jin Mao Tower, China (Korista, Sarkisian & Abdelrazaq, 1997) and the 415 m tall International Financial Centre, Hongkong (Carroll et al, 2009). Conventionally reinforced concrete and structural steel reinforced concrete composites and hybrids continue to be the materials of choice for early 21st century high-rise construction due to their ability to provide compact floor plates over long spans, thermal, acoustic and fire insulation, durability and strength. The different types of construction are inherent with varying degrees of axial shortening in the short and long term thereby creating the demand for a very high degree of precision and monitoring to provide strength and performance of

high rise buildings. Axial shortenings of tubular structural steel filled with concrete members are quantified by scaling the linear elastic numerical models of reinforced concrete (structural steel encased in concrete) as a common design practice due to the non-availability of well established numerical methods to capture the true non-linear and time dependent load response. However, accuracy of these scaled models is questionable (Uy, 1998; Uy & Das, 1997).

Axial shortening is cumulative over the height of a structure so that detrimental effects due to differential axial shortening become more pronounced with increasing building height. For example, in an 80 storey concrete building, it has been reported that the elastic shortenings of columns is 65mm and that due to shrinkage and creep is 180 to 230mm (Fintel, Gosh & Iyengar, 1987). The combination of these shortening components is unacceptable as a structural performance criterion. It is therefore necessary to accurately predict linear and non-linear components of differential axial shortening and control performance with design.

Unacceptable cracking and deflection of floor plates, beams and secondary structural components, damage to facades, claddings, finishes, mechanical and plumbing installations and other non-structural walls can occur resulting from differential axial shortening. In addition, common effects on structural elements are sloping of floor plates, secondary bending moments and shear forces in framing beams (Fintel & Fazlurl, 1987). Figure 1-3 illustrates the behavior of a wall panel subjected to differential axial shortening.

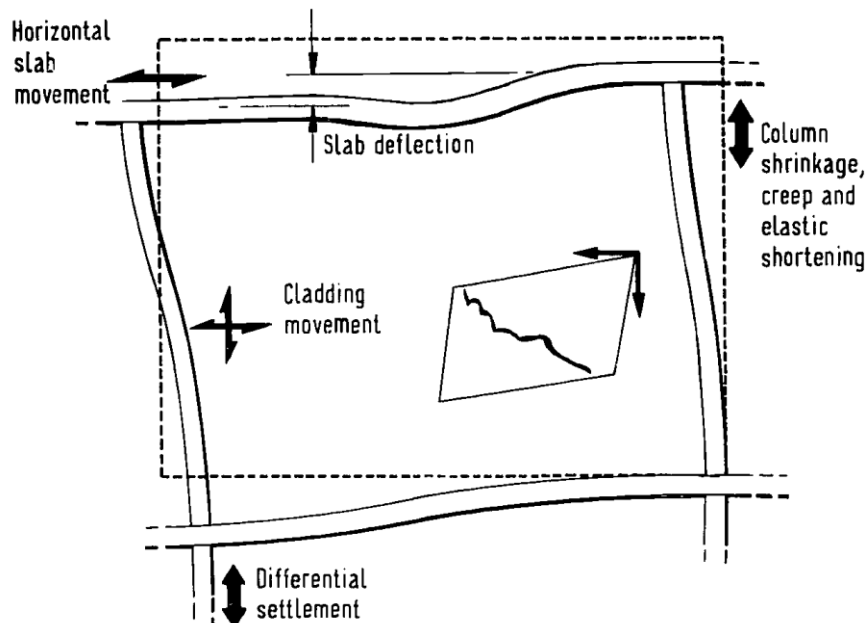


Figure 1-3: Failure of wall panel due to differential axial shortening (Fintel & Fazlur, 1987)

Concrete has three significant modes of volume change after pouring. Shrinkage, as the name implies causes the concrete volume to decrease as the water within it dissipates and the chemical process of concrete causes hardening to occur. Elastic shortening occurs immediately as hardened concrete is loaded and is a function of the applied stress, length of the concrete element, and modulus of elasticity. Creep is a long-term effect that causes the concrete to deform under exposure to sustained loading. These three phenomena occur in every concrete structure (Neville, 2005). A combination of these three time dependent phenomena causes axial shortening.

Shrinkage and creep deformations are impacted by volume and surface area. Figure 1-4 illustrates cross sections of structural elements emphasizing variation of the volume and surface area of elements at a certain level in a building. The combination of elastic, shrinkage and creep strains cause differential axial shortening, deformation and distortion of building frames. The load carrying capacity and integrity of structural frames are not adversely impacted by these effects as they are a natural phenomenon associated with loaded concrete structures. Gravity load bearing elements in high rise

buildings are subjected to a large number of load increments during and after the construction process. Each load increment causes immediate elastic shortening of already constructed gravity load bearing elements such as walls and columns which are followed by shrinkage and creep over a long period of time. Typically, core shear walls in a high rise building are designed to resist the combination of shear and gravity loads while columns carry mainly gravity loads. As a result, height-dependent, significant stress differentials can exist between these elements due to gravity loads resulting in differential axial shortening. Increasing column sizes to balance stresses is not an acceptable solution. Additionally, designing and constructing geometrically complex high rise buildings with belt and outrigger systems comprising stiff shear walls is a well established practice today. Non vertical paths resulting from these stiff shear walls and the geometrical complexities amplify differential axial shortening between the elements.

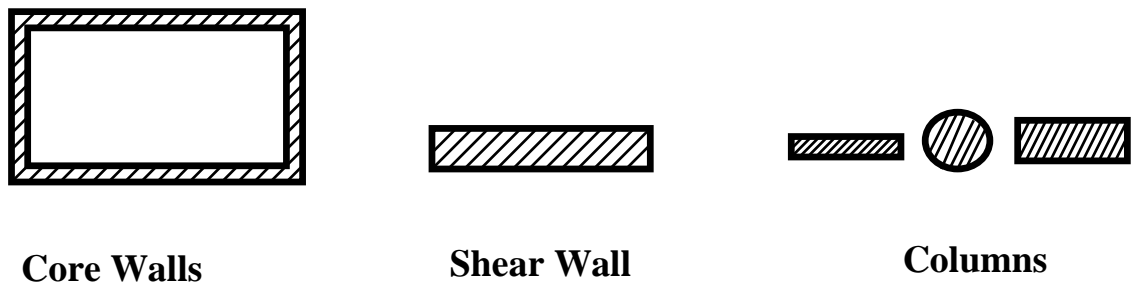


Figure 1-4: A typical view of cross sections of structural elements

(Uy, 1998; Uy & Das, 1997) recommended further studies to develop numerical models to capture the true behavior of creep, shrinkage and elastic deformations of the composite elements because of existing non-rigorous numerical models. Consequently, methods proposed in this thesis are based on the well established material models of reinforced concrete, whereas if required, the proposed methods can be applied to structures with composite elements by modifying the creep, shrinkage and young's modulus parameters since these modifications do not affect to the main concept of the methods.

1.2 Prediction and Monitoring Methods

Problems due to differential axial shortening have been observed and reported, especially as building height increases. A number of methods have been developed to quantify the differential axial shortening and they are based on laboratory tests where the long term time dependent material properties are predicted using previously established criteria. Designers normally rarely have the opportunity and facilities to observe and measure the long term material behaviour of concrete in actual buildings. On the other hand, concrete tested under laboratory conditions does not simulate the exact behaviour of in situ constructed structural elements. Designers therefore depend on numerical analysis methods based on established performance criteria and the influence of available parameters, for predicting the mechanical behaviour of structural components (Boonlualoah et al, 2005).

Analytical and test procedures that are available to quantify the differential axial shortening are limited to a very few parameters and are not adequately rigorous to capture the complexity of true time dependent material response. These techniques do not also address adequately the dynamic aspect of load application and the load migration that takes place during construction. Such non-rigorous analytical methods therefore fail to predict within a reasonable degree of accuracy the true behavior of tall and geometrically complex structural framing systems. The rigorous numerical method and the practical procedure developed in this research incorporate all time dependent parameters illustrated in Figures 1-5 to 1-7. Figure 1-5 illustrates the variation of Young's Modulus of concrete with time, and Figure 1-6 shows the time variation of the stress and the (creep, elastic and shrinkage) strains in a concrete element respectively. Figures 1-7a and 1-7b depict typical load time histories of self weight and superimposed dead loads, and the static and fluctuating live loads respectively.

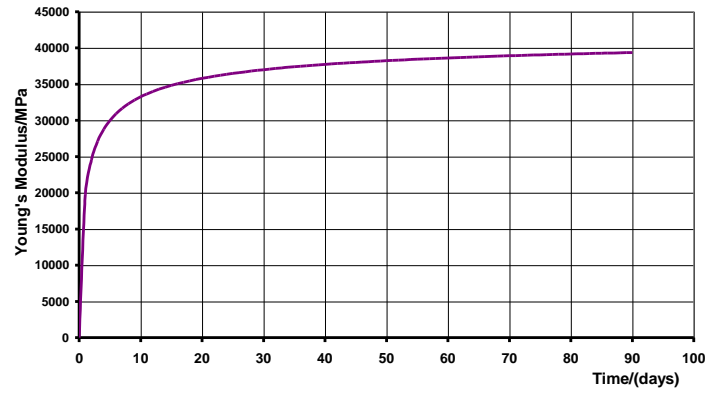


Figure 1-5: Variation of Young's Modulus with time

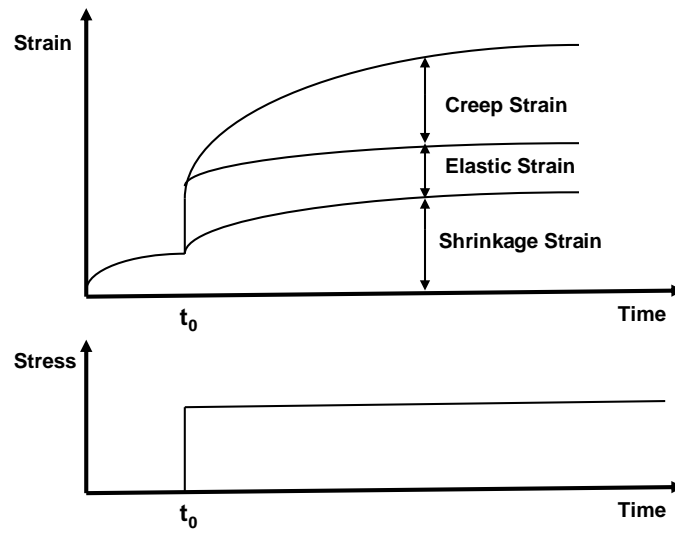


Figure 1-6: Time variations of stress and strains in concrete

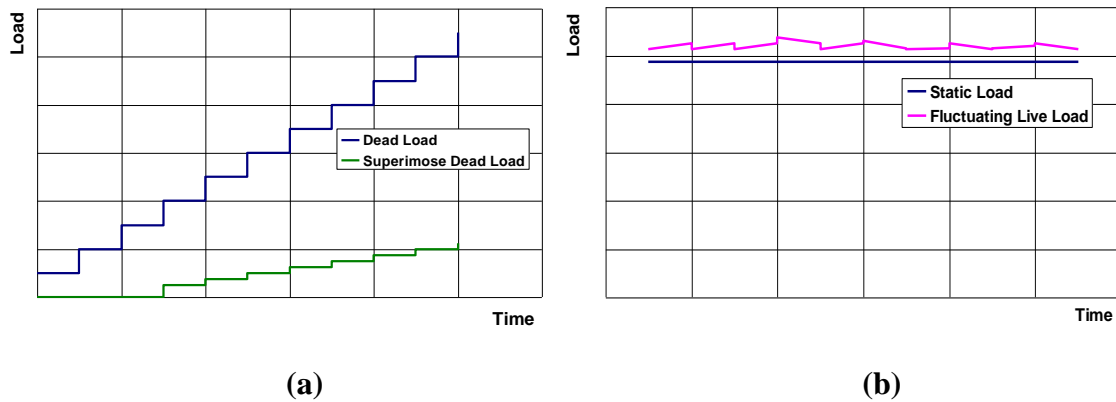


Figure 1-7: (a) Construction load time histories and (b) load time histories after the construction, for a typical element.

Vibrating wire, external mechanical and electronic strain gauges can be used to measure axial shortening in order to verify the pre estimated values used at design stage result in mitigate the adverse effects of differential axial shortening. These gauges are placed on or in elements during construction in order to acquire continuous measurements during construction and service stages. The protection of the gauges that are used in laboratory environments requires a degree of care and precision that is difficult to achieve on a construction site. More details on these gauges are discussed in Chapter 2.

1.3 Objectives

The main objectives of this research are to:

- Develop a numerical method incorporating time dependent parameters to predict during design the axial shortening of column and core shear wall components of concrete buildings that will occur during construction and service life.
- Develop a post construction monitoring procedure that incorporates time dependent behavior to quantify axial shortening using ambient measurements of vibration characteristics.

These developments are based on the assumption, that the Young's Modulus of concrete at the incremental load application during the construction is constant.

Additional objectives are to:

- Incorporate the influence of time dependent parameters such as construction sequence, creep, shrinkage, time varying Young's Modulus of reinforced concrete into the developments
- Examine influence of belt and outrigger systems on axial shortening
- Develop Dynamic Stiffness Matrixes (DSM)s of a beam/column, a shear wall elements and structural framing systems with load transferring elements
- Develop a relationship between axial deformations (elastic shortening) and vibration characteristics
- Assess effectiveness of the developments through illustrative examples

The numerical method and the vibration based practical procedure developed in this research will be through dynamic computer simulations using Finite Element (FE) techniques. According to available options in the software, time dependent parameters such as the Young's Modulus of reinforced concrete, time dependent load application, creep and shrinkage, are incorporated into the analysis using pre-processing and post-processing methods.

1.4 Research Problem

Differential axial shortening is more pronounced with increasing height as well as geometrical complexity of buildings. The available numerical methods are limited to a few parameters and not adequately rigorous to capture complexity of true time dependent material properties as well as load migration. Quantifying differential axial shortening through ambient vibration measurements using strain measuring instruments is not common in construction practice due to unreliability and practical difficulties experienced with implementation. The research is hence conducted to develop a rigorous numerical method and a convenient procedure based on vibration characteristics to measure and monitor actual performance of building structures during and after construction.

1.5 Significance and Innovation of Research

Planning is underway worldwide for the construction of geometrically complex high rise buildings. Differential axial shortening of vertical members and its consequent adverse effects on these buildings have been identified as a major concern. Based on the information presented in the above sections, it is evident that there is a need to develop a comprehensive numerical method and a convenient practical procedure to quantify and measure axial shortening. These developments will be innovative as they will take the following important parameters into consideration (i) load time histories associated with the construction process, (ii) time varying values of Young's Modulus of reinforced concrete (iii) creep, shrinkage models that account for variability resulting from environmental considerations and (iv) non linear material response. In addition to these parameters, the procedure for post construction measuring and monitoring will be based on the vibration characteristics of the structure during construction and service life of the building. These developments are comprehensive as they can incorporate a wider range of behavioural influences such as time dependent, non-linear material response and load applications, load migration and axial load variations. The method can be applied to any type of structure that uses concrete as a primary construction material without limitations. Special capabilities of these developments will be addressed using illustrative examples.

1.6 Outline of the Thesis

Chapter 1 – Introduction

Background information, research problem and its significance as well as innovation are described in detail. Aims and objectives of the research is presented.

Chapter 2 - Literature review

Problem of axial shortening in tall buildings and design methods used in actual buildings, creep, shrinkage and elastic deformations and their governing factors are discussed. Phenomena governing differential axial shortening and its adverse effects are also discussed. Interactive behaviour of structural framing systems with belt and

outrigger systems due to differential axial shortening is demonstrated. Existing methods used to quantify axial shortening and their limitations are reviewed.

Chapter 3 – this chapter presents a developed numerical method to quantify the axial shortening. Unique capabilities of the development such as capturing influences of load migration and axial load variations are demonstrated through an illustrative example.

Chapter 4 presents development of dynamic stiffness matrices of -axially loaded beam element representing a column and a structural frame comprising the similar elements.. The relationship between the axial deformation and vibration characteristics is developed through a novel vibration based parameter called Stiffness Index (SI) Which is capable of capturing influence of the boundary conditions, load migration and axial load variation. The method is illustrated with examples.

Chapter 5- demonstrates developments of dynamic stiffness matrices of plate elements and a structural framing system comprising core shear walls in order to examine the influence of axial deformation on vibration characteristics. Capabilities of the vibration based parameter, Stiffness Index (SI) introduced in Chapter 4 are further interrogated using the structural framing systems.

Chapter 6 describes enhancement of SI presented in Chapters 4 and 5 in order to develop a procedure to quantify axial shortening during construction and service life of buildings using ambient vibration data. Unique features in the developed method are illustrated through numerical model of a geometrically complex high rise building with outrigger and belt systems.

Chapter 7 summarises the thesis providing main conclusions and practical applications of the developed methods.

2 LITERATURE REVIEW

Columns and core shear walls of high-rise buildings are constructed in concrete with any one or a combination of conventional steel bars, structural steel sections and tubular encasing steel. These key structural members are subjected to axial shortening caused by a combination of creep, shrinkage and elastic effects that increase with building height. At Present rigorous numerical techniques are not available to design engineers to reliably quantify the non-linear and time dependent impact of creep, shrinkage and elastic strains on axially loaded structural members that use concrete as a primary construction material in high-rise buildings. Quantification of axial shortening at design stage of high-rise buildings with composite members is hence based on scaled well established numerical models of reinforced concrete. Further studies to improve these scaled models to capture the true behaviors of the composite action have been recommended in recent research work (Uy, 1998; Uy & Das, 1997). Methods proposed in this thesis are hence based on the well established material models of reinforced concrete using conventional bar reinforcements. The fundamental principles and computational techniques developed in this research work can be applied to structural components that are reinforced with structural steel encased in concrete or tubular structural steel filled with concrete. One other aspect that requires due consideration is the inability to validate the findings through a process of monitoring performance of tall buildings during and after construction. Experimental testing of components under laboratory conditions cannot simulate the true behaviour of large and complex component systems in the open environment. Techniques available for field measurements and monitoring have not been feasible due to practical implementation problems (Boonlualoah, Fragomeni & Loo, 2005).

(Kim & Cho, 2005) predicted and measured axial shortenings of two reinforced concrete core walls and four steel embedded concrete columns (composite columns) in a 69 storey building. Axial shortenings of these composite columns were predicted using the numerical models of reinforced concrete with limitations. This study recommended further studies to develop a method to quantify axial deformations of composite columns with high steel ratios.

Columns of Taipei 101 tower, which is the second highest building in the world, was designed and constructed in steel box section filled with high strength concrete. The composite action between concrete and steel plates of the steel section impacts on elastic, creep and shrinkage strains and hence this impact was incorporated into the design procedure (Shieh, Cang & Jong, 2010).

Baker, Korista & Novak (2008) presented quantification of axial shortening of Burj Khalifa Tower in the UAE using 15 separate three dimensional finite element analysis models. Each model represents a discrete time steps during construction and time dependent load application and stiffness change of concrete were employed into the models at the time steps. The compensation methodology was employed to mitigate the adverse effects of differential axial shortening. The main drawback of this quantification procedure is that due to the wide discrete time steps considered during the axial shortening quantification, capturing accurately the variations of time dependent creep, shrinkage, concrete stiffness and load application incorporating non vertical load paths resulting from stiff shear walls of outrigger and belt systems and the geometrical complicity at the intermediate construction stage is questionable. It is well known that after the opening this tower, it was not occupied around two weeks due to failure of the lifts. This may be a result of adverse effects of differential axial shortening.

Luong et al (2004) demonstrates quantification of differential axial shortening at the design stage and strategies used to control the adverse effects of differential axial shortening of two international financial center, Hong Kong. The packing shims at the contact surfaces between the outrigger and the mega columns were employed to minimize the massive forces and moments generated due to differential axial shortening between these structural members. However, this strategy is unable to control the detrimental effects such as tilting floor plates, and distortion and deformation of non structural components and services. (Shahdapuri, Mehrkar-Asl & Chandunni, 2010) presented a method used to quantify axial shortenings of mega composite columns and cores of A1 Mas tower. This method was based on material models of reinforced

concrete in ACI codes. Capturing the true behaviour of creep, shrinkage and elastic shortenings of the composite members using this implemented method is therefore uncertain. Moreover, Laser equipments were proposed to measure axial shortenings of the columns and the core shear walls during and after the construction. Jin Mao tower is an 88 storey building comprising mega composite columns and a reinforced concrete core. These key load bearing members are connected by several outrigger and belt systems at certain locations. It is necessary to quantify axial shortenings of these key members incorporating effects of non vertical load paths resulting from the belt and outrigger systems since these load paths impact significantly on axial shortening.

(Uy, 1998) studied the effects of composite action on creep and shrinkage strains and concluded that these strains are low than those of reinforced concrete members because of the confinement effects. This study also presented the factors limited to three concrete strengths and these factors can be used to predict the creep strain of the composite members comprising the limited concrete strengths.

As a primary material, concrete governs the behaviors of the key members of buildings and their axial shortening. Concrete is subjected to time dependent deformations and distortions after being placed which govern life time serviceability and performance of a structure during its life as stated in the introduction.

2.1 Deformation of Concrete

Firstly, concrete undergoes shrinkage soon after being poured, if moisture is allowed to transfer to the environment. Shrinkage is independent of load and depends on the quality of concrete. Secondly, concrete undergoes a further deformation which depends on the load present. This is known as creep which is both load and time dependent (Neville, 2005).

The total strain in a concrete member, $\delta_{\text{total}}(t, t_0)$, at any time, $t(\text{days})$ after loading at time $t_0(\text{days})$ can be expressed as

$$\delta_{\text{total}}(t, t_0) = \delta_{\text{Elastic}}(t, t_0) + \delta_{\text{Creep}}(t, t_0) + \delta_{\text{Shrinkage}}(t) \quad (2.1)$$

Where the elastic strain, $\delta_{\text{Elastic}}(t, t_0)$ and the creep strain, $\delta_{\text{Creep}}(t, t_0)$ depend on the time that loading took place. The shrinkage strain, $\delta_{\text{Shrinkage}}(t)$ depends on the time that drying started. Figure 2-1 depicts time variations of stress and strains in concrete.

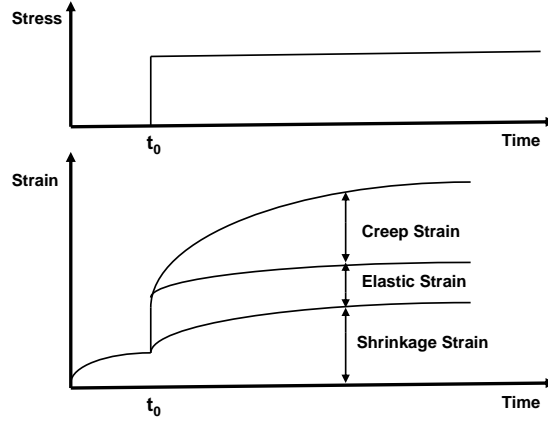


Figure 2-1: Time variations of stress and strains in concrete

Figure 2-1 illustrates that immediately after concrete sets or at the end of moist curing, the shrinkage strain begins to develop and continues to increase at a decreasing rate. Meanwhile, stress applied at time (t_0) causes a sudden increment in the strain diagram. This strain is called instantaneous strain which also follows an additional increase in strain due to creep.

2.2 Elastic Deformation

2.2.1 Definition

Elastic strain $\delta_{\text{Elastic}}(t, t_0)$ occurs immediately on application of stress and depends on the magnitude of the stress, the rate at which the stress is applied, and on the age of concrete (Young's Modulus) (Neville, 2005).

2.2.2 Influencing Factors

The moduli of elasticity of concrete vary with strength. Several factors govern strength and the modulus. The water cement ratio is the most dominant factor since when

increasing the water cement ratio, the modulus decreases significantly. Aggregate properties also affect the modulus. When increasing the modulus of aggregates, the modulus of concrete increases. Figure 2-2 demonstrates the stress Vs. strain variation of aggregate, cement and concrete (Fintel,Ghosh & Iyengar,1987).

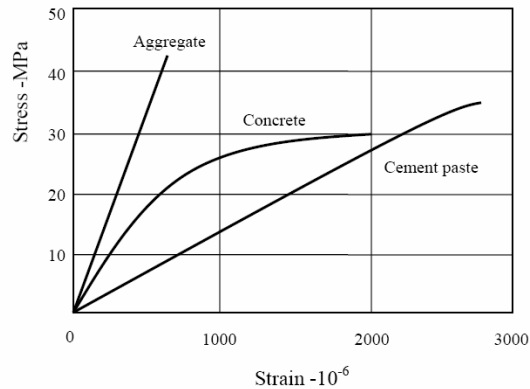


Figure 2-2: The stress Vs. strain variation of aggregate, cement and concrete (Fintel,Ghosh & Iyengar,1987)

2.2.3 Elastic Modulus of Concrete

The modulus of elasticity or “Young’s Modulus” reflecting the capability of concrete to deform elastically is a very important mechanical property. The modulus of elasticity is defined as the slope of the stress strain curve within the proportional limit of a material (Liu, 2007). Figure 2-3 illustrates the stress-strain plot of a concrete member subjected to loaded and unloaded conditions.

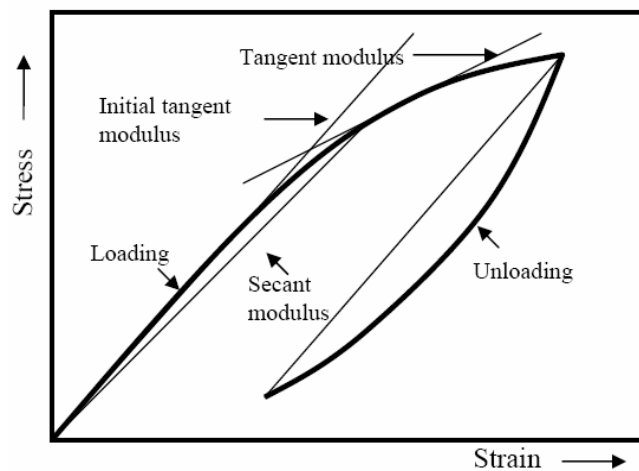


Figure 2-3: Representation of the stress-strain relationship for concrete (Liu, 2007)

The most commonly used value in structural designs is the secant modulus (static modulus), which is defined as the slope of the straight line drawn from the origin of axes to the stress-strain curve at some percentage of the ultimate strength. This modulus is used to design structures subjected to static loads (Liu, 2007).

Since no portion of the stress strain curve is a straight line, the method of determining the modulus of elasticity is to measure the tangent modulus (dynamic modulus), which is defined as the slope of the tangent to the stress-strain (where the curve is non-linear). This modulus is used to design structures subjected to dynamic loadings (Liu, 2007).

2.3 Shrinkage Deformation

2.3.1 Definition

Shrinkage is independent from the load applied and only occurs due to the loss of water during the dehydration process. The converse of shrinkage is swell age, which denotes volumetric increase due to moisture gain in the hardened concrete. This is because the cement gel either shrinks or expands with its volume. Additionally, shrinkage phenomenon takes place in fresh as well as in hardened concrete and hence this phenomenon can be categorized into two groups; drying and plastic. Shrinkage occurring before the concrete hardens is called “plastic shrinkage” while shrinkage occurring after the concrete hardens is called “drying shrinkage” (Fintel & Fazlur, 1987).

2.3.2 Influencing Factors

Shrinkage is affected by all the factors which affect the drying of concrete so that it depends on environmental conditions. Additionally, the aggregate controls amount of shrinkage since increment of the aggregate content reduces shrinkage and shrinkage is small when stiffer aggregate is used. i.e. aggregate with higher elastic modulus (Liu, 2007).

The water-cement ratio influences enormously on shrinkage. This ratio is directly proportional to shrinkage due to the fact that strength of concrete and its porosity depend on a large extent on the water-cement ratio. The higher this ratio (more porous concrete) therefore assists to increase the moisture interchange between concrete and the ambient condition and higher water content reduces volume of the restraining aggregates (Fintal, Ghosh & Iyengar, 1987).

The environmental condition affects magnitude of shrinkage. High relative humidity decreases shrinkage. The magnitude of shrinkage is governed by several factors such as surface area of concrete member exposed to the environment, temperature, wind velocity and bond between reinforcements and concrete. The water in the concrete member evaporates from the exposed area to the environment so that when raising this area, amount of shrinkage also amplifies. Shape and size of the concrete member therefore control shrinkage. Additionally, factors such as temperature growth and amplification of wind velocity accelerate the drying and evaporation respectively and hence leads to high shrinkage. Shrinkage decreases slightly when increasing confinement effects between reinforcements and concrete (Fintal, Ghosh & Iyengar, 1987).

2.4 Creep Deformation

2.4.1 Definition

Creep continues with time under the sustained stress. Creep associates with shrinkage since several governing factors common for both phenomena occur simultaneously. Creep phenomenon can be categorized into two groups; basic and drying. Basic creep takes place under conditions of no moisture movement between the environment and the concrete. Drying creep is an additional creep caused by drying. However, this distinction is not considered in practice and creep is simply considered as a time- dependent deformation under load in excess of shrinkage (Neville, 2005).

A concrete structural member can deform freely under a permanent constant stress with the influence of creep. As a result, creep problems involve the calculation of deformations under a known sustained stress history. Alternatively, if the free

development of deformation due to creep is suppressed, the original stress is reduced. It means that relaxation takes place. The relaxation problems hence involve the deformation of stress at any time under specified conditions of strains or deformations. However, in reinforced concrete structures, it is impossible to explore situations which are categorically separated into either creep or related problems. Pure creep is not achievable as internal restraint is provided by the reinforcement, while real support conditions provide significant external restraint. In addition, pure relaxation is unachievable since the members are seldom restrained completely so that no deformation of concrete is possible. Concrete members in buildings are therefore subjected to a combination of both creep and relaxation (Elnimeiri & Joglekar, 1989).

2.4.2 Original Mechanism

Creep commences with hardening cement paste which consists of solid cement gel containing numerous capillaries. The cement gel is made up of colloidal sheets of calcium silicate hydrates separated by spaces containing absorbed water. Creep is thereby a paste property and aggregates in concrete serve to act as a restraint. Many theories have been proposed to describe the mechanism of creep in concrete (Neville, 2005).

The internal mechanism of creep takes place due to any one or combination of followings (Neville, 2005).

01. Sliding of the colloidal sheets in the cement gel among the layers of absorbed water (viscous flow).
02. Flow of water out of the cement gel due to external load and drying.
03. Elastic deformation of the aggregate and the gel crystals as viscous flow and seepage occurs within the cement gel
04. Local fracture within the cement gel involving the breakdown of physical bonds, micro cracking and closing of internal voids.

Concrete with high shrinkage performs high creep. This does not mean that these two phenomena occur due to the same causes, however, they associate with the same structure of hydrated cement paste.

2.4.3 Influencing Factors

Magnitude of creep and its rate of development are influenced by many factors depending on properties of concrete, environmental and loading conditions. The individual factors interrelate and affect not only the final magnitude of creep, but also its development. These factors are described as follows (Fintel & Fazlur, 1987).

- Age of concrete at loading

The magnitude of creep depends on age of concrete at instant of loading or more precisely on the degree of hydration at first loading. Creep will be low when concrete is loaded later.

- Strength of concrete

Strength of concrete is inversely proportional to magnitude of creep. Creep depends on factors such as the water-cement ratio and the cement type as these factors associate with strength of concrete.

- Ambient Conditions

Creep behaves differently for the factors which affect drying. Creep increases, once environmental humidity decreases. Also, temperature growth helps to amplify creep since deformability of cement paste is increased by an increased temperature and drying is accelerated.

- Aggregate type and volume

Amount of creep depends on size and stiffness of the aggregate content. If the size and stiffness are very high, creep reduces dramatically. Increasing the content of aggregate also reduces creep.

- Cross sectional dimensions of structural members.

The most important factor is the area exposed to the environment because of the moisture movement to the environment. Creep is directly proportional to area of concrete member. Size of the concrete member such as surface to volume ratio controls creep development which means that actual shape of the member is insignificant.

- Magnitude of stress

Creep depends on the stress level of loaded concrete member. When the sustained stress is less than about one half of the compressive strength of concrete, the creep strain is directly proportional to the stress level. This is called “Linear Creep”. At higher stress levels (i.e. higher than $0.5 f_c'$ where f_c' = characteristic strength of concrete) creep increases rapidly and becomes nonlinear with respect to stress. In practice, compressive stress rarely exceeds $0.5 f_c'$ in concrete members in buildings under loaded condition so that the creep is direct proportional to the stress.

- Reinforcements of structural member.

Stress is directly proportional to creep strain as described earlier. Stress of reinforced concrete member transfers to reinforcements and hence the higher reinforcement ratio reduces creep and vice versa. Columns and core shear walls in high rise buildings comprise 2-4% reinforcement ratio and these reinforcement ratios govern their creep strains noticeably.

2.5 Axial Shortening

Combination of axial creep, shrinkage and elastic shortenings causes axial shortening. In high rise buildings, perimeter columns tend to be more heavily stressed compared to shear walls of internal core. These perimeter columns thereby tend to deform axially at higher rates compared to the shear walls. This leads to differential axial shortening (DAS) between the columns and shear walls. DAS increases with building height and non vertical load path as a result of geometric complexity of structural framing systems and causes serviceability related problems; impacting on floor flatness, load

redistribution and cracking. Axial shortening is influenced by several variables as outlined in Figure 2-4.

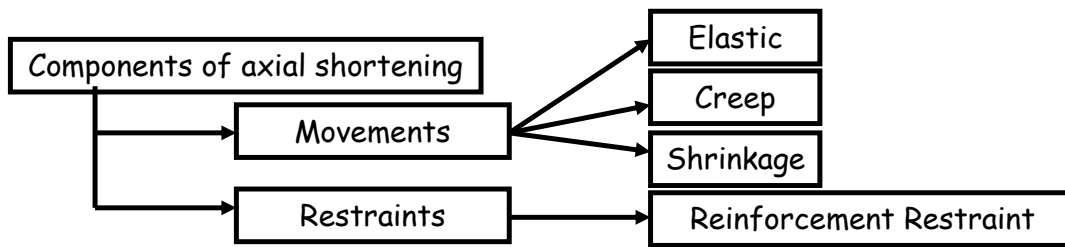


Figure 2-4: Components of axial shortening

Accurate prediction and management of axial shortening in buildings help to minimize potential problems as described earlier. Proactive measures can be made in optimizing building layout to limit differential axial shortening. However, it is not always practical when considering architectural and constructional constraints. Allowance can be made for additional stress induced for strength requirements. Serviceability can also be improved by pre-stressed slabs in tall buildings. Effective prediction of the shortening requires the use of appropriate analysis models and assumptions including consideration of both structural and material modeling.

Engineers predict DAS using different methods and none of them are comprehensive enough to capture complexities of modern high rise concrete buildings, such as load migration during and after construction, load –time histories, and outrigger and belt systems. Most of these methods are based on discrete models of an member and or building representing few stages of the construction and the field measurements acquired during the limited time frame. Consequently, these methods are unable to capture the time dependent load migration resulting from structural geometric complexities highlighting that there are no widely accepted rigorous procedures and guidelines in design codes suitable for quantifying axial shortening of geometrically complex new generation high rise buildings. Some of studies conducted to examine the axial shortening are outlined as follows.

Pfeifer et al (1970) determined the axial shortening of load bearing members of a 70 story building and allowed gaps in the construction to mitigate adverse effects of differential axial shortening. Elnimeiri & Joglekar (1989) developed a procedure to predict the long-term deformations of reinforced concrete columns, walls and composite columns. This procedure includes the effects of concrete properties, construction sequence and loading history. Ghosh (1997) presented the outcome of calculated axial shortenings of load bearing members of the 80 story Jin Mao Tower, Shanghai and recommended a few structural modifications which need to be incorporated into the design procedure in order to mitigate detrimental effects of differential axial shortening. Using this procedure, the Differential Axial Shortening (DAS) effects for three high rise buildings in Chicago are designed and six years of field measurements of the column shortenings are compared with the predicted values. Baker, Korista & Novak (2007) presented a design procedure for the Burj Tower, the world's tallest building in which a procedure for calculating the axial deformation of vertical load bearing members was incorporated. This involved 15 separate three dimensional finite element models, each representing a discrete time during construction, to calculate axial shortenings of members.

2.6 Quantify the Axial shortening using Ambient Measurements

Measuring shortenings of columns and shear walls of cores to verify the predicted levels of shortening is an acceptable method. Russell & Corley (1997) presented outcomes of axial shortening measurements of Water Tower Place, a 75 storey reinforced concrete building in Chicago. Axial shortenings of selected vertical load bearing members at six levels of the building were measured using mechanical strain gauges during the first three years of a five year project and effects of differential movements on the strength and serviceability of the structure were examined.

Beresford (1970) studied suitable measuring instruments to quantify the axial shortening. In this study, the instruments were categorized into two main groups such as macro and micro based on their real potential to capture the axial shortening. Macro scale measuring instruments are virtual scales, optical leveling, liquid manometers and

displacement gauges. Micro scale measuring instruments are manual strain, acoustic strain, electrical resistance strain, hydraulic stress and photo elastic stress gauges. This study also identified that obtaining accurate in-situ measurements is a inconvenient activity since these measurements depend on environmental conditions and the construction process concluding that “a great deal of practical data on long-term shrinkage behavior and effects in buildings is required so that theoretical methods can be accurately applied at the design stage” Beresford (1970).

External mechanical strain, vibrating wire and electronic strain gauges are used to measure axial shortening in the fields. These gauges are embedded on or in the concrete members, although this may not be the most effective due to the fact that deploying and protecting of these gauges are uneconomical and inconvenient (Carreira & Poulos, 2007).

The most well established gauges used in the fields to measure axial shortening are described as follows.

2.6.1 Vibrating Wire Gauge

Bakoss, Burfitt & Cridland (1977) investigated the suitability of vibrating wire gauges to measure axial shortenings of structural members. The operation of this gauge is based on magnetic and electrical concepts. Figure 2-5 shown below is a typical view of the wire gauge.

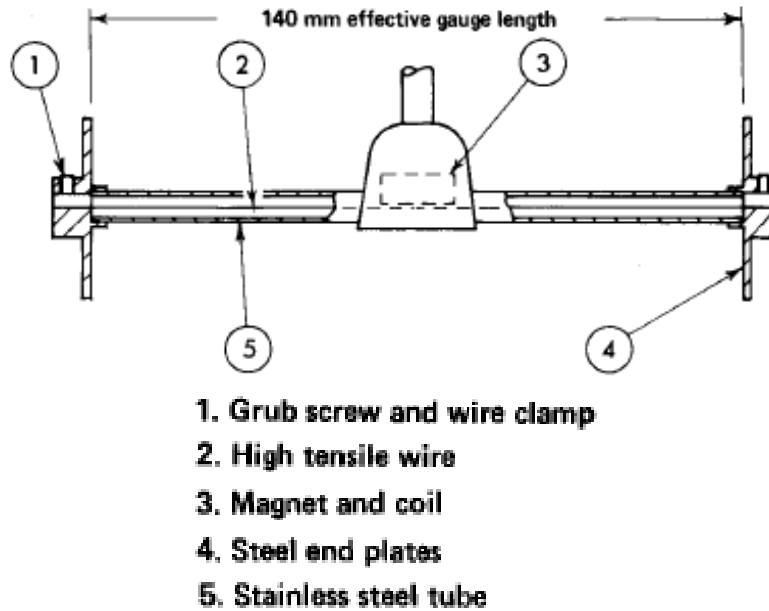


Figure 2-5: A vibrating wire gauge (Bakoss, Burfitt & Cridland, 1977)

Basic theory behind of vibrating wire gauge operation is that an electric impulse causes the electromagnet to pluck the wire and hence the frequency of the resulting free vibration of the wire can be measured. The coil of the electro magnet can also be used as a resistance thermometer. When the end plates of the gauge undergo relative movements, strain of the wire produces a change in the frequency of the wire. Consequently, this frequency change can be used to quantify the relative strains so that the axial shortening at a certain time can be evaluated by multiplying the obtained strain measurements and height of the member (Bakoss, Burfitt & Cridland, 1977).

2.6.1.1 The use of Briquette Gauges

Vibrating wire gauge should be embedded in members during its construction. This gauge is therefore placed into a small briquette of concrete before installation to protect from immersion vibrators, so that normal pouring and compacting procedures can be used. The shape of the briquette enhances its bonding to the encasing concrete and to minimize the formation of voids beneath the briquette. Figures 2-6 and 2-7 shown below illustrate the gauge with a briquette and the location of the gauge placed in a structural member respectively while Figure 2-8 depicts vibrating wire gauges prior to use.

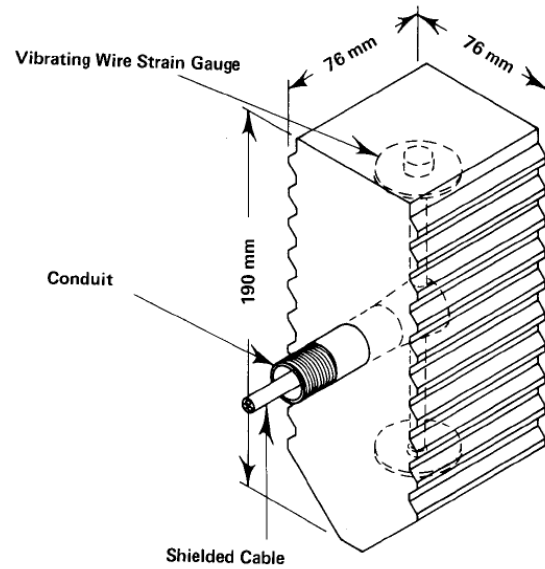


Figure 2-6: A briquette for vibrating wire gauge (Bakoss, Burfitt & Cridland, 1977)

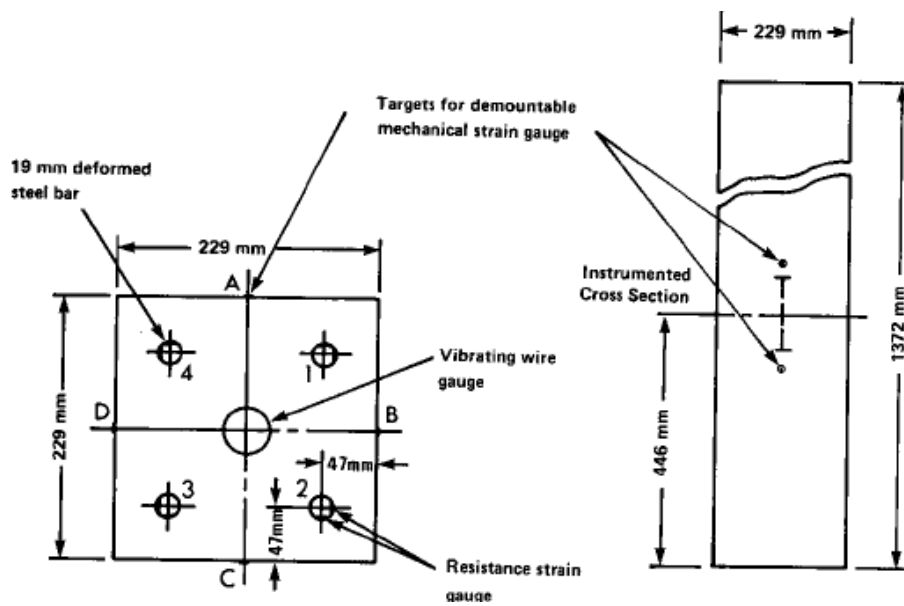


Figure 2-7: A typical view of the detailed of reinforced column with the location of the Vibrating Wire gauge (Bakoss, Burfitt & Cridland, 1977)

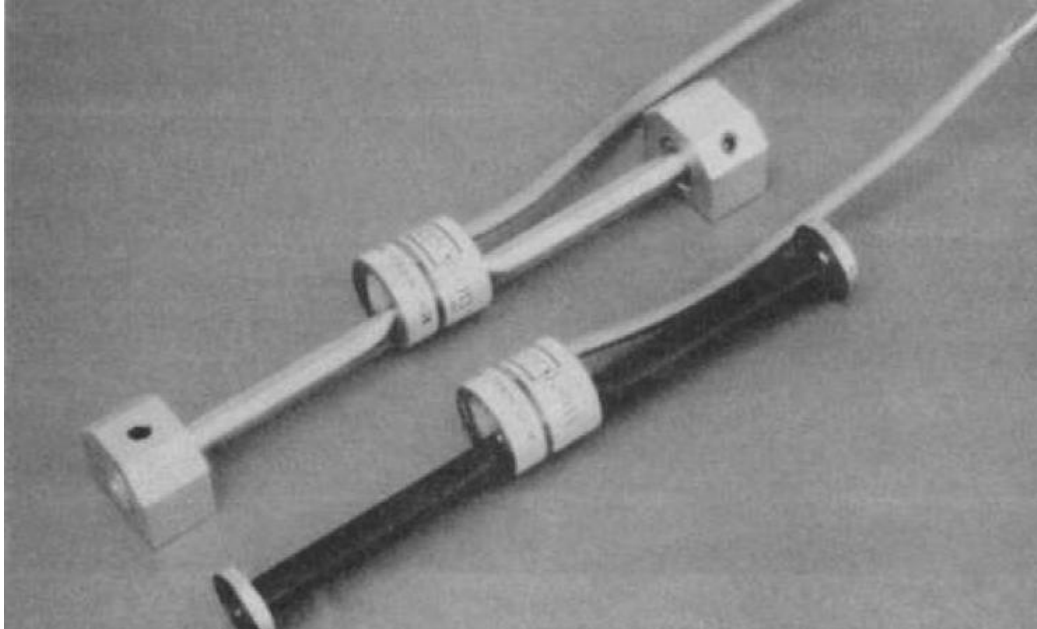


Figure 2-8: Vibrating wire gauges prior to installation (Implementation program on high performance concrete,2008)

Bakoss, Burfitt & Cridland (1977) also investigated the accuracy of strain readings from vibrating wire gauge comparing with strain measurements from resistance strain gauges attached to reinforcement or surface and from demountable mechanical gauges applied to the surface. The errors caused by temperature changes can be made insignificant for practical purposes, or can be estimated. Furthermore, this study explored that reliability of the readings is unaffected by distance of the gauge from the reading instrument concluding that remote monitoring or logging is not affected.

A comprehensive field study was carried out at New South Wales University of Technology, Australia to determine axial deformations of columns in a reinforced concrete building (Cridland et al, 2007 ; Cridland, Heiman & Burfitt,1973). Strains of the concrete columns in a medium rise building were measured at three levels using vibrating wire gauges. Meanwhile, the column deformations were measured by precise leveling. Several laboratory experiments relevant to creep and shrinkage were conducted to verify the proactive measurements. These measurements were then compared with calculated value from the ACI code. Outcome depicted a good agreement on accuracy of the data from the code and the laboratory tests while highlighting appreciable

differences between shrinkage and creep strains measured in the laboratory and those from the ACI code provided method.

2.6.2 External Mechanical Strain Gauges

Long term surface strain like axial shortening can be measured using external mechanical strain gauge as well. The distance between two points on the concrete surface is compared with the length of a standard reference bar used as the reference. Use of this gauge involves the installation of special points on the concrete surface which is labor intensive, and cannot be used effortlessly with an automated data acquisition system. It is particularly suitable for measurements of strand transfer length and as back up for long-term strain measurements by other means. The sensitivity of Mechanical Strain Gauge measurements is occasionally insufficient to provide reliable data. Measurements of concrete surface temperatures and standard reference bar temperatures also require when using mechanical strain gauge. The frequent comparisons with the reference bar are also needed to maintain accuracy of this method (Carreira & Poulos, 2007).

External Mechanical Gauge comprises the installation of brass knobs on concrete surfaces after form work removal. The gauge length is 508 mm. The installation does not interfere with the placing of concrete. However, brass knobs on concrete surface can be damaged or removed accidentally during the construction, or covered by column finishing when progressing the construction process. To minimize such damages, they are placed flush with the concrete surface in a drilled hole and bonded with epoxy. The number of strain readings is usually small and accessibility may be limited or impossible with the time. External mechanical gauge is embedded on the surface of the measured concrete columns so that the readings may include extreme fiber strains induced by load eccentricity and by temporary or seasonal temperature and moisture changes (Carreira & Poulos, 2007). Figure 2-9 demonstrates a typical view of the gauge being used.



Figure 2-9: A typical view of a mechanical gauge being used to measure transfer length in a pre stressed concrete girder (Implementation program on high performance concrete,2008)

Several field studies have been conducted using External Mechanical gauges. The field study conducted by Donald, et al (1980) on a 70 storey building is very comprehensive. Time dependent shortening of concrete columns and core walls of the structure were measured. Meanwhile, laboratory tests were performed to determine creep and shrinkage properties of the concrete mixes for the columns and the core walls. External Mechanical Strain gauges were used to measure axial shortening at 27 different levels of interior columns and core walls. This study concluded that “ in the design of a building where the structural system indicates that differential shortening require to be considered, the range in material properties should be determined (preferably by laboratory tests on concrete mixes to be used) and the subsequent range of differential shortening should be calculated”(Donald et al,1980).

Russell & Corley (1978) measured axial shortenings of vertical load bearing members of the high rise concrete building, Water Tower Place, a 75-storey building, located Chicago, Illinois using External Mechanical Strain gauges. In this study, the measurements were acquired at the six levels selected to provide measurements for each of the different concrete strengths. Air temperature and concrete surface temperature

were recorded for every strain reading. Laboratory test of concrete from the field were performed in order to calculate the creep, shrinkage and elastic deformations.

2.6.3 Electronic Strain Gauge

This gauge is embedded at the center of columns and shear walls. As a result, this gauge does not have the limitations as of external gauges, and can be wired to a central automatic collection panel for data recording. Implementing these gauges is initially more expensive than the exterior gauges since they require embedding in concrete members. Additionally, concrete placement in the members requires extra precautions to avoid damage from vibrators and falling concrete from form work. Electronic strain gauges were successfully used since the construction of large dams in the 1930's and more recently in laboratory testing of structural members and in nuclear containments. A dual system comprising external mechanical strain gauges and embedded electronic strain gauges is recommended for measuring axial shortening (Carreira & Poulos, 2007).

Beresford (1970) studied the suitability of Electronic Strain gauges to measure axial shortening and identified that the use of a precision level with targets located at a designated elevation on columns is another useful tool to determine differential axial shortening between columns and shear walls at a certain floor. This study also reported that a total station can also be utilized to relate the absolute differences in height in adjacent floors with the necessary target points. These measuring methods become even more problematic as construction progresses and architectural members commence to cover the structural members. Measuring axial shortening should therefore be discussed with the entire project team prior to start of construction and pricing of the structure. The installation, measurements, documentation and interpretation of the strain data are responsibility of an independent testing agency hired by the Owner and reporting to the Architect/Engineer.

Based on the above, embedding Vibrating Wire, External Mechanical Strain and Electronic Strain gauges on or in the structural members to acquire continuous measurements and protecting them during and after construction stages are inconvenient

and uneconomical highlighting the need of a comprehensive convenient procedure/method to quantify axial shortening using ambient measurements.

2.7 Vibration Measurements

Accelerometers used to estimate the modal parameters can be installed on structural elements more convenient than the gauges above. Presently, use of these parameters to assess health and or performance and to validate the numerical model of structure is increasingly popular. Ellis & Ji (1996) conducted a broad study to establish the dynamic characteristics of a building during and after its construction. The study was carried out using a reasonably large building model to simulate its behaviour. The aims of that study were to provide information on the dynamic characteristics at different construction stages of the building and to understand the behavior of structural components under dynamic excitations such as wind, traffic loads, and earthquakes. Using both a long-range laser interferometer and accelerometers, the dynamic characteristics of the laboratory model at several selected construction stages were studied under free and forced vibrations. Meanwhile, finite element analysis was carried out for each construction stage and the results were compared with the experimental results and achieved a satisfactory agreement. Damage assessment of structural members in a seven story building after the earthquake was performed using ambient vibration measurements by Ivanovic et al (2000) and outcomes provide a guide for future implementations of recording systems in buildings. This study also highlighted that ambient vibration measurements are more convenient since they can be acquired using light equipments and few operations. Ambient Vibration Test (AVT) on the Republic Plaza, one of the tallest buildings in Singapore, was conducted over two years from the commencement of construction to the service stage. Sensors such as accelerometers, GPS (Global Position System) and strain gauges were deployed on the structure to examine its behaviour during and after construction. Meanwhile, Finite Element (FE) models were developed applying micro and macro model updating methods and were analyzed to simulate the construction and service stages. The comparison study between results from the FE analysis and the ambient measurements showed a satisfactory agreement (Brownjohn, Pan & Deng ,2000). Ventura et al (2003) conducted ambient

vibration tests on a base-isolated building in Japan in order to investigate its dynamic response characteristics under low excitation. The natural frequencies and mode shapes of the building in the longitudinal, transverse and torsional directions were determined to calibrate finite element model of the building. Li et al (2004a, 2004b) reported that measured dynamic characteristics facilitate to understand the real structural behavior especially for modern tall buildings under wind action due to the fact that many critical phenomena can be investigated by full scale experiments only. Additionally, these measurements are very useful to calibrate numerical model of building. Kanwar et al (2008, 2010) identified damages of building models using Damage Index method associated with vibration characteristics. Different limits for Damage Index were defined based on the damages. This method was then applied to a real building to examine accuracy of the defined limits. Results depicted that Damage Index method with its limits can be used to identify damages of structures successfully. This research also emphasized that ambient vibration characteristics can be employed to locate damages of structures successfully after subjected to natural hazards.

Olmer (1980) presented the development of an innovative vibration measuring gauge called “Pick-up”. These gauges were installed on a 16 story building in order to measure its dynamic response. Results show that Pick up(s) have an ability to extract smaller natural frequencies (ranging from 0.2Hz) and modal vectors (modal displacement ranging from micro meter) which are more accurate than those obtained from present instruments such as GPS and accelerometers. This study concluded that accurate ambient vibration measurements of building structures can be acquired conveniently and accurately.

The practical procedure developed in this research will depend on modal parameters. Quantification of axial shortening is hence more convenient than methods associated with vibrating wire, external mechanical strain and electronic strain gauges. Another benefit of this development is that these modal parameters can be used to assess health and performance of structure.

2.8 Structural System

Geometrical complexities of high-rise buildings are increasing dramatically. Regular classification of high-rise buildings with respect to their structural system is difficult. However, general classification as listed below can be made with respect to effectiveness in resisting lateral loads.

- Moment resisting frame systems
- Braced frame, shear wall systems
- Belt and outrigger and shear wall systems
- Tubular system
 - ▲ Framed tubes
 - ▲ Trussed tubes
 - ▲ Bundled tubes
- Hybrid systems that combine advantages of different structural and material systems (Buyukozturk & Gunes,2008).

Figure 2-10 illustrates how these systems can be utilized according to their effectiveness in resisting lateral loads.

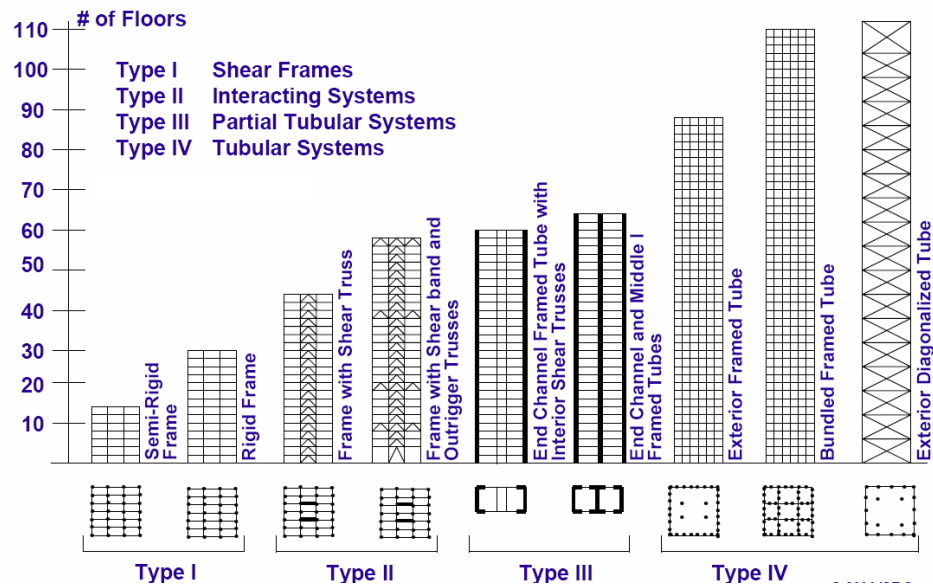


Figure 2-10 : Classification of structural systems based on their effectiveness in resisting lateral loads (Buyukozturk & Gunes,2008)

2.8.1 Belt and Outrigger Systems

Outrigger and belt systems are relatively stiff framing systems connecting the shear cores and mega perimeter columns to enhance resistance to transient lateral force induced by wind and earthquakes. These systems reduce lateral deflection and the base overturning moment in the core and are introduced into building frames at various intervals ranging from 10-25 floors to allow the building to regain its stiffness after a significant load enhances with height. Outrigger and belt systems can be several stories deep connecting between cores and mega perimeter columns so that they assist to increase the bending rigidity and shear resistance. Mechanical plant floors are an ideal location for installation of outrigger and belt systems in high-rise buildings. These stiff framing systems also control the relative movement between the structural elements and hence reduce the differential axial shortening. Several buildings with this type of stiff framing systems have been built during the last three decades especially in America, England, Australia and Dubai. . Introducing these systems into buildings has become very common in design practice today. Figure 2-11 demonstrates a schematic diagram of outriggers located in a building.

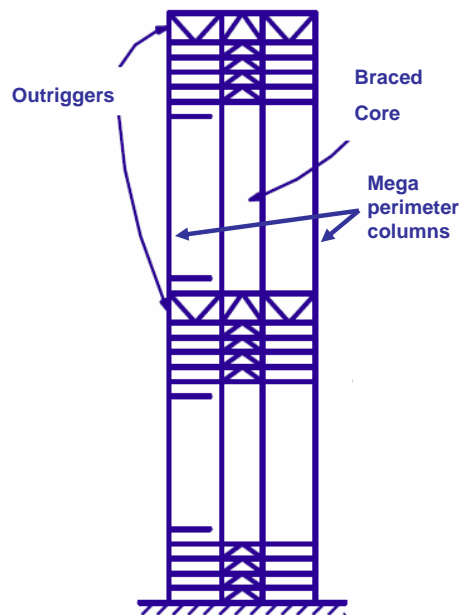


Figure 2-11 : A schematic diagram of outriggers located in a building.

Gibbons, Lee & MacArther (1998) examined impact of outrigger and belt systems on differential axial shortening and concluded that jacking and shim packing would be implemented at connections which are between outrigger systems and the perimeter columns, effectively allowing the differential axial shortening between the core and the mega perimeter columns to occur during construction without developing additional significant shear forces and bending moments in these systems. This approach reduces influence of extreme stresses developed due to differential axial shortening between the core and the perimeter columns. After a majority of the relative movements/differential axial shortening occur, the connections are then to be permanently fixed. However, during the above procedures, the core and the perimeter columns are not connected so that lateral load capacity of the building is very low. This is a significant issue when the structure is subjected to considerable lateral forces from the natural or manmade events such as earthquakes, hurricanes, blasts etc. Such a situation occurred during construction of the Taipei 101 tower, which is the second tallest building in the world (Taipei 101, 2008). During construction of the tower (at 2.52 p.m, 31st March 2002), it was subjected to an earthquake with a magnitude 6.8 in Richter scale. The tower was undamaged while significant damages occurred in temporary works when a crane at the top crashed down killing 2 people. Another disadvantage of above procedure introduced by (Gibbons, Lee & MacArther, 1998) is that differential axial shortening between perimeter columns and core shear walls becomes more pronounced and impacts significantly on life time serviceability and performance of the structures, when these structural members are not connected through outrigger and belt systems which control the differential axial shortening of those members.

Gibbons, Lee & MacArther (2002) reported strategies used to control adverse effects of differential axial shortening. The most significant strategy was the 20mm limit for facades attached to the floors. The effects of creep, shrinkage and patterned imposed load require to be considered to determine this limit. These effects along with axial shortening of core and columns were incorporated in the construction to ensure that the building was constructed within acceptable tolerance of the determined limit. However, the differential axial shortening is more or less than 20mm depending on several factors

such as structural systems, environmental conditions, the construction materials and so on. Further, differential axial deformation impacts significantly on non structural elements and horizontal structural members such as slabs and beams as well as other services such as plumbing, electrical conduits. This limiting strategy implemented for facades attached to the floors is thus an unacceptable solution for geometrically complex new generation high-rise buildings.

Tianyi & Xiangdong (2007) studied the influence of outrigger systems on differential axial shortening. The results of this study revealed that these systems control significantly the vertical deformations and forces of the columns by attracting additional moments and shear forces. Furthermore, the additional forces in these systems are controlled by the number of floors constructed on the top of these systems, but are not sensitive to total height of the building. This study also highlighted that differential axial shortening between the columns and the cores is very low where outrigger systems are placed.

Previously, many outrigger and belt systems are designed using steel because steel is not subjected to creep and shrinkage shortenings. However, when increasing height and length of building constructed in urban areas, lifting large steel sections and their installation become very difficult. Additionally, extensive analysis requires conducting to assess the precise characteristics of the interface between steel trusses used for outrigger systems and concrete members to ensure strain compatibility for minimizing the potential for cracking on the concrete surfaces. Another key issue is potential impact on the construction program/sequence when using different materials, process and systems. The cores of buildings are constructed with relative speed (typical cycle times achieved on core are 3-4 days) using a slip or jump form construction system. Stopping the constructing system at the outrigger levels to permit the steelwork contractor to install the outrigger system is not conducive to optimizing continuity of skills and processes highlighting that installing steel outrigger systems delays the whole construction program (Gibbons, Lee & MacArther, 2002). Presently, designers are thereby willing to design buildings with concrete outrigger and belt systems. Accurate

quantification of differential axial shortening is thus necessary at design stages to improve performance of the whole structural framing system. .

2.9 Ambient Measurements of Modal Parameters/Vibration Characteristics

Significant works has been conducted in area of Structural Health Monitoring(SHM) of civil engineering structures using change of modal parameters such as natural frequencies and mode shapes which can be measured conveniently. These modal parameters depend on mass and stiffness distributions of structure and any subsequent changes of these distributions reflect in changes in the frequency and mode shapes (Catbas, Brown & Aktan, 2006).

During the construction stage, new structural members are incorporated into the structure according to the time schedule so that mass and stiffness of the structure change with construction progress. During the service stage, stiffness of members and mass of the structure change due to service loads/live loads. Consequently, the modal parameters change during these two stages and can be used to examine the behaviour of members of a structure. More information on change of the modal parameters during these two stages will be presented in Chapter 6.

Sensor systems including accelerometers, GPS (Global Position System), FBG (Fiber Bragg Grating) sensors are being used to measure modal parameters of structures. Presently, these sensor systems are installed on structures to assess their health and performance (Xu & Chen, 2008). Bridges comprise small number of discontinuous and determinate structural systems while buildings comprise massive number of continuous members and indeterminate structural systems. It is hence clear that measuring vibration characteristics of buildings require a comprehensive schedule. Figure 2-12 demonstrates SHM system for a building.

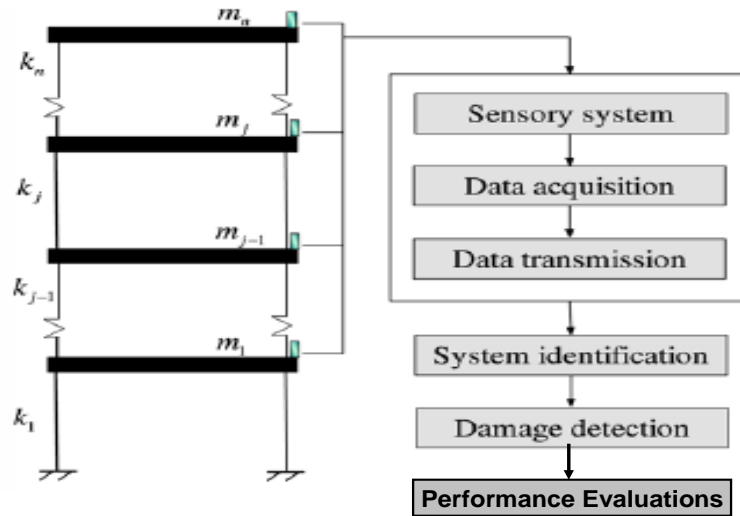


Figure 2-12: SHM system for a building

2.10 Characterization of Structural Phenomena

One of the main purposes of the SHM operation is to monitor the development of specific structural phenomena in a structure. Depending on types of loads such as loads coming from vehicles, people, goods, wind and so on acting on the structure during the monitoring, different phenomena can occur.

The probable cause, such as internal and external loads, for these phenomena needs to be identified to be able to determine which parameters should be measured. Examples of parameters are forces, stresses, displacements, rotations, vibrations, and strains. Also environmental parameters such as temperature, humidity, precipitation, wind and traffic can influence the phenomena. For example, environmental parameters directly combine with the material used for structural members so that changes of these parameters govern health of the structures (Atkan et al, 2003).

2.11 Time strategies

The time strategy describes the duration and the frequency of the measurements. Basically, time dependent strategies are characterized as short-term, long-term, periodic, continuous, and triggered monitoring. The strategy selection depends on the phenomena to be observed. For example if the width of an existing crack requires to be observed, a

periodic, long-term monitoring program can be recommended. If the damping of a structure needs to be measured, a short-term manually triggered program can be selected. In this research, the measuring effects are continuously changing over long periods of time (30-40 years). Hence, a long term continuous monitoring strategy can be recommended. Figure 2-13 shows further explanation of time strategies.

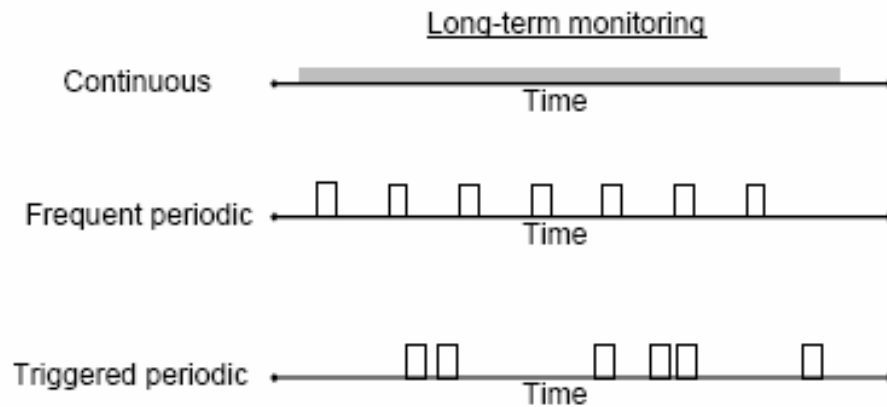


Figure 2-13: Time monitoring strategies (Atkan et al ,2003)

2.11.1 Sensor System

Selecting the most suitable sensor systems is one of the most important factors in SHM since the accuracy of data obtained from these sensors depends on identification of parameters to be observed. Different types of sensors are well established to monitor civil engineering structures based on the requirements. The sensor system must be designed especially for the application and the kind of measurements that should be performed (Hejll, 2007). Natural frequencies and the corresponding modal vectors of the structure can be monitored during and after the construction using a sensor system comprising accelerometers, and GPS (global position systems). According to the parameters to be observed, the sensors can be categorized as follows (see Table 2-1).

Table 2-1: Examples of structural phenomena, strategies and suitable sensors. T: Time dependent strategies, C: Condition dependent strategies and L: Load dependent strategies (Sohn et al, 2003)

Phenomenon	Monitoring Strategies	Suitable sensor types	Comments
1 Foundation displacement and settlements	Local ^C Continuous ^T Static measurement ^L Long-term ^T	LVD Laser Hydrostatic liquid systems All types	Reference position is important Whether dependent, no Accuracy limitations
2 Displacement	Global ^C Short-term ^T or Long-term ^T Periodic ^T or Triggered ^T Static ^T or dynamic ^T	LVD Laser GPS	Reference position is important Whether dependent Accuracy limitations
3 Inclinations and Rotations	Local ^C Short-term ^T or Long-term ^T Continuous ^T	Inclinometers	Slow sample rates
4 Crack detection and localisation	Damage detection ^C Global ^C Dynamic ^T	Fiber optical crack detection systems	Unpractised
5 Crack widths	Local ^C Damage detection ^C Periodic ^T Static ^L	LVD Crack sensors	Stable, only local monitoring possible Possibility to detect cracks
6 Vibrations	Global ^C Short-term ^T Periodic ^T Continuous ^T Triggered ^T Dynamic ^L	Accelerometers	Expensive
7 Corrosion	Local ^C Long-term ^T Continuous ^T Static ^L	Scanning sensors Imbedded sensors	Manually triggered. Only possible to install at new structure

Modal Flexibility Method (MFM) comprising modal vectors and natural frequencies are widely used to examine the health/performance of members of structures because of easy

of computation, accuracy as well as convenient to apply to any structure (Shibukumar, Leslie & Girija,2008 ; Zhao & Dewolf,2006).

2.11.2.1 Definition

Modal Flexibility (MF) associates with modal parameters of a structure, such as modal vectors and natural frequencies and is a measure of the structural state (Adewuyi & Wu, 2010; Shih et al, 2009; Zhao and Dewolf, 2006). This phenomenon will be used to develop an innovative vibration based procedure to quantify axial shortening of building from the ambient measurements. More information on this development will be presented in Chapters 4 to 6.

Modal Flexibility, F_x of element x of a structure can be obtained from (Adewuyi & Wu, 2010 ; Zhao and Dewolf, 2006, as

$$F_x = \sum_{r=1}^n \frac{1}{\omega_r^2} \phi_{xr} \phi_{xr}^T \quad (2.2)$$

Where

x - the element considered

r and n - the mode and total number of modes considered respectively

ϕ_{xr} -magnitude of modal vector of mode r at element x

Note- ϕ_{xr} is a single entity at element x and hence F_x is a scalar. However, Equation (2.2) is presented in the above format to be compatible with expressions in previous publications in the literature mentioned above.

Since, the ω^2 term is in the denominator of Equation (2.2), the modal contribution decreases with increasing frequencies, resulting in the rapid convergence of F_x Modal Flexibility is inversely proportional to the stiffness.

2.12 Summary

From the literature survey, it can be summarized

- ⤴ Analytical methods available to quantify axial shortening at design stage are limited to a very few parameters and not adequately rigorous to capture the complexity of true time dependent load migration and material response
- ⤴ There is a need to develop a comprehensive numerical method to quantify axial shortening of structural members in high rise buildings especially those with complex geometrical structural framing systems.
- ⤴ There are NO convenient and practical methods/procedures available to quantify axial shortening using ambient measurements in order to update previous predictions of axial shortening.
- ⤴ There is a need for a convenient and practical procedure to update axial shortening during construction and service of the building.
- ⤴ This research will be based on the well established numerical models of reinforced concrete. However, if required, these methods can be applied to buildings with the composite members by scaling the creep, shrinkage and elastic parameters.

3 DEVELOP A RIGOROUS NUMERICAL METHOD TO CALCULATE AXIAL SHORTENING IN HIGH RISE BUILDINGS

This chapter demonstrates development of a load time history based analytical procedure to quantify axial shortening capturing influence of the construction sequence combined with the time varying values of Young's Modulus, load migration resulting from structural geometric complexity, creep and shrinkage models of reinforced concrete elements of high rise buildings. This procedure can be used to incorporate axial shortening effects into design procedure.

3.1 Introduction

In recent applications, design engineers have adopted creep , shrinkage and elastic models included in code based methods such as ACI, AS 3600, CEB and GL2000 (ACI committee 2009,1993 ; AS3600,2001 ;CEB-FIP,1990 ;Gardner,2004). GL2000 method has been developed more recently and creep, shrinkage and elastic models included in this method has become increasingly popular compared to the other methods because of it accuracy (Gardner,2004). Goel, Kumar& Paul (2007) conducted a comprehensive study to investigate the most accurate methods among ACI-209R- 82, the B3, the CEB-FIP (1990) and GL2000. The predicted values of creep and shrinkage were compared with the available experimental results from the RILEM (RILEM TC-107-GCS,1995), which is the computerized data bank. Outcome was revealed that the creep and shrinkage models of GL2000 method are more accurate.

3.1.1 Time varying Young's Modulus

The time varying value of Young's Modulus of concrete is one of the major governing factors controlling the behaviour of axial shortening. The time varying value of the Young's Modulus of concrete, $E_c(t)$ is calculated using the equations given by Gardner (2004)

$$E_c(t) = E_{cmt} = 3500 + 4300(f_{cmt})^{0.5} \quad (3.1)$$

where E_{cmt} is the mean modulus of elasticity (in MPa) at age t and f_{cmt} in the mean concrete strength at age t .

The following equation is used if the experimental results for the development of concrete strength with time are not available. This equation depends on the cement type since it affects the strength development of concrete (Gardner,2004).

$$f_{cmt} = \beta_e^2 f_{cm28} \quad (3.2)$$

Where

$$\beta_e = \exp \left[\frac{s}{2} \left(1 - \sqrt{\frac{28}{t}} \right) \right] \quad (3.3)$$

In the above equation, s is a strength development parameter and β_e relates strength development to cement type. According to the type of the cement, s varies as given in Table 3-1.

Table 3-1: variation of s with cement type

Cement Type	S
I	0.335
II	0.4
III	0.13

When a reinforced concrete element is subjected to sustained loads, the stress is gradually transferred to the reinforcement with a simultaneous decrease in overall concrete stress. Therefore, creep and elastic shortening of the concrete are significantly influenced by the reinforcement (Alexandar, 2001). The reinforcement and concrete strains are assumed to be equal under the load so that the material behaviour can be represented by the set of equations (see Equation (3.4)) in which $E_c(t)$ at different time frames can be calculated by Equation (3.1). Effect of reinforcements can be incorporated into the analysis though Equation (3.4) in a simplified way in order to

reduce the complexity and hence to become more attractive procedure among practicing engineers.

$$\begin{aligned}
\xi_T &= \xi_C = \xi_R \\
F_T &= F_C + F_R \\
\sigma_T A_T &= \sigma_C A_C + \sigma_R A_R \\
E(t)_T \xi_T A_T &= E(t)_R \xi_R A_R + E(t)_C \xi_C A_C \\
E(t)_T &= \frac{E(t)_R A_R + E(t)_C A_C}{A_T}
\end{aligned} \tag{3.4}$$

In Equation (3.4), ξ , F , σ , A and E are strain, force, stress, area and Young's Modulus respectively, and the subscripts T, C and R refer to reinforced concrete, concrete and reinforcement respectively and (t) denotes time dependence. The influence of reinforced concrete is introduced into the analysis as a time dependent parameter through Equation (3.4) above.

3.1.2 Staged Construction Process

High rise buildings commonly have floor plans with perimeter and interior columns as well as shear core (s). Slip and jump forms systems used to construct shear cores increase the age difference and loading history of gravity load bearing elements on the same floor and hence have an enhance influence on differential axial shortening. Thus, the construction system and its sequences have a significant impact on the evaluation of axial shortening along with the loading history and the construction time lag. In the preliminary study carried out time history analysis using compression only (gap) elements located at the interface of all vertical load bearing elements and the slabs, as shown in Figure 3-1. This analysis is used to simulate the impact of construction sequence and time based on load application.

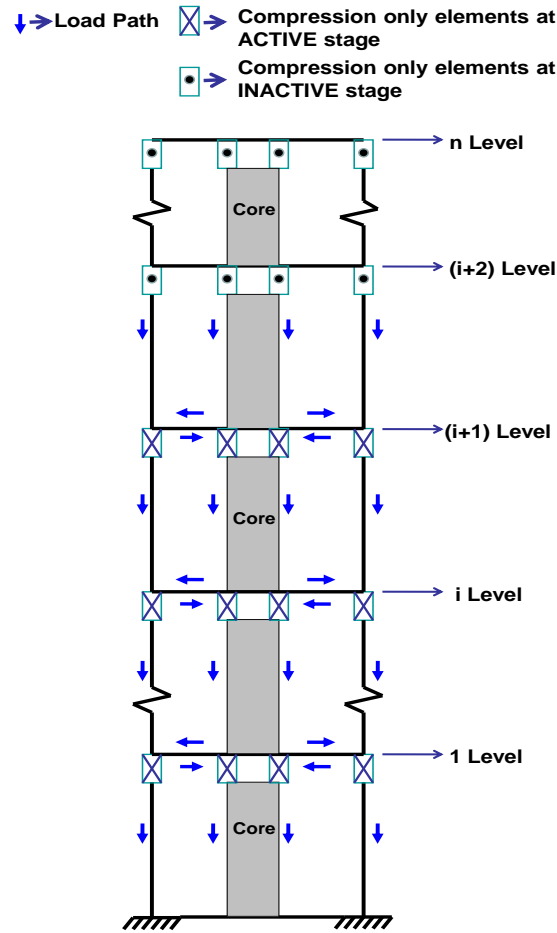


Figure 3-1: Compression only elements and load migration during construction

These compression only (gap) elements transfer the compression only loads to the vertical members at a certain level due to all construction loads applied above that level. The time history of load transfer through these elements at any particular level will depend on the construction sequence. The finite element model representing the whole structure will incorporate these elements at all levels as shown in Figure 3-1. The elements at any one level will initially be in an “inactive” stage until construction proceeds to one level above the level of these elements, after which they will be an “active” throughout the rest of the construction process. Such a guide of load transfer will be able to simulate the exact staged construction process. With reference to Figure

3-1, when the loads from the storey above level (i+2), the compression only elements at level (i+2) and above that level, such as those at levels (i+3), (i+4), etc will be in the inactive stage. Meanwhile, the compression only elements below level (i+2), such as those at (i+1), (i), (i-1), etc will all be in the active stage. The load migration among structural elements below the (i+2) level is therefore simulated according to the real construction sequence. Note that this model is only valid for structural systems where tension loads are not induced across the “gap element” interface.

3.1.3 Compression only Element

Compression only (gap) elements are strategically utilized at the locations to introduce the staged construction procedure as described above after being developed in the finite element model of the whole structure. Figure 3-2 shows a typical compression only element (SAP2000 Ver 10, 2004). In this element, all internal deformations are independent. The presence of the gap (inactive stage) or its closure (active stage) influences only the vertical element below the gap element and do not affect the deformations of the other structural elements. The stiffness function, $f(k)$, of this element can be represented by Equation (3.5).

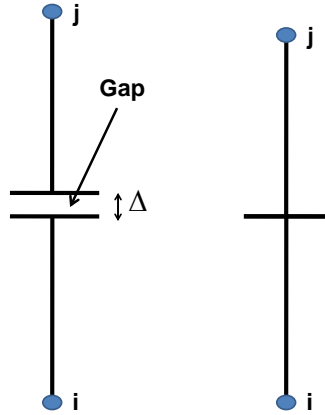


Figure 3-2: A schematic diagram of the compression only element at inactive stage (left) and active stage (right)

$$f(k) = \begin{cases} k & \Delta = 0 \\ 0 & \Delta > 0 \end{cases} \quad (3.5)$$

Where k is the compressive stiffness of the element and Δ is the initial gap opening, which must be zero or positive. In the analysis, the stiffness of the compression only elements k determined from the axial stiffness of the vertical structural elements below them. Equation (3.6) can be used to calculate the axial stiffness of the structural element.

$$k = \frac{EA}{L} \quad (3.6)$$

Where

E-the Young' Modulus of the structural element

A-the Area of the structural element

L-the length of the structural element

3.1.4 Sub Models

High rise buildings may have complex geometric configurations and large number of small components with insignificant distortional stiffness. They tend to increase the computational demand without significant influence on the outcome. Separate finite element models are thus developed for such complex sub framing systems to determine the loads transferred to the main structural frame that is investigated in the finite element analysis. Thereby, the main framing system is isolated from the less significant sub frames to reduce the magnitude of the numerical problem that includes the time dependent variables.

3.1.5 Load Application and Analysis

A typical time varying load history of a concrete element in a building can be represented by the stepped diagram shown in Figure 3-3. It is assumed in this diagram that there is instantaneous load transfer (vertical lines) from any storey, such as the one between $(i + 1)$ and $(i + 2)$ levels to the vertical elements below the level $(i + 1)$. As a consequence, the Young's Modulus of concrete in these elements can be deemed to be constant at this instance. This instantaneous load transfer stage is followed by a “no

load transfer” stage (horizontal lines) until the next storey is constructed. In addition, the stress developed in the concrete elements below level (i + 2) due to the instantaneous dead load from floor above can be acquired as $0.5 f_c'$, where f_c' is the characteristic strength of concrete (Smith & Loull, 1991; Alexander, 2001). Consequently, these vertical elements are in the linear elastic region enabling the principle of superposition to be applied.

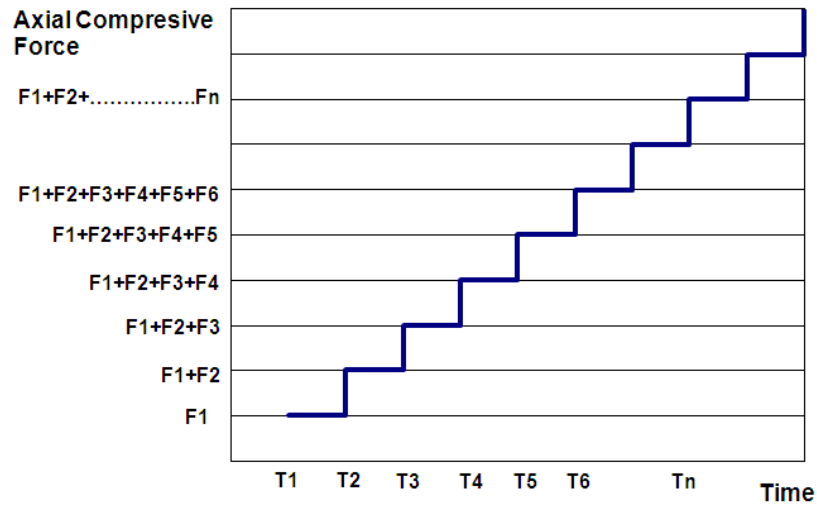


Figure 3-3: The load –time history of a typical concrete element

After the loads have been placed as described above (using sub models where necessary) in the finite element model of whole structure, time history analysis is used to activate the time dependence of these loads according to the construction sequence. As shown in Figure 3-4, Load 11, Load 12, etc are applied at nodes 11, 12 etc, (with the nodes located below the respective floor levels) according to the construction method.

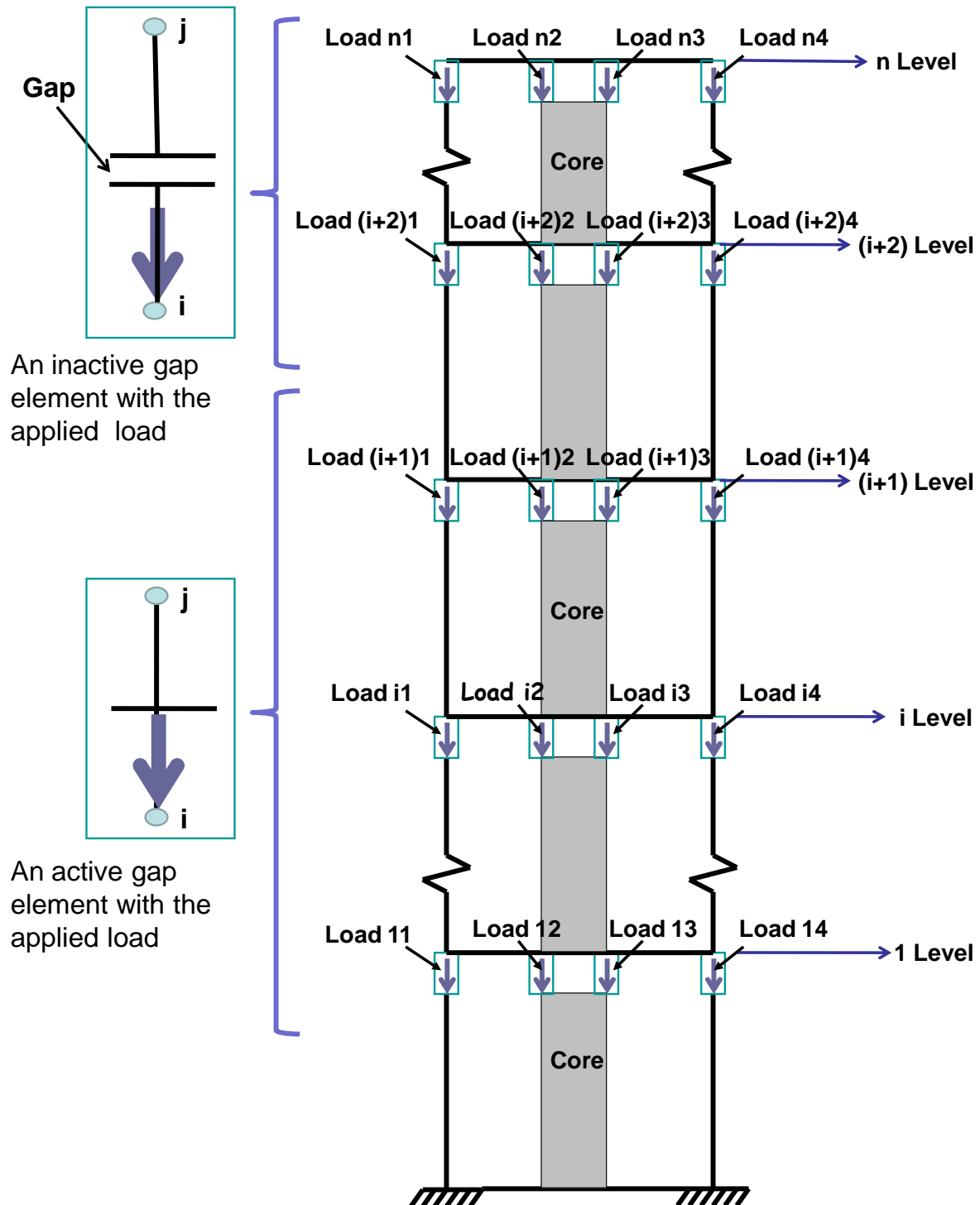


Figure 3-4: Load application to the structure

3.1.6 Analysis

The flow chart illustrated in Figure 3-5 represents the steps in the analysis. The initial condition of the structure is considered as unstressed and settlements due to the soil are neglected.

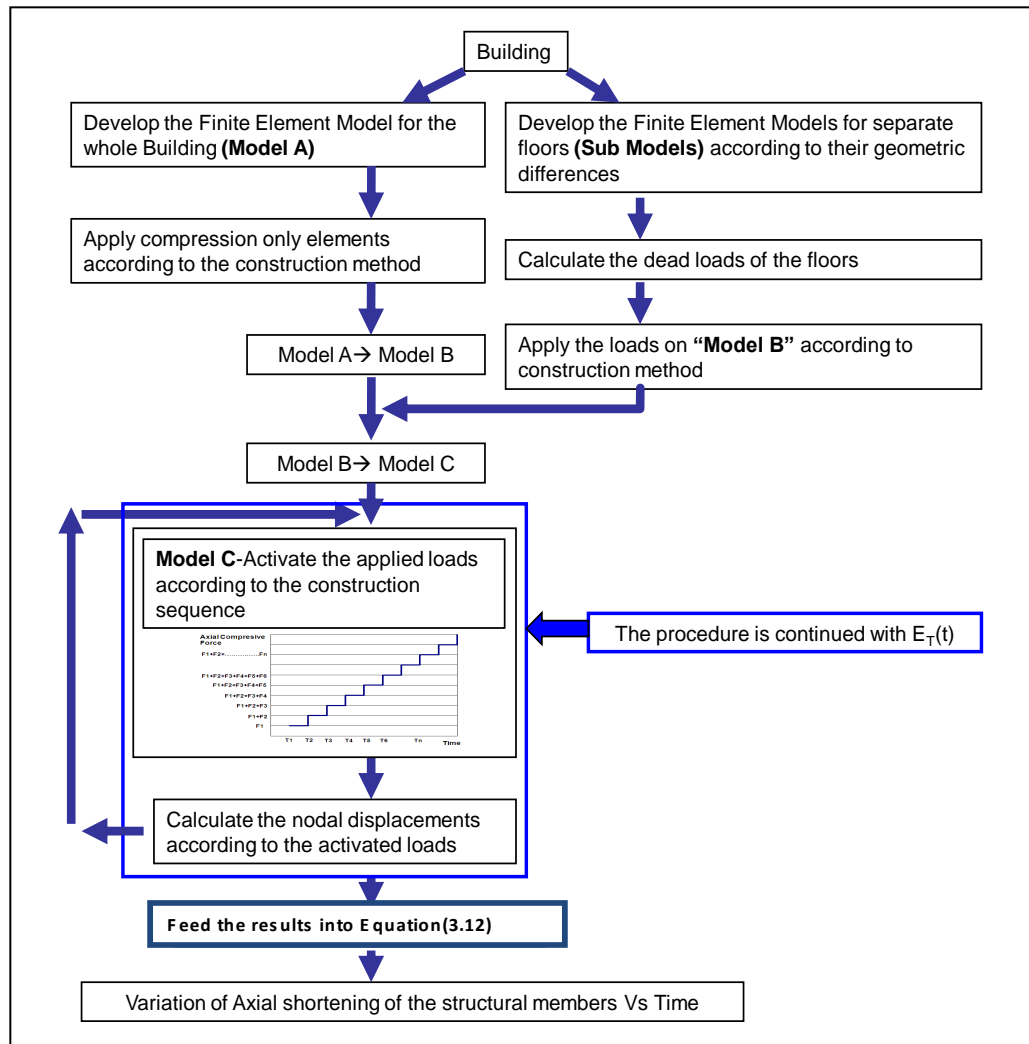


Figure 3-5: Flow chart of the analytical process

3.1.7 Calculation-Creep, Shrinkage and Elastic Deformation

The relative nodal displacements $\Delta U(t)$ at each time step can be obtained from the time history analysis discussed above. The total axial shortening of each element can then be obtained from the procedure developed below.

An equation representing the total strain and hence the axial shortening at any given time due to elastic, creep and shrinkage using relevant expressions in GL2000 method is developed in the following format to facilitate convenient computation (Gardner ,2004).

$$\delta_{\text{total}}(t, t_0) = \delta_{\text{Elastic}}(t, t_0) + \delta_{\text{Creep}}(t, t_0) + \delta_{\text{Shrinkage}}(t) \quad (3.7)$$

Where $\delta_{\text{total}}(t, t_0)$, $\delta_{\text{Elastic}}(t, t_0)$, $\delta_{\text{Creep}}(t, t_0)$ and $\delta_{\text{Shrinkage}}(t)$ are total, elastic, creep and shrinkage strains respectively for an element.

$$\delta_{\text{total}}(t, t_0) = \sigma \left[\frac{1}{E_{\text{cm}t_0}} + \frac{\phi_{28}}{E_{\text{cm}28}} \right] + \left(900K \left[\frac{30}{f_{\text{cm}28}} \right]^{1/2} \times 10^{-6} \right) \left(1 - 1.18h^* \right) \left[\frac{t - t_c}{t - t_c + 0.12(v/s)^2} \right]^{0.5} \quad (3.8)$$

Where

σ -the axially developed stress, $E_{\text{cm}t_0}$ - the modulus of elasticity at the time of loading t_0 , $E_{\text{cm}28}$ - the mean modulus of elasticity at 28 days, $E_{\text{cm}t_0}$, $E_{\text{cm}28}$ and ϕ_{28} - the creep coefficient which can be calculated using formulae presented in GL2000 method, using the relevant data pertaining to the problem being treated, K -the correction term for the effect of cement type which can be calculated using the table presented in GL2000 method, $f_{\text{cm}28}$ -the concrete mean compressive strength(in MPa) h -the humidity as a decimal, t -the age of concrete (days), t_c -the age drying commenced end of moist curing, (v/s) - the volume to surface area ratio (mm)

$$\sigma = \frac{E(t) \Delta U(t)}{L} \text{ where } \Delta U(t) \text{ is the difference in the nodal displacement}$$

(or the relative displacement) and can be obtained from the time history analysis, L -the length of the element. The above equation can be written as

$$\delta_{\text{total}}(t, t_0) = \left[\frac{\Delta U(t)}{L} + \frac{E(t)_T \Delta U(t)}{L} \frac{\phi_{28}}{E_{cm28}} \right] + \left(900K \left[\frac{30}{f_{cm28}} \right]^{1/2} \times 10^{-6} \right) \left(1 - 1.18h^4 \right) \left[\frac{t - t_c}{t - t_c + 0.12(v/s)^2} \right]^{0.5} \quad (3.9)$$

Using the principle of superposition, the total strain of a concrete element at time t_n subjected to the force history shown in Figure 3-3 can be written as

$$\delta_{\text{total}}(t, t_0)^0 = \sum_{i=1}^n \left[\frac{\Delta U(t_i)}{L} + \frac{E(t)_T \Delta U(t_i)}{L} \frac{\phi_{28}}{E_{cm28}} \right] + \left(900K \left[\frac{30}{f_{cm28}} \right]^{1/2} \times 10^{-6} \right) \left(1 - 1.18h^4 \right) \left[\frac{t - t_c}{t - t_c + 0.12(v/s)^2} \right]^{0.5} \quad (3.10)$$

The cumulative elastic, creep and shrinkage shortening of a single element can be written as

$$\Delta h(t_r) = L \delta_{\text{total}}(t, t_0)^0 \quad (3.11)$$

In order to obtain the vertical displacement (or axial shortening) at a particular level (n) relative to the foundation (base), all the elements below that level have to be considered. The cumulative elastic, creep and shrinkage shortening at a location on level (n) due to all elements below that level (n) can be obtained from the equation shown below as

$$H(t_r) = \sum_{j=1}^n \Delta h_j(t_r) \quad (3.12)$$

Equation 3.12 represents the axial shortening, $H(t_r)$ of the element at the time, t_n .

3.1.8 Comparison

The procedure developed and presented in this chapter and the method developed by (Fintel, Ghosh & Iyengar, 1987) are applied to a column subjected to load history to compare the axial shortening predictions. As this example treated a single column, interactive effects which are incorporated into the present research, are not treated. The properties of the column and other factors considered in the example are presented in Table 3-2.

Table 3-2: The properties used for the compassion study

Property	
Size	1.5 x1.5x 4m
Concrete strength	60MPa
Reinforcement content in relation to the cross section area	4%
Young's Modulus of the reinforcements	200GPa
Humidity	50%

Figures 3-6 and 3-7 show the variations of elastic and axial shortenings respectively. It can be seen from Figure 3-6 that the elastic shortenings compare very well. The axial shortenings in Figure 3-7 have some variations at larger values of time. This is because of the use of different material models to predict creep and shrinkage in these two approaches. As stated earlier, the method developed in this research is based on the widely accepted material models of GL2000 method, while Fintal's method is based on material models of the much older ACI code (ACI committee 209). However, both results display similar shapes and trends.

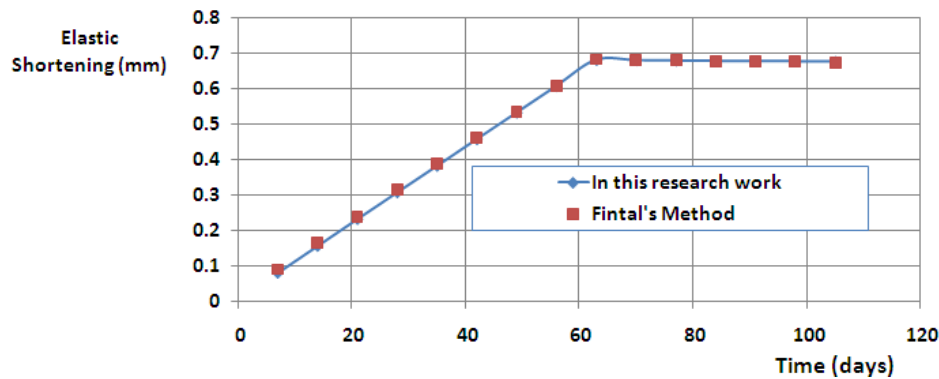


Figure 3-6: Variation of the elastic shortenings

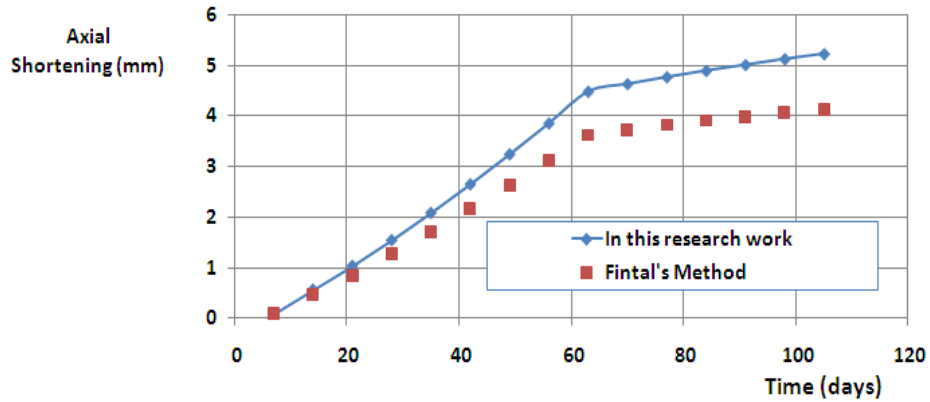


Figure 3-7: Variation of the Axial shortenings

3.1.9 Application

A high rise building with 64 storeys and storey height 4m as shown in Figures 3-8 and 3-9 is used to illustrate the methodology described above. This building has two outrigger and belt systems constructed with 60 MPa concrete and they spread over two floors; between 10 and 12 and between 42 and 44. The columns and the core are constructed with 80 MPa and 60 MPa concrete respectively, while the slabs are constructed with 40 MPa concrete. The reinforcement content of the structural elements is considered as 3% in relation to the cross-sectional area of the element. The sizes of the structural elements are presented in Tables 3-3 and 3-4. The analyses are conducted taking into account the dead and superimposed dead loads and it is assumed that these loads are constant over the time. The core is connected to the columns using sixteen shear walls at the locations where the outrigger systems are placed. The analysis is carried out after 4500 days from commencement of construction and taking into account the construction sequence of 7 days per floor. The axial shortening of columns X and Y and the core, (highlighted in Figure 3-8), and differential axial shortening between these members are determined and discussed. The columns X and Y were selected in order to study the influence of location and hence different tributary areas.

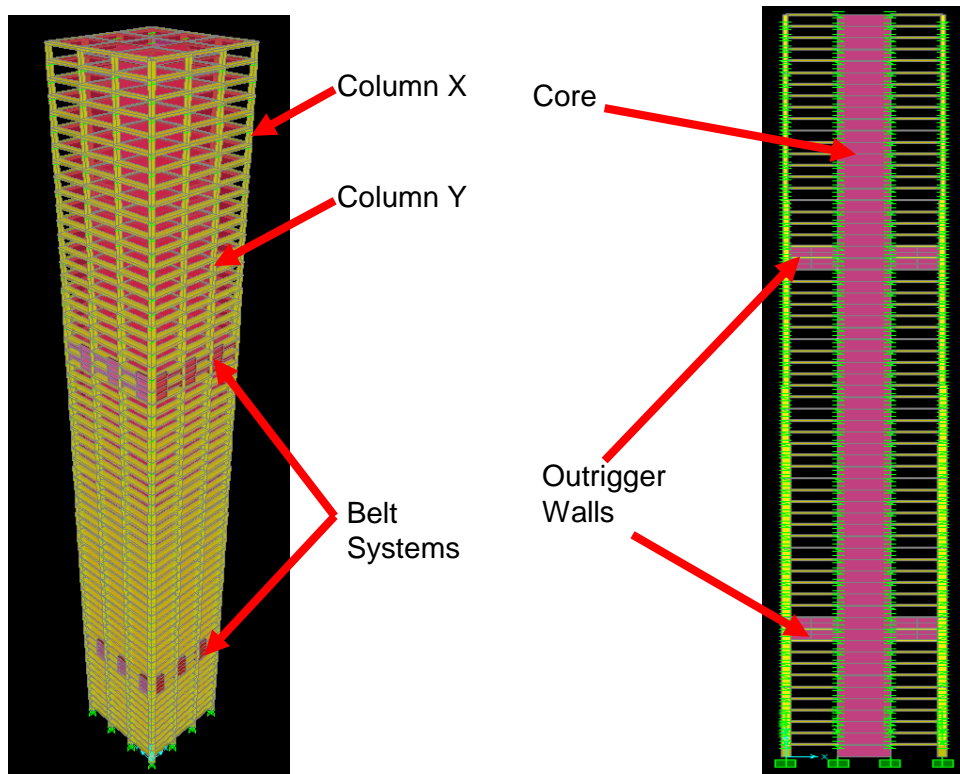


Figure 3-8: The isometric view (left) and the sectional end view (right) of the building

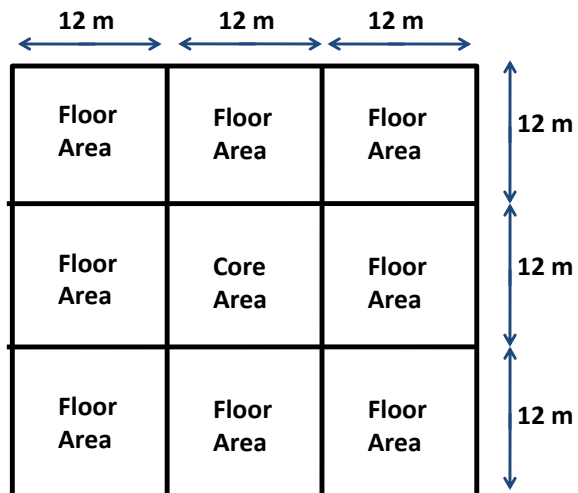


Figure 3-9: A typical plan view of the building

Table 3-3: Sizes of the columns and thicknesses of the core walls

Location(Floor Number)	Column Size(m)	Core Wall(m)
0-16	2.0 x 2.0	1.2
17-32	1.8 x 1.8	1.0
33-48	1.6 x 1.6	0.8
49-64	1.4 x 1.4	0.6

Table 3-4: Thicknesses of the shear walls in the outrigger and belt systems

Location	Size of the Wall (m)
Lower (floors between 10-12)	1.2
Upper(floors between 42-44)	0.8

3.1.10 Results and Discussion

A combination of compression only elements, time varying Young's Modulus of reinforced concrete and time history analysis is used to formulate the real staged construction procedure and to capture load migrations during and after the construction. Incorporating creep, shrinkage and elastic models of GL2000 method into the above staged construction procedure, axial shortenings of selected vertical elements at a given period in time (4500 days from commencement of construction in the present case) are calculated as described below. The axial shortenings of the selected structural elements are shown in Figure 3-10, while the elastic shortening of the elements are shown in Figure 3-11. The influence of creep and shrinkage on the axial shortening is obvious by comparing the results in these two Figures.

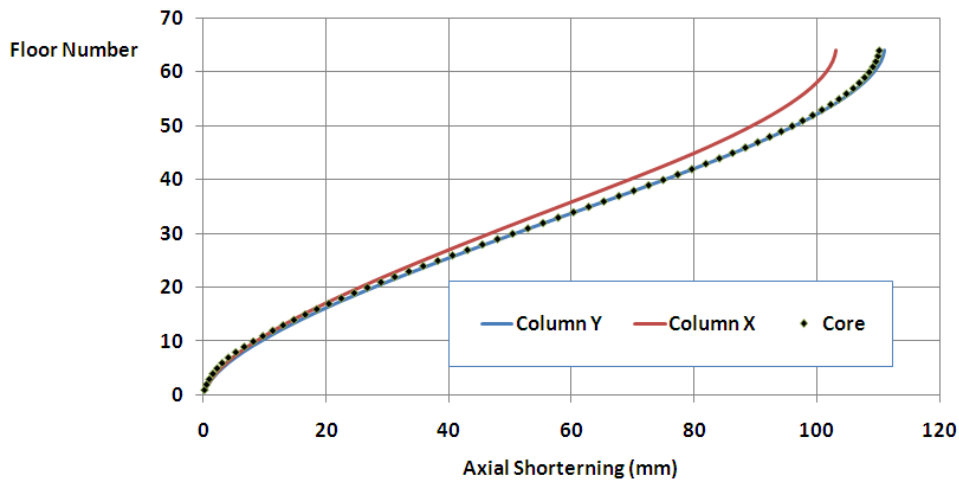


Figure 3-10: The axial shortening of the core, Column X and Column Y at 4500 days from commencement of construction

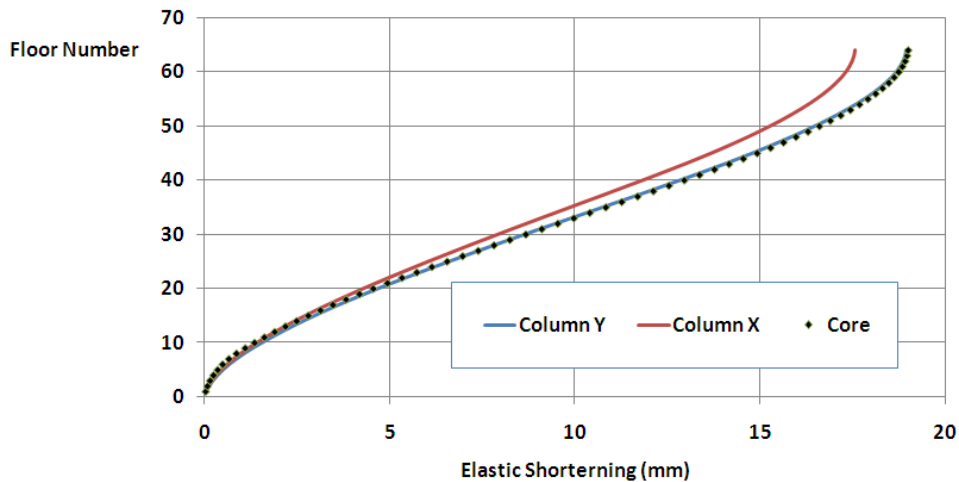


Figure 3-11: The elastic shortening of the core, Column X and Column Y at 4500 days from commencement of construction

The load migration during the analysis can be identified by examining the variation of elastic shortening of the elements since this is directly proportional to the forces acting on the elements. Figure 3-11 shows that the magnitude of the elastic shortening of the core is higher than that of Column X and Column Y due to a considerable amount of load transfer to the core through the outrigger and belt systems. This is a very important consideration as most of the existing axial shortening calculation procedures do not

capture this important time dependent load migration. Column and core axial stiffness as well as the shear and flexural stiffness of the outrigger system (all time dependent phenomena) play a significant role in this process. Furthermore, this load migration has a significant post construction impact on the axial shortening due to creep as evident from Figure 3-10 depicting axial shortenings of Columns X and Y and the core.

The differential axial shortening between Columns X and Y is shown in Figure 3-12, while that between these columns and the core are shown in Figures 3-13 and 3-14. It can be seen from these figures that there is considerable amount of differential axial shortening between Column X and Column Y due to the interaction between column axial stiffness and load tributary in relation to belt frame stiffness.

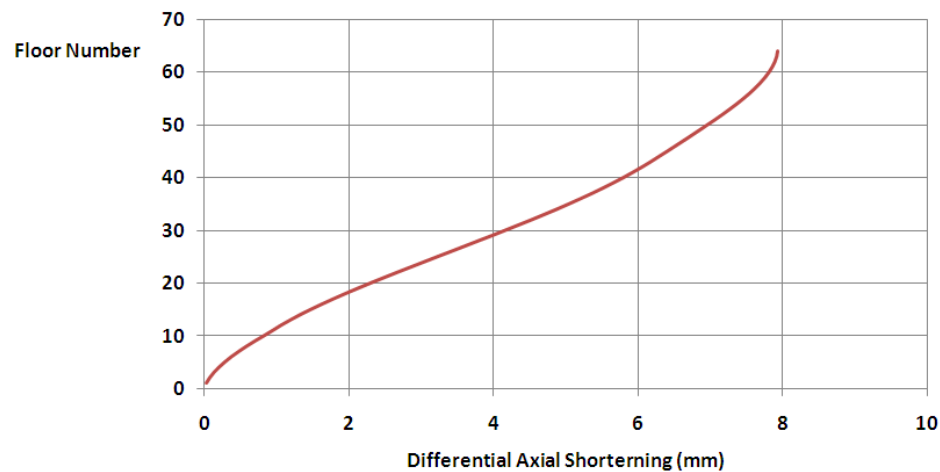


Figure 3-12: Differential axial shortening between Column X and Column Y at 4500 days from commencement of construction

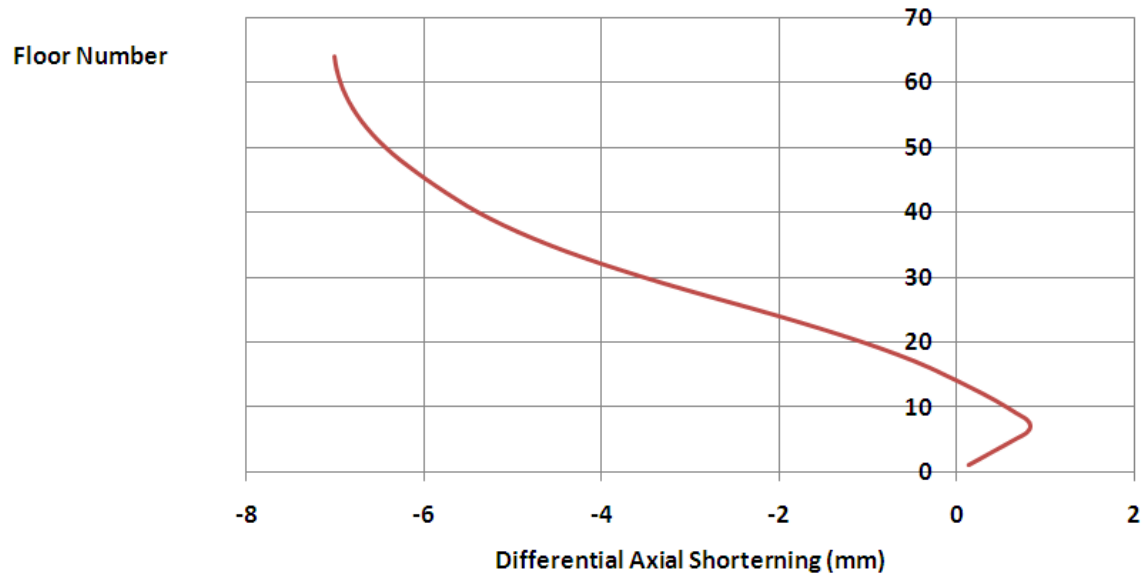


Figure 3-13: Differential axial shortening between the core and Column X at 4500 days from commencement of construction

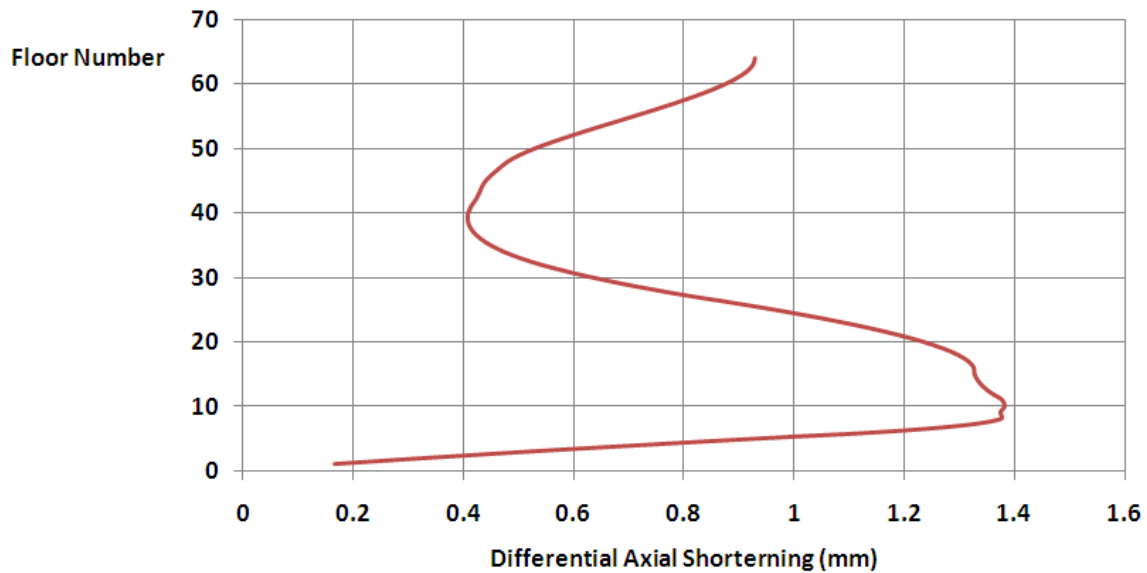


Figure 3-14: Differential axial shortening between the core and Column Y at 4500 days from commencement of construction

Figures 3-15 and 3-16 illustrate the absolute values (moduli) of the differential axial shortening between the core and the two columns. From these figures, it is interesting to observe the influences of the outrigger and belt systems on the differential axial

shortenings. Variation of the differential axial shortening between the core and the columns are different at where the belt and outrigger systems are located as the stiff elements in these systems significantly control the relative movements between the core and the columns. In addition, it is evident that the differential axial shortening (absolute values) of Column Y, (with respect to the core), is much less than that of Column X, at the locations of the outrigger-belt systems. This is due to the fact that Column Y and the core are directly connected with the shear walls which control the relative movements between them. Shear walls radiate from the central core to connect with some of the perimeter columns (at the locations of the outrigger-belt systems) and as a result those perimeter columns have relatively smaller differential axial shortenings (with respect to the core) at these locations.

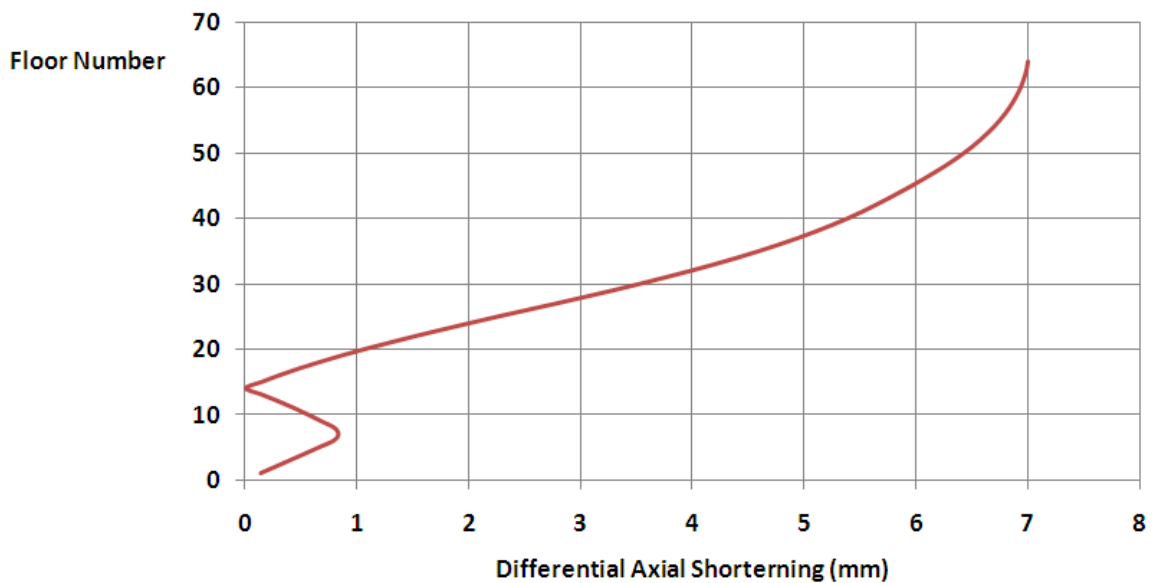


Figure 3-15: Absolute value of graph of Figure 3-11

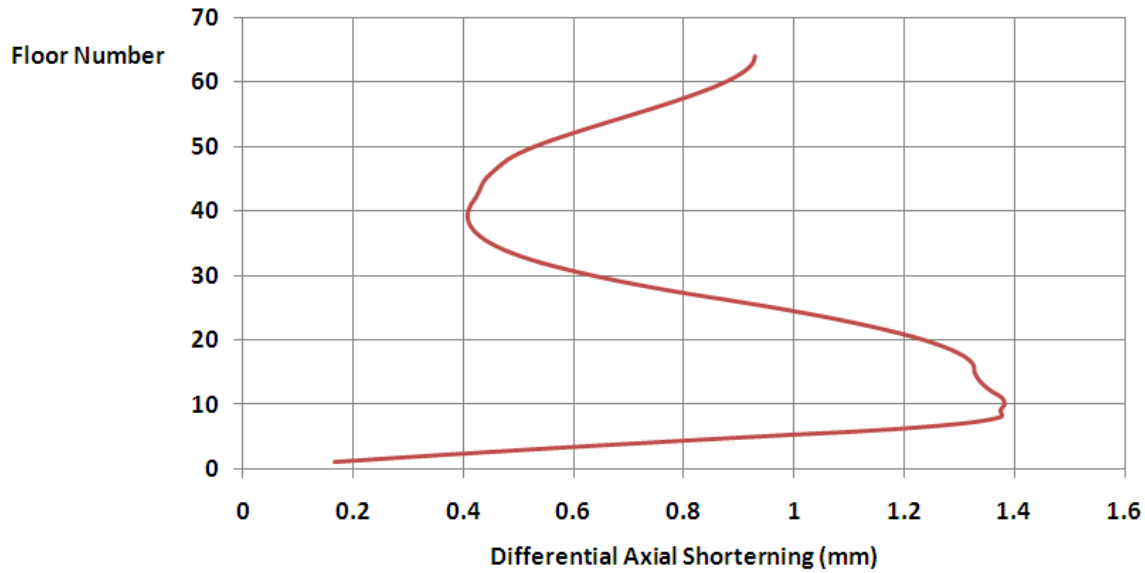


Figure 3-16: Absolute value graph of Figure 3-12

3.2 Conclusion

This chapter presents development of a numerical procedure used to predict the differential axial shortening of vertical members in a high rise concrete building. Finite element time history analysis together with compression only elements and time varying Young's Modulus of reinforced concrete are used to formulate the actual construction process and to capture load migrations during and after the construction. The effects of creep and shrinkage are then integrated in the procedure to calculate the axial shortenings of elements at any particular time. The procedure developed and illustrated in this section is for a 64 storey building. Results for selected elements are presented. The interaction of outrigger-belt frame systems with columns and cores and the resulting time dependent load migration is investigated. The influence of non linear time dependent parameters on the construction process and the impact on differential axial shortening is discussed. A rigid outrigger system has a mitigating impact on differential axial shortening between perimeter columns and the cores. The differential axial shortening between perimeter columns are influenced by the axial stiffness of the columns in proportion to load tributary with assistance from the belt frames.

The proposed procedure is general enough to be applicable to all concrete high rise buildings to predict differential axial shortening between vertical elements. This will enable appropriate action to be undertaken at the planning and design stages to mitigate the adverse effects. Two main strategies such as varying sizes (volume to surface ratio) and concrete strengths of structural elements can be implemented at design stage to control differential axial shortening between structural components due to the fact that these two strategies enable to control elastic, creep and shrinkage shortenings. Accurate quantification of differential axial shortening is necessary at design stage in order to implement such strategies accurately and successfully.

4 INFLUENCE OF AXIAL DEFORMATIONS OF COLUMNS ON THEIR VIBRATION CHARACTERISTICS

This chapter presents the development of a dynamic stiffness matrix of a structure used to examine the influence of axial force on the vibration characteristics. Additionally, a relationship between axial deformation as a result of axial force of elements and Modal Flexibility (MF) phenomenon comprising modal vectors and natural frequencies is presented through a vibration based parameter called Stiffness Index (SI). This parameter can be used identify the individual behaviour of the axially loaded elements.

4.1 Introduction

Axial loads in members influence significantly on the vibration characteristics of the structural framing system. Several researchers have investigated influence of axial loads on vibration characteristics of individual load bearing elements with different boundary conditions and established a relationship between the frequency and the axial load (Yesilce & Demirdag, 2008; Shaker 1975; Della & Shu, 2009). Their methods can be used to quantify axial force and or buckling load of an element using natural frequencies. However, as the natural frequencies are a property of the entire structure, these methods are limited to individual elements only.

The influence of axial force on vibration characteristics such as nodal vectors and natural frequencies of structural elements has been studied. Aeronautics and Space Administration) technical note, NASA TN-D-8109, Shaker (1975) reported findings of a numerical study in which equations are derived to capture effect of axial force on modal parameters of beam elements with different boundary conditions. This study concluded that while increasing axial compressive force of beam elements with different boundary conditions, the frequencies become low and mode shapes change considerably. This is because the axial force reduces the stiffness of the beam elements. It was also observed that the boundary conditions impact on mode shapes of the element. Bokaian, (1988a 1990b) studied the influence of axial force on the modal parameters using Timoshenko

beam theory and reported that the presence of a tensile axial load increases all of the bending natural frequencies whereas the compressive load decreases all of the bending natural frequencies. The magnitude of the compressive axial load can amplify up to the point where the first bending frequency reaches zero, and then the beam is subjected to buckling action. Walter & Kang (1996) investigated impact of axial force on vibration characteristics of a beam element and developed a stiffness equation incorporating influence of axial force. Findings show that the developed equation can be used to estimate buckling load of the beam element as well. Yesilce & Demirdag (2008) examined the exact solutions of the first five natural frequencies and corresponding mode shapes of a Timoshenko multi-span beam subjected to the axial force. Results highlighted that the frequency values obtained for this beam decrease when the axial compressive force increases demonstrating that the stiffness of the beam element is a function of the axial force. The stiffness change due to the axial force impacts on the modal vectors as well. Bahra & Greening (2008) have carried out a comprehensive study to examine axial load pattern updating using ambient vibration data from a physical frame. Equations developed by these authors were validated using ambient vibration data and confirmed that axial compressive force reduces the stiffness of the elements. NASA (National Della (2009) studied impact of axial compressive force on the modal parameters of natural frequencies and modal vectors of beam elements and concluded that a monotonic relation exists between the natural frequency and the axial compressive force. The axial compressive force impacts significantly on the first vibration mode shape of the beam and reduces with the mode number.

Based on the above, it is evident that when axial compressive forces increase, the natural frequencies and mode shapes of a framed structure change significantly. According to the best of author's knowledge, there is not existing methods have an ability to calculate axial deformation (elastic shortening) resulting from axial force of load bearing elements in a structural framing system using both natural frequencies and mode shapes capturing load migration among vertical load bearing elements due to horizontal stiff structural elements. This is another reason to motivate to develop a rigorous vibration based method to quantify axial deformations of elements of structural framing systems.

4.2 Dynamic Stiffness Matrix of a beam/column element

The following sets of equations are derived to present influence of axial force on modal vectors and natural frequencies of an element and thereby extend to the entire structural framing system. A beam element with a fixed end condition under free vibration with axial compressive force is shown in Figure 4-1.

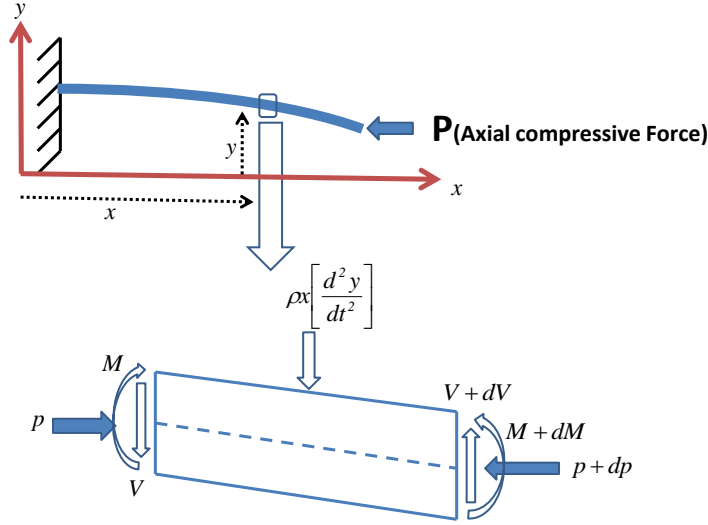


Figure 4-1: An element with axial compressive force under free vibration

In Figure 4-1, where P - axial compressive force, M -moment, V -Shear Force, ρ -mass per unit length, y, x -distances considered, t -time

Equations 4-1 and 4-2 can be formed as follows for moments and forces of the element respectively.

$$\frac{dM}{dx} + P \left[\frac{dy(x, t)}{dx} \right] + V = 0 \quad (4.1)$$

$$\frac{dV}{dx} - \rho \left[\frac{d^2 y(x, t)}{dt^2} \right] = 0 \quad (4.2)$$

For elementary beam theory

$$M = EI \left[\frac{d^2 y(x, t)}{dx^2} \right] \quad (4.3)$$

Where EI- flexural rigidity of the element

Equation (4.4) can be derived using Equations 4.1 to 4.3.

$$EI \left[\frac{d^4 y(x, t)}{dx^4} \right] + P \left[\frac{d^2 y(x, t)}{dx^2} \right] + \rho \left[\frac{d^2 y(x, t)}{dt^2} \right] = 0 \quad (4.4)$$

Equation (4.4) is a fourth order homogeneous differential equation. This equation can be solved using variable separation method and $y(x, t)$ can be written using two parameters such as $Z(x)$ and $w(t)$ to represent the influence of deflection and time respectively

$$y(x, t) = Z(x)w(t) \quad (4.5)$$

Equation (4.5) is substituted into Equation (4.4) in order to form Equation (4.6) as follows

$$\frac{EI \left[\frac{d^4 Z(x)}{dx^4} \right] + P \left[\frac{d^2 Z(x)}{dx^2} \right]}{Z(x)} = \frac{-\rho \left[\frac{d^2 w(t)}{dt^2} \right]}{w(t)} = \omega^2 \quad (4.6)$$

Where ω - natural frequency

From Equation (4.6), Equations (4.7) and (4.8) can be written as follows

$$\frac{EI \left[\frac{d^4 Z(x)}{dx^4} \right] + P \left[\frac{d^2 Z(x)}{dx^2} \right]}{Z(x)} = \omega^2 \quad (4.7)$$

$$\frac{-\rho \left[\frac{d^2 w(t)}{dt^2} \right]}{w(t)} = \omega^2 \quad (4.8)$$

Solution of Equation (4.7) is

$$z(x) = D_1 \sinh(\alpha_1 x) + D_2 \cosh(\alpha_1 x) + D_3 \sin(\alpha_2 x) + D_4 \cos(\alpha_2 x) \quad (4.9)$$

Where

$$\alpha_1^2 = \frac{-P + \sqrt{P^2 + 4EI\omega^2}}{2EI} \quad (4.10)$$

$$\alpha_2^2 = \frac{-P - \sqrt{P^2 + 4EI\omega^2}}{2EI} \quad (4.11)$$

D_1, D_2, D_3, D_4 - vector constants

Solution of Equation (4.8) is

$$w(t) = A_1 \sin(\beta_1 t) + A_2 \cos(\beta_2 t) \quad (4.12)$$

Where

$$\beta_1 = \sqrt{\frac{\omega^2}{\rho}} \quad (4.13)$$

$$\beta_2 = -\sqrt{\frac{\omega^2}{\rho}} \quad (4.14)$$

A_1, A_2 -constants determined from initial conditions of the vibration.

Displacement of the element under free vibration can be expressed as follows using Equations (4.9) and (4.12)

$$y(x, t) = \{D_1 \sinh(\alpha_1 x) + D_2 \cosh(\alpha_1 x) + D_3 \sin(\alpha_2 x) + D_4 \cos(\alpha_2 x)\}w(t) \quad (4.15)$$

Considering boundary conditions and the initial conditions of vibration, Equation (4.16) can be formed as follows

$$\{Y\} = [A]\{D\} \quad (4.16)$$

Where

$$\{Y\} = \begin{Bmatrix} y(0, t) \\ y'(0, t) \\ y(L, t) \\ y'(L, t) \end{Bmatrix} \quad (4.17)$$

$$[A] = \begin{bmatrix} 0 & 1 & 0 & 1 \\ \alpha_1 & 0 & \alpha_2 & 0 \\ \sinh(\alpha_1 L) & \cosh(\alpha_1 L) & \sin(\alpha_2 L) & \cos(\alpha_2 L) \\ \alpha_1 \cosh(\alpha_1 L) & \alpha_1 \sinh(\alpha_1 L) & \alpha_2 \cos(\alpha_2 L) & -\alpha_2 \sin(\alpha_2 L) \end{bmatrix} \quad (4.18)$$

$$\{D\} = \begin{Bmatrix} \overline{D_1} \\ \overline{D_2} \\ \overline{D_3} \\ \overline{D_4} \end{Bmatrix} \quad (4.19)$$

Where $\overline{D_1}, \overline{D_2}, \overline{D_3}, \overline{D_4}$ -vector constants

Equation (4.20) can be written considering moment, M and shear force, V

$$\{F\} = [B]\{D\} \quad (4.20)$$

Where

$$\{F\} = \begin{Bmatrix} M_{x=0} \\ V_{x=0} \\ M_{x=L} \\ V_{x=L} \end{Bmatrix} \quad (4.21)$$

$$[B] = \begin{bmatrix} 0 & EI\alpha_1^2 & 0 & -EI\alpha_2^2 \\ -(\rho\alpha_1 + EI\alpha_1^3) & 0 & -(\rho\alpha_2 - EI\alpha_2^3) & 0 \\ EI\alpha_1^2 \sinh(\alpha_1 L) & EI\alpha_1^2 \cosh(\alpha_1 L) & -EI\alpha_2^2 EI \sin(\alpha_2 L) & -EI\alpha_2^2 EI \cos(\alpha_2 L) \\ -(\rho\alpha_1 + EI\alpha_1^3) \cosh(\alpha_1 L) & -(\rho\alpha_1 + EI\alpha_1^3) \sinh(\alpha_1 L) & -(\rho\alpha_2 - EI\alpha_2^3) \cos(\alpha_2 L) & -(\rho\alpha_2 - EI\alpha_2^3) \sin(\alpha_2 L) \end{bmatrix} \quad (4.22)$$

$$\{D\} = \begin{Bmatrix} \overline{D_1} \\ \overline{D_2} \\ \overline{D_3} \\ \overline{D_4} \end{Bmatrix} \quad (4.23)$$

$$M = EI \left[\frac{d^2 y(x, t)}{dx^2} \right] \text{ and } V = - \left(\frac{dM}{dx} + P \left[\frac{dy(x, t)}{dx} \right] \right) \quad (4.24)$$

Equation (4.25) can be formed using Equations (4.16) and (4.20) as follows

$$\{F\} = [B][A]^{-1}\{Y\} \quad (4.25)$$

$$\{F\} = [k]_L \{Y\} \quad (4.26)$$

Where $[k]_L$ -dynamic stiffness matrix and subscript, L- local coordinate system

Modal parameters of the beam element can be estimated from Equation (4.27) presented below using the dynamic stiffness matrix $[K_{\text{Dyn}}]$

$$[k]_L \{\phi\} = 0 \quad (4.27)$$

Where

$\{\phi\}$ - modal vector of the element

The above stiffness matrix is defined based on the local coordinate system so that transformation matrix, $[T]$ can be employed (West & Geschwindner 2002) as follows to establish the stiffness matrix based on the global coordinate system.

$$[k]_G = [T]^T [k]_L [T] \quad (4.28)$$

Where subscript G refers the global coordinate system

The dynamic stiffness matrix of the structure, $[\bar{K}]$, incorporating the influence of axial loads can then be formed by assembling stiffness matrices of the elements considering compatibility of the nodes. With the use of the dynamic stiffness matrix $[\bar{K}]$, the equation of free vibration of a structure with the influence of the axial forces in elements can be represented as

$$[\bar{K}]\{\phi\} = \{0\} \quad (4.29)$$

Where Φ - modal vector

It is clear from Equation (4.28) that there is an influence of the axial compressive force on the modal parameters of the entire structural framing system. However, it is not convenient to solve Equation (4.28) to examine the modal parameters with the influence of the axial forces of a complex structural framing system with shear walls. Therefore, Finite Element (FE) software is employed for this research. The Finite element package, ANSYS (ANSYS Inc., 2007) is modified considering the theory presented above to capture effects of the applied axial compressive loads and incorporated into the modal analysis. Using this modified FE program, a FE model was developed for an element used to study the effect of axial force from previous publications (Banerjee, 2000 ; Banerjee & Williams, 1994; Friberg, 1985) to study the accuracy of the program. Analysis results were then compared with the previous publications and found a satisfactory agreement confirming the accuracy of the modified program. The first example presented in the next section illustrates the validation.

Modal Flexibility (MF) for an element (element x) without the axial load (unloaded case) can be written as (using Equation 2.2 in Chapter 2)

$$F_{XU} = \left[\sum_{r=1}^n \frac{1}{\omega_r^2} \phi_{xr} \phi_{xr}^T \right]_U \quad (4.30)$$

Where subscript U denotes the unloaded case

The stiffness matrix of an element changes due to the influence of the axial force and consequently the modal parameters and MF of such an element change significantly. Modal Flexibility (MF) for element x with the axial load (loaded case) can be written as

$$F_{XL} = \left[\sum_{r=1}^n \frac{1}{\omega_r^2} \phi_{xr} \phi_{xr}^T \right]_L \quad (4.31)$$

Where subscript L denoted the loaded case

In order to amplify the effects of these modal flexibility changes, reciprocals of the two MFs for unload and loaded cases are considered as shown below:

$$\frac{1}{F_{XU}} = \frac{1}{\left[\sum_{r=1}^n \frac{1}{\omega_r^2} \phi_{xr} \phi_{xr}^T \right]_U} \quad (4.32)$$

$$\frac{1}{F_{XL}} = \frac{1}{\left[\sum_{r=1}^n \frac{1}{\omega_r^2} \phi_{xr} \phi_{xr}^T \right]_L} \quad (4.33)$$

MF is a function of the stiffness matrix which changes with the axial force. In order to capture the influence of the axial force on the MF or the vibration characteristics, the parameter, called Stiffness Index (SI) is introduced through Equation (4.34). This parameter is directly proportional to the stiffness reduction which occurs due to the axial load.

$$SI = \frac{1}{F_{xu}} - \frac{1}{F_{xl}} \quad (4.34)$$

4.3 Validation of the modified FE program and study the capabilities of Stiffness Index (SI)-for column elements

Four numerical examples are presented in this section. The first example is for validating the modified FE program used for the other examples which are used to illustrate the capability of the proposed vibration based parameter, Stiffness Index (SI) of elements in a multi storey structural framing systems such as capturing influences of the load migration, different tributary areas.

4.3.1 Validation of the modified FE program-for column elements

Banerjee (2000); Banerjee & Williams (1994) and Friberg, (1985) examined an axially loaded beam with cantilever end condition using different approaches. Results from all approaches agreed well confirming their accuracy. The example used by these researchers was selected to study the accuracy of the modified FE program in this research. Figure 4-2 shows a cross section of a beam element while Table 4-1 presents the material properties and other data used in the vibration analysis. More information on the selected element can be found in references (Banerjee, 2000 ; Banerjee & Williams, 1994; Friberg, 1985).

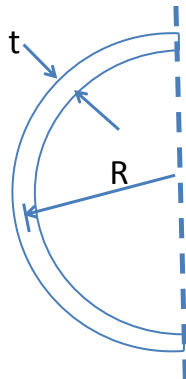


Figure 4-2: Cross section of the beam structure

Table 4-1: Material properties and other data used in the vibration analysis

Beam Parameter	Numerical Value
R(mm)	24.5
t(mm)	4
L(mm)	820
m(Kg/m)	0.835
E(GPa)	68.9
G(GPa)	26.5

A finite element model of this element was developed using the modified FE program and was first subjected to an axial compressive force of 1790N and then to an axial tensile force of the same magnitude. The axial load was applied as a pressure load along the circumference of this beam with a semi-circular cross-section, while maintaining fixed and free boundary conditions at the 2 ends. These loads were used in the previous publications (Banerjee, 2000 ; Banerjee & Williams, 1994; Friberg, 1985)). The natural frequencies of first three modes and the corresponding mode shapes with and without axial loads are extracted from the analysis results and compared with results from the previous publications. Tables 4-2 to 4-4 show comparison of the results for the natural frequencies of the first three modes for three cases,

Table 4-2: Comparison of natural frequencies without axial load

	Natural Frequency(rad/s)		
	Axial force=0		
Frequency Number	Pervious Publications	Modal Analysis	Difference (%)
1	391.70	390.40	0.33
2	816.00	815.00	0.12
3	1629.00	1625.00	0.25

Table 4-3: comparison of natural frequencies with compressive axial load

	Natural Frequency(rad/s)		
	Axial force=1790N(compression)		
Frequency Number	Pervious Publications	This research	Difference (%)
1	405.80	404.00	0.44
2	826.70	826.00	0.08
3	1649.00	1650.00	0.06

Table 4-4: comparison of natural frequencies with tensile axial load

	Natural Frequency(rad/s)		
	Axial force=-1790N(tension)		
Frequency Number	Pervious Publications	This research	Difference (%)
1	376.80	377.00	-0.05
2	805.10	804.00	0.14
3	1609.00	1608.00	0.06

It is evident from Tables 4-2 to 4-4 that variations between the present results and those from the previous publications are less than 1%. In addition, the corresponding mode shapes obtained from the present analysis, where the first mode is bending and the next two modes are mostly torsional, compare well with the previous publications highlighting the accuracy of the modified FE program.

4.3.2 Study the Capability of Stiffness Index (SI) applied to column elements

4.3.2.1 Impact of boundary conditions on SI

A column, 0.5 x 0.5 x 4 m is selected to demonstrate an ability of Stiffness Index (SI) defined in the previous section. The material properties of the column are presented in Table 4-5. These properties were selected to be representative columns with high

strengths. 10 axial compressive loading cases with loads ranging from 1, 2, 3 up to 10 MN are applied to the column to deform maintaining it in the linear elastic region. Effects of the boundary conditions were studied by considering Cases A and B shown in Figure 4-3. The first three frequencies of vibration and the associated modes were obtained for both cases. These boundary conditions depict the differences in allowing or restraining the in-plane and out of plane bending rotations at the top of the columns.

Table 4-5: material properties of the column

Material Property	Numerical Value
Density/(kNm^{-3})	2300
Poisson Ratio	0.2
Young's Modulus /(GPa)	30

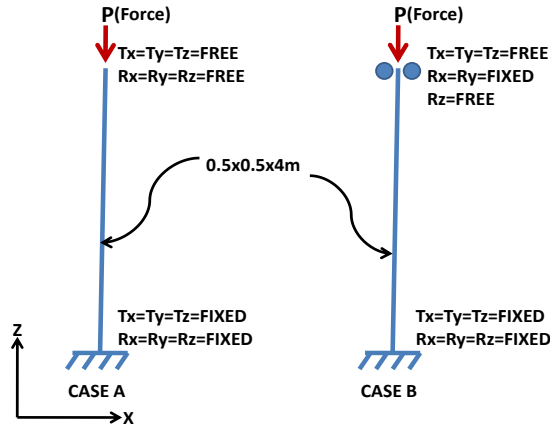


Figure 4-3: the columns with two different boundary conditions

The first three free vibration modes and corresponding natural frequencies are used for calculating SI. The modes indicate that the first and second modes are bending while the third mode is a combination of bending and torsional. Percentages of the changes in the frequencies for each mode due to the axial compressive force are depicted in Figure 4-4. It is interesting to note that this change is largest for the first mode and reduces with the mode number. This highlights that the stiffness matrix change, indicated by the change in the defined parameter SI, under axial force can be essentially captured by using the

first mode. This observation was also made in a previous study conducted by Della & Shu (2009).

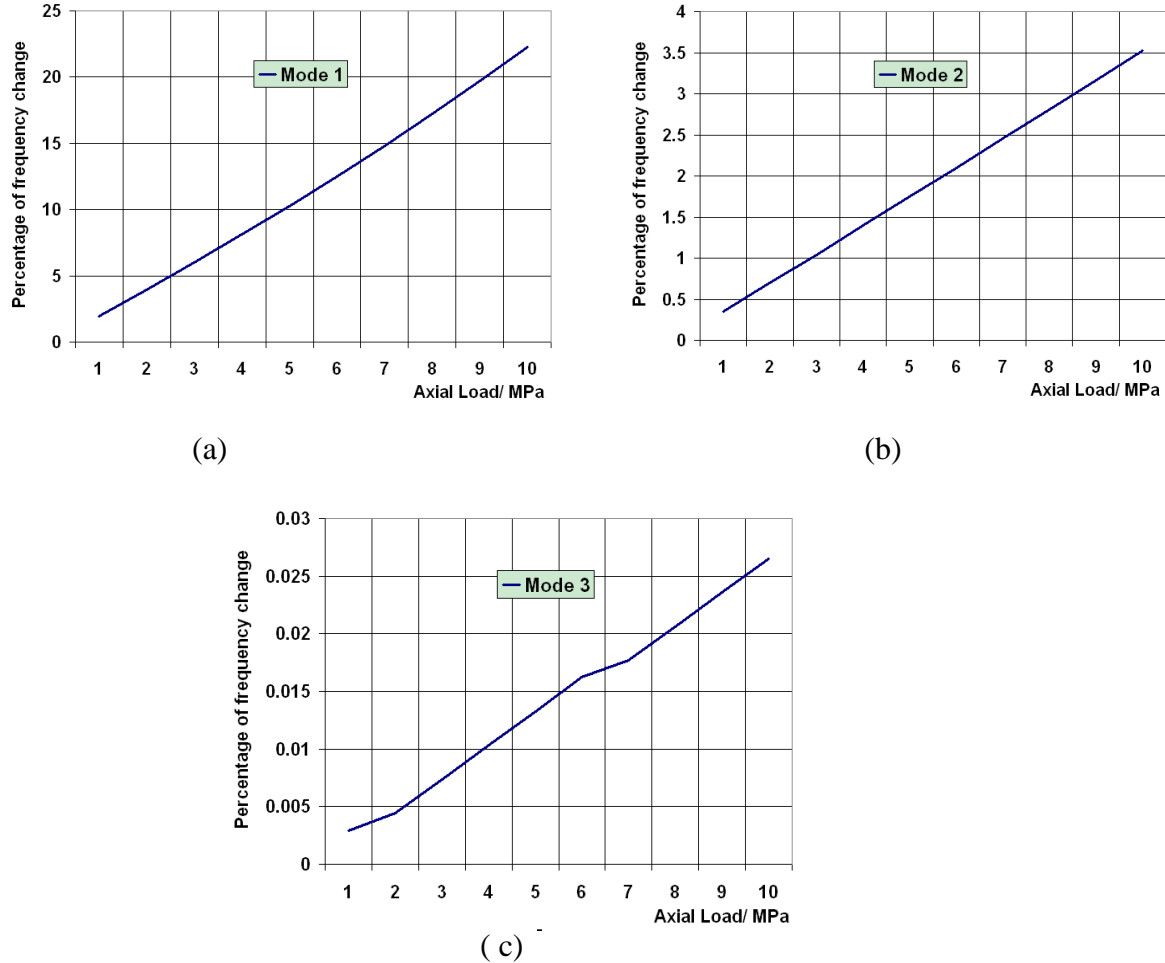


Figure 4-4: Percentage of frequency change (a)-first mode, (b)-second mode and (c)- third mode

For each applied axial force, the modal parameters (natural frequencies and modal vectors) were extracted from the modified FE program and Equation (4.33) was used to calculate the Stiffness Index (SI). The corresponding axial deformation is obtained using static analysis. Figure 4-5 shows the variations of SI with the axial deformation for three different cases – using the (i) first mode, (ii) first two modes and (iii) first three modes.

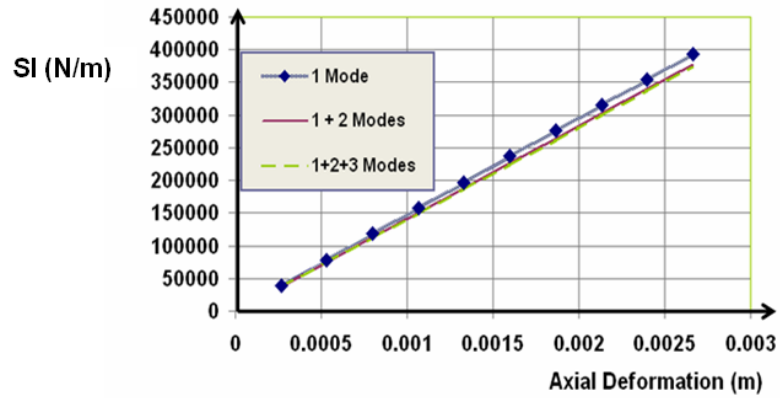


Figure 4-5: variation of stiffness index, SI with the axial deformation for case A

It is clearly revealed from Figure 4-5 that SI does not deviate significantly when increasing number of modes incorporated into the calculation. This confirms that impact of number of modes on Case A is very low.

For Case B, the frequency changes with axial loads are similar to those in Case A with the largest changes occurring for first mode. Though the first two modes are bending while the third mode is a combination of bending and torsional, as also observed for Case A, the shapes of the modes for Case B are different from those of Case A due to the impact of the different boundary conditions.. It was also observed that there was a significant change in shape of first mode due to the influence of the axial load as also observed by Della & Shu (2009).

Figure 4-6 shows variation of Stiffness Index (SI) with the axial deformation, where the impact of number of modes can be seen. In case B, the boundary conditions influence the variation of the mode shapes and hence SI. Consequently, the graphs (see Figure 4-6) deviate considerably when the number of modes used in the calculation is increased. This feature is different to that observed for Case B and highlights the effect of boundary conditions in this study.

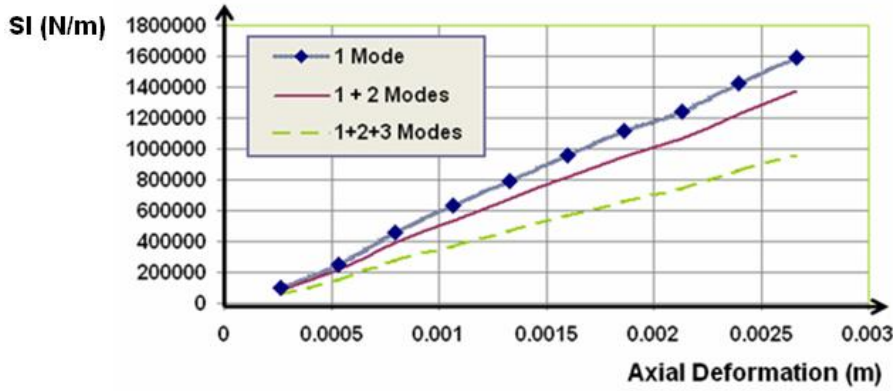


Figure 4-6: variation of stiffness index, SI with the axial deformation for case B

4.3.2.2 Capture the behaviour of column elements in a structural framing system

As the third example, a two storey 2D structural framing system shown in Figure 4-7 is considered with different axial compressive loads acting on the columns. The column sizes and the material properties are selected to be the same to maintain the equal stiffness before applying the axial loads. Consequently, impact of the differential axial forces on Stiffness Index (SI) can be investigated in this example. Another reason for selecting this example is that it can be used to examine the capabilities of the proposed SI when introduced into elements of a structural framing system. Different axial compressive loads such as P1,P2,P3 and P4 are applied on the columns (as shown in Figure 4-7) as different load cases defined in Table 4-6. This was conducted to illustrate the case in which columns at different levels subjected to different loads from different tributary areas, especially in system with geometrically complex floor plates and framing systems.

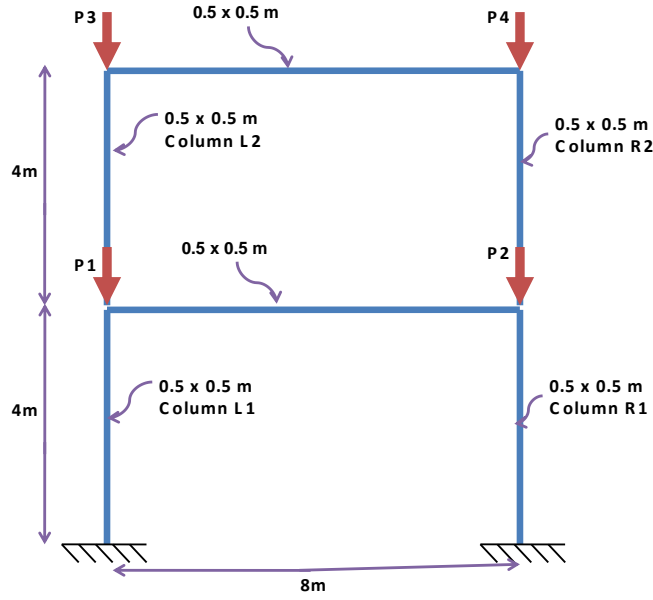


Figure 4-7: two storey structural framing system

Table 4-6: the applied axial loads for the columns

Loads(MN)	Case				
	1	2	3	4	5
P1	10	15	20	25	30
P2	20	30	40	50	60
P3	5	10	15	20	25
P4	10	20	30	40	50

Figure 4-8 shows percentage of frequency change of the first two modes as a result of the axial force. This figure demonstrates that the percentage frequency change for the first mode is higher than that of the other. It was also examined that the frequency changes for the higher modes were less pronounced and hence it could be neglected, as was also observed by Della & Shu (2009). Consequently, modal vectors and natural frequencies corresponding to first two modes are taken into account to calculate Stiffness Index, (SI).

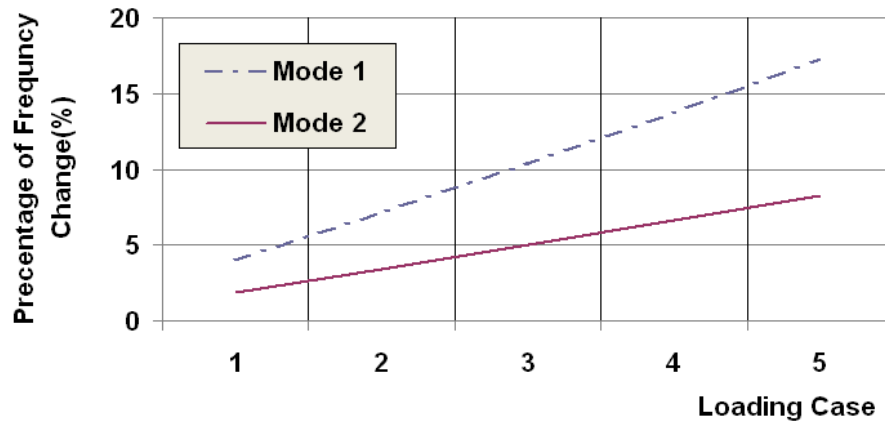
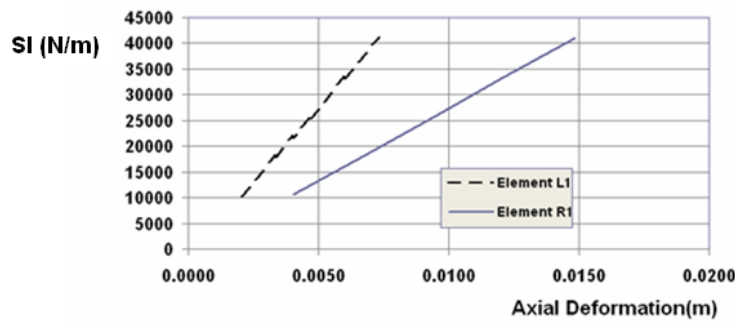
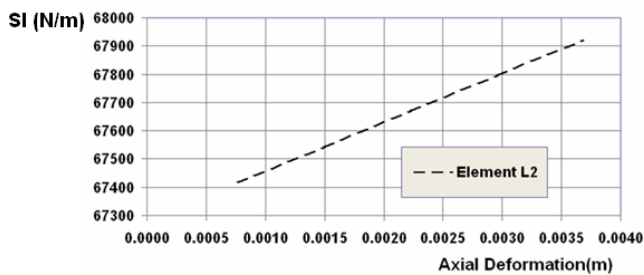


Figure 4-8: Percentage of frequency change of the first two modes

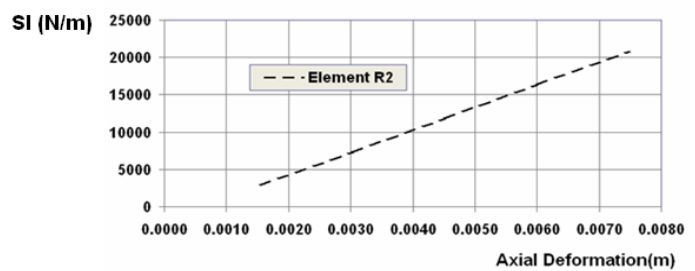
Figures 4-9(a), 4-9(b) and 4-9(c) depict Stiffness Indexes, SI(s) of columns L1, R1, column L2 and column R2 respectively. Variations of SI(s) of columns R2 and L2 are separately plotted due to the different ranges of the variables required along the axes.



(a)



(b)



(c)

Figure 4-9: variation of SI of the elements (a)- columns L1, R1, (b)- column L2 and (c)- column R2

It is evident from Figure 4-9 that even though the selected columns in the structure have equal stiffness before applying the axial loads, SI of such columns deviate significantly from each other after applying the axial loads. This highlights that mode shapes incorporated in the Modal Flexibility (MF) parameter enables to capture the influence of the axial loads on the columns even though the natural frequencies are a property of the entire structural framing system. Additionally, stiffness change is inversely proportional to the axial deformation so that it is revealed from Figures 4-9 (a) and 4-9 (b) that gradient of variation of SI of column R1 subjected to more axial load is low in comparison to column L1 while gradient of variation of SI of column R2 carrying more loads is less compared to that of column L2. Based on the outcomes above, it can be concluded that SI is a good indicator for identifying the variations of axial deformations resulting from the different axial forces applied to element in the same floor level in a structural framing system.

4.3.2.3 Capture the effects of the load migration and different tributary areas

A 10 storey structural framing system with shear walls located at certain places is used to examine the impact of load migration due to the shear walls on the Stiffness Index (SI). The material properties of all elements are selected to be same as those in the pervious examples. Sizes of columns and beams are 1x1m and 0.5 x0.5 m respectively while 0.5m thickness shear walls are employed in locations as shown in Figure 4-10. Because of these shear walls, load migration occurs among the columns as in structural framing system with belt and outrigger systems as discussed in Chapter 3. This example will enable us to study the capability of SI to capture the load migration. Floor height of the selected structure is 4m. Columns in this structure are across the total height of the building, while horizontal shear walls connect the columns at levels 4 and 8. Different axial compressive loads are applied on columns as tabulated in Table 4-7. These loads facilitate to simulate vertical elements of the structure subjected to different loads from different tributary areas. Using the modified FE program, the analysis is performed with increasing all the applied loads by 0.25MN in order to develop several loading cases

incorporating effects of axial deformations. The first two modes of vibration (both of which are bending modes) and the corresponding frequencies are extracted from analysis to calculate $SI(s)$ of columns as higher modes do not impact significantly on SI as indicated in the previous examples. Stiffness Indexes, $SI(s)$ of columns C1, C2, C3 and C4 shown in Figure 4-10 at the certain floor levels are selected to examine their behavior. $SI(s)$ of columns in floor levels 2, 6 and 10 represent their behavior at lower, middle and upper levels respectively, while $SI(s)$ of columns in levels 4 and 8 represent the behavior under load migration occurring due to shear walls located in these levels.

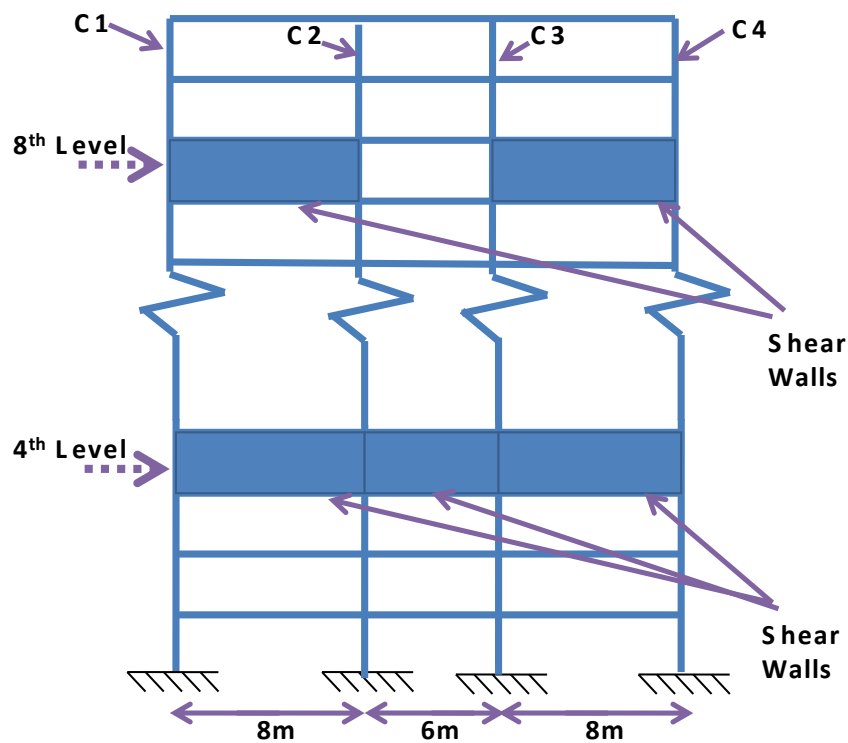
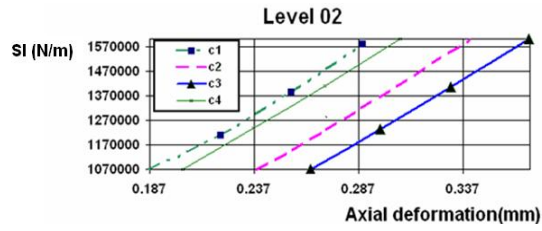


Figure 4-10: Structural framing system with shear walls.

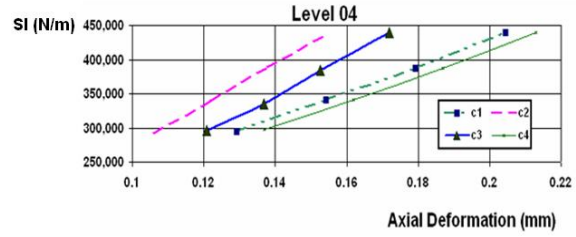
Table 4-7: the applied axial compressive loads on columns initially

Floor Number	Force/ MN			
	Column			
	C1	C2	C3	C4
1	1	1.5	2	1
2	1	1.5	2	1
3	2	3	3.5	2
4	1	1.5	2	1
5	1	1.5	2	1
6	1	1.5	2	1
7	2	2.5	3	2
8	1	1.5	2	1
9	1	1.5	2	1
10	1	1.5	2	1

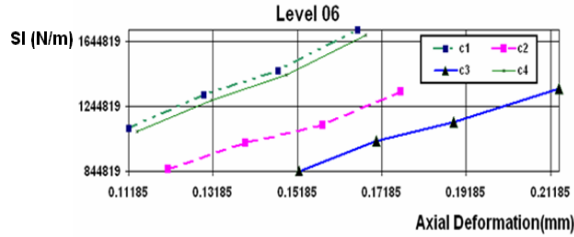
Using the modified FEM programme, separate modal analysis are performed incorporating effect of the applied axial compressive loads for each loading case. Stiffness Indexes, SI(s)) are calculated incorporating natural frequencies and the corresponding modal vectors of the first two modes for each column at the selected floor levels, while static analysis is used to calculate the axial deformations of the columns. Figure 4-11 shows variation of SI(s) of the columns with their axial deformations at the selected floor levels.



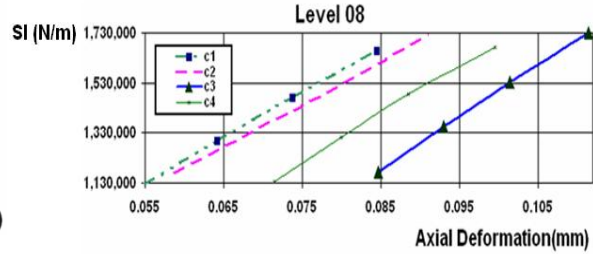
(a)



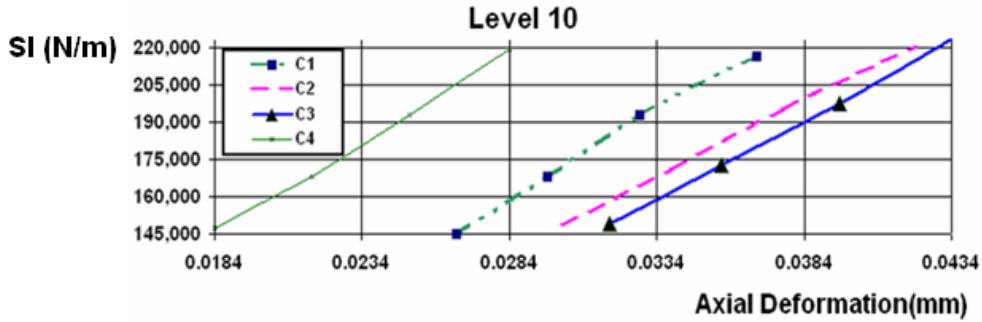
(b)



(c)



(d)



(e)

Figure 4-11: variation of SI(s) of the columns, (a)-2nd level, (b)- 4th level, (c)-6th level, (d)-8th level and (e)-10th level

Figures 4-11 (a),(c) and (e) depict that SI of column C3 is lower than that of the other columns while SI of column C2 is low compared to columns C1 and C4. This is because column C3 is subjected to more axial compressive load than others and column C2 is subjected to higher axial load than that of columns C1 and C4 (see Table 4-7). However, SI of column C1 is higher compared to column C4 at 2nd and 6th levels and SI of column C4 is higher than that of column C1 at 10th level, though these two columns are subjected to equal axial loads (see Table 4-7). This is because load migration due to the

shear walls impacts on axial deformations of columns C1 and C4. In 4th level, axial load of column C3 migrates to columns C4 and C3 via the shear walls while axial load of column C2 migrates to column C1 only via the shear wall. Load migration from columns C3 to C4 is much higher compared to that of other two columns since axial load of column C3 is subjected to high axial load. Column C4 therefore acquires more loads than column C1. Consequently, Figure 4-11(b) depicts that variation of SI of column C4 is low compared to the other columns and variation of SI of column C1 is lower than that of columns C2 and C3. This Figure also shows that SI of column C3 is lower in comparison to column C2 due to the fact that axial load and hence axial deformation of column C3 is more pronounced than the others. According to shear wall configuration in 8th level (see Figure 4-10), axial load of column C3 migrates to column C4 while axial load of column C2 migrates to column C1 only. However, axial load of column C3 is higher than other columns so that load migration from columns C3 to C4 is higher than other columns. Axial deformation of column C4 is thereby more pronounced than the other columns and hence SI of that column is low in comparison to column C3 as shown in Figure 4-11(d). Figure 4-11(d) also shows that variations of SI(s) of columns C1 and C2 are similar to columns C3 and C4 because of the load migrations. Nevertheless, the difference between columns C1 and C2 is low in comparison to the other two columns due to the fact that column C2 is subjected to low axial load than column C3 and hence load migration from columns C2 to C1 is low.

Figures 4-5, 4-6, 4-9 and 4-11 indicate a relationship between SI and axial deformation exists and linear positive gradients of SI with axial deformation for the different structural systems concluding that the elements deform axially in the linear elastic range and hence the stiffness reduces linearly.

4.4 Conclusion

Several methods have been developed to study the axial effects of beam elements comprising different boundary conditions based on their natural frequencies. These methods are unable to capture the effects of the elements in a structural framing system

as natural frequencies are a property of a whole structural framing system. This gap in the present knowledge is reorganized.

Chapter 4 presents the development of dynamic stiffness matrixes of a beam element and a structural framing system to study the influence of the axial affects on the vibration characteristics. This chapter introduces a vibration based parameter called Stiffness Index (SI) which can be used to identify the individual axial effects of the elements in a structural framing system capturing influences of different tributary areas, the boundary conditions and the load migration.

5 INFLUENCE OF AXIAL DEFORMATIONS ON VIBRATION CHARACTERISTICS OF CORE SHEAR WALLS

This chapter presents the development of a dynamic stiffness matrix of a building structural framing system with core shear walls and this development is implemented to examine the influence of the axial forces on the vibration characteristics. Capabilities of the vibration based parameter, Stiffness Index (SI) defined in Chapter 4 are further investigated through illustrative examples.

5.1 Introduction

Many researchers have investigated the influence of axial load and hence deformation of a plate element on its natural frequency with different boundary conditions. Subrahmanyam (1985) developed expressions for the buckling of annular plates and established convergence. Outcome of this study highlighted that these expressions can be applied to the buckling of any polygonal plate. Tameroglu (1986) presented a method to determine general solutions for plates using the variable separation method. This method incorporates additional terms to treat different types of rectangular plate problems using Levy's method. Kapania & Yang (1986) examined the buckling, post buckling and non linear vibration of imperfect laminated plates. Chen & Liu (1990) developed a numerical method to study the static deflection and natural frequencies of plates using a Levy-type solution. The developed numerical method was compared with previously published works and achieved a close agreement highlighting the accuracy of the development. Abrate (1993) used the Levy's method to find exact solutions for static deflections, free vibration and buckling loads for rectangular plates with two opposite edges simply supported. Chang, Hu. & Jane (1998) studied the vibration analysis of a delaminated composite plate subjected to in-plane load. Results highlighted that fundamental natural frequency decreases as the applied axial compressive force increases and vice versa. Zhou (2002) studied a rectangular plate element incorporating stiffening effect of dead load on dynamic behavior of plates using Finite Element (FE) method. Outcome concluded that the stiffness of plate increases when the effect of dead

load is included into the calculation and that the effect is more significant for plate with a smaller stiffness. Xiang, Zhao & Wei (2002) investigated the vibration behavior of multi span rectangular plates using Levy's method which can be applied to rectangular plates with two parallel simply supported edges. The impact of the internal line supports on the vibration behavior of the plates was also studied.

Based on the above, it is clear that the previous developments are limited to individual plate elements with their natural frequencies. Consequently, these developments can't apply to investigate the axial effects/ axial deformations of plate elements in a structural framing system as experienced from beam/column elements in Chapter 4.

Shear wall elements of cores and column elements in high rise buildings are subjected to huge loads during construction and service stages. Axial deformations of these elements are thereby more pronounced and their effects increase with height and structural geometric complexity. Chapter 4 demonstrates the effect of axial deformations of column elements on the vibration characteristics. Results highlighted that axial deformations of the elements impact significantly on the natural frequencies and modal vectors of first few modes of structural framing system and such an impact reduces with the modal number. This chapter also concluded that axial compressive forces of column elements reduce their stiffness and the frequency of the entire structural framing system. Swaddiwudhipong, Sidji, & Lee (2002); Swaddiwudhipong, Lee & Zhous (2001) investigated the effects of axial deformations and axial forces on the vibration characteristics of tall buildings. Findings confirmed that axial forces and axial deformations in vertical elements reduce the stiffness of the building and result in higher natural periods. Results of this study also demonstrated that the effects of axial deformations should be included for vibration analysis of structures especially for tall and or slender buildings. Chapter 3 presented a method to quantify axial shortenings and highlighted the need to quantify the elastic shortenings accurately incorporating effect of load migration among vertical elements occurring due to horizontal stiff shear walls, It is thus important to discuss the ability of the proposed method to capture such a load migration.

5.2 Dynamic Stiffness Matrix of Plate Element

Dynamic stiffness matrix of a plate element subjected to axial (or in-plane) compressive loads can be formed as follows in order to examine the impact of axial compressive load on the modal parameters.

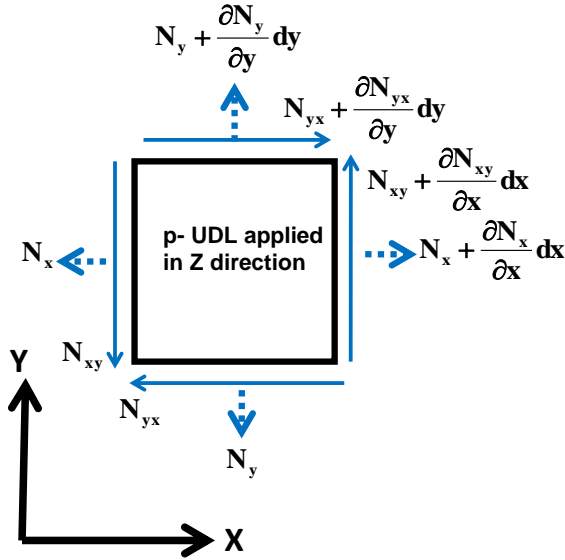


Figure 5-1: The plate element with forces - plan view

A plate element subjected combined lateral and direct in-planes loads is shown in Figure 5-1 in which N_x , N_y , N_{xy} , N_{yx} are in plane forces, x and y are distances along axes depicted in the Figure and p is the pressure load applied in Z the direction

The governing differential equation of the plate shown in the Figure can be written as follows (Ventsel & Krauthammer , 2001).

$$\frac{\partial^4 w}{\partial x^4} + 2 \frac{\partial^4 w}{\partial x^2 \partial y^2} + \frac{\partial^4 w}{\partial y^4} = \frac{1}{D} \left(p + N_x \frac{\partial^2 w}{\partial x^2} + N_y \frac{\partial^2 w}{\partial y^2} + 2 N_{xy} \frac{\partial^2 w}{\partial x \partial y} \right) \quad (5.1)$$

Where

w - transverse displacement and D - Flexural rigidity of the plate

A dynamic stiffness matrix of an axially compressive plate shown in Figure 5-2 to treat free vibrations is developed and presented in this Chapter. Boundary conditions of this plate element are selected to be representative of shear walls in a core of a building. According to D'Alambert's principle, Equation (5.1) can be written for free vibration analysis.

$$\frac{\partial w^4}{\partial x^4} + 2 \frac{\partial w^4}{\partial x^2 \partial y^2} + \frac{\partial w^4}{\partial y^4} + \frac{1}{D} \left(N_y \frac{\partial w^2}{\partial y^2} \right) = \frac{1}{D} \left(-\mu \frac{\partial w^2}{\partial t^2} \right) \quad (5.2)$$

Where μ is the mass of the element

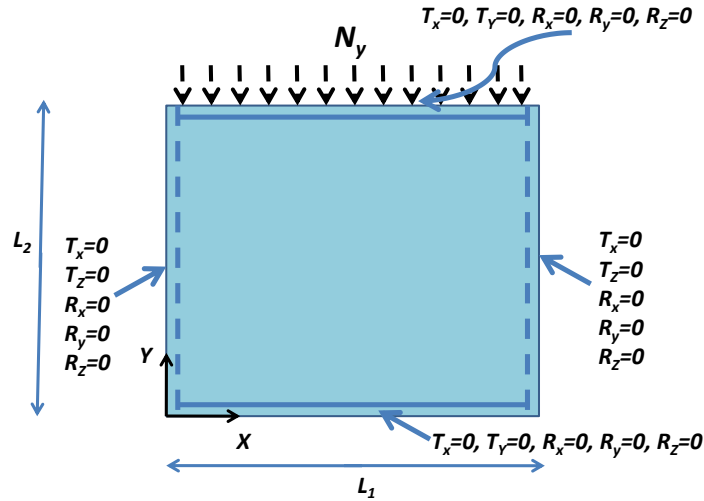


Figure 5-2: A plate element with axial compressive load

The above equation can be solved using a combination of variable separation method and Levy's Method. According to variable separation method, the following equation can be formed as

$$w = w(x, y, t) = v(x, y)g(t) \quad (5.3)$$

Equations (5.4) and (5.5) can be formed after substituting Equation (5.3) into Equation (5.2)

$$\frac{1}{g} \left(-\frac{\partial g^2}{\partial t^2} \right) = \omega^2 \quad (5.4)$$

$$\frac{D}{v\mu} \left(\frac{\partial v^4}{\partial x^4} + 2 \frac{\partial v^4}{\partial x^2 \partial y^2} + \frac{\partial v^4}{\partial y^4} + \left(\frac{N_y}{D} \frac{\partial v^2}{\partial y^2} \right) \right) = \omega^2 \quad (5.5)$$

.

Where

ω - natural frequency

Solution of Equation (5.4) can be written as follows

$$g = g(t) = A \cos(\omega t) + B \sin(\omega t) \quad (5.6)$$

Equation (5.7) is selected as a solution of Equation (5.5) based on Levy's Method (Xiang, Zhao & Wei, 2002)

$$v = v(x, y) = f(y) \sin \left(\frac{m\pi x}{L_1} \right) \quad (5.7)$$

Where

$m=1,2,3 \dots$

L_1 - shown in Figure 5-2

At the boundary,

$$v(0, y) = 0 \quad (5.8)$$

And

$$v(L_1, y) = 0 \quad (5.9)$$

Substituting Equation (5.7) into Equation (5.5), $f(y)$ in Equation (5.7) can be determined as follows

$$f(y) = A_1 e^{\lambda_1 y} + B_1 e^{\lambda_2 y} + C_1 \cos(\lambda_3 y) + D_1 \sin(\lambda_4 y) \quad (5.10)$$

Where

A_1, B_1, C_1 and D_1 - vector constants

$$\lambda_1 = \sqrt{a+b} \quad (5.11)$$

$$\lambda_2 = -\sqrt{a+b} \quad (5.12)$$

$$\lambda_3 = -\sqrt{a-b} \quad (5.13)$$

$$\lambda_4 = \sqrt{a-b} \quad (5.14)$$

$$a = \frac{\left(-\frac{N_y}{D} + 2\left(\frac{m\pi}{L_1} \right) \right)^2}{2} \quad (5.15)$$

$$b = \frac{\sqrt{\frac{N_y}{D} \left(\frac{N_y}{D} - 4\left(\frac{m\pi}{L_1} \right)^2 \right) + \frac{4\mu\omega^2}{D}}}{2} \quad (5.16)$$

Combining Equations (5.7) and (5.6), the deflection at any point on the plate can be represented from Equation (5.17) at any time $t=T$ as follows

$$w(x, y, T) = \left(\bar{A}e^{\lambda_1 y} + \bar{B}e^{\lambda_2 y} + \bar{C}\cos(\lambda_3 y) + \bar{D}\sin(\lambda_4 y) \right) \sin\left(\frac{m\pi x}{L_1} \right) \quad (5.17)$$

Where $\bar{A}, \bar{B}, \bar{C}, \bar{D}$ -vector constants as at a specific time $t=T$, $g(t)$ remains constant.

At the boundaries, $y=0$ and $y=L_2$, the deflections and rotations can be determined as follows

$$w(x, 0, T) = \left(\bar{A} + \bar{B} + \bar{C} \right) \sin\left(\frac{m\pi x}{L_1} \right) \quad (5.18)$$

$$w(x, L_2, T) = \left(\bar{A}e^{\lambda_1 L_2} + \bar{B}e^{\lambda_2 L_2} + \bar{C}\cos(\lambda_3 L_2) + \bar{D}\sin(\lambda_4 L_2) \right) \sin\left(\frac{m\pi x}{L_1} \right) \quad (5.19)$$

$$\vartheta(x, 0, T) = \left(\bar{A}\lambda_1 + \bar{B}\lambda_2 + \bar{D}\lambda_4 \right) \sin\left(\frac{m\pi x}{L_1} \right) \quad (5.20)$$

$$\vartheta(x, L_2, T) = \left(\bar{A}\lambda_1 e^{\lambda_1 L_2} + \bar{B}\lambda_2 e^{\lambda_2 L_2} - \bar{C}\lambda_3 \sin(\lambda_3 L_2) + \bar{D}\lambda_4 \cos(\lambda_4 L_2) \right) \sin\left(\frac{m\pi x}{L_1} \right) \quad (5.21)$$

Where

$$\mathfrak{g}(x, y, T) = \frac{\partial w(x, y, T)}{\partial y} \quad (5.22)$$

The following equation (Equation (5.23)) can be formed combining Equations (5.18) to (5.21)

$$\{Y\} = [A]\{D\} \quad (5.23)$$

Where

$$\{Y\} = \begin{Bmatrix} w(x, 0, T) \\ \mathfrak{g}(x, 0, T) \\ w(x, L_2, T) \\ \mathfrak{g}(x, L_2, T) \end{Bmatrix} \quad (5.24)$$

$$[A] = \begin{bmatrix} 1 & 1 & 1 & 0 \\ \lambda_1 & \lambda_2 & 0 & \lambda_4 \\ e^{\lambda_1 L_2} & e^{\lambda_2 L_2} & \cos(\lambda_3 L_2) & \sin(\lambda_4 L_2) \\ \lambda_1 e^{\lambda_1 L_2} & \lambda_2 e^{\lambda_2 L_2} & -\lambda_3 \sin(\lambda_3 L_2) & \lambda_4 \cos(\lambda_4 L_2) \end{bmatrix} \sin\left(\frac{m\pi x}{L_1}\right) \quad (5.25)$$

$$\{D\} = \begin{Bmatrix} \overline{A} \\ \overline{B} \\ \overline{C} \\ \overline{D} \end{Bmatrix} \quad (5.26)$$

Equations (5.27) and (5.28) below represent the moment, M_y and shear force, V_y respectively

$$M_y = -D \left[\frac{\partial^2 w}{\partial y^2} + \nu \frac{\partial^2 w}{\partial x^2} \right] \quad (5.27)$$

$$V_y = -D \frac{\partial}{\partial y} \left[\frac{\partial^2 w}{\partial y^2} + (2 - \nu) \frac{\partial^2 w}{\partial x^2} \right] \quad (5.28)$$

Where, ν - Poisson's ratio

Equation (5.29) is formed using the moments and shear forces at the boundaries

$$\{F\} = [B]\{D\} \quad (5.29)$$

Where

$$\{F\} = \begin{Bmatrix} v_y(x,0,T) \\ M_y(x,0,T) \\ v_y(x,L_2,T) \\ M_y(x,L_2,T) \end{Bmatrix} \quad (5.30)$$

$$[B] = -D \begin{bmatrix} b_{11} & b_{12} & b_{13} & b_{14} \\ b_{21} & b_{22} & b_{23} & b_{24} \\ b_{31} & b_{32} & b_{33} & b_{34} \\ b_{41} & b_{42} & b_{43} & b_{44} \end{bmatrix} \sin\left(\frac{m\pi x}{L_1}\right) \quad (5.31)$$

where

$$b_{11} = \lambda_1^3 - \left(\frac{m\pi}{L_1}\right)^2 (2 - \nu)\lambda_1 \quad (5.32)$$

$$b_{12} = \lambda_2^3 - \left(\frac{m\pi}{L_1}\right)^2 (2 - \nu)\lambda_2 \quad (5.33)$$

$$b_{13} = 0 \quad (5.34)$$

$$b_{14} = -\lambda_4^3 - \left(\frac{m\pi}{L_1}\right)^2 (2 - \nu)\lambda_4 \quad (5.35)$$

$$b_{21} = \lambda_1^2 - \left(\frac{m\pi}{L_1}\right)^2 \nu \quad (5.36)$$

$$b_{22} = \lambda_2^2 - \left(\frac{m\pi}{L_1}\right)^2 \nu \quad (5.37)$$

$$b_{23} = -\lambda_3^2 - \left(\frac{m\pi}{L_1} \right)^2 v \quad (5.38)$$

$$b_{24} = 0 \quad (5.39)$$

$$b_{31} = \lambda_1^3 e^{\lambda_1 L_2} - \left(\frac{m\pi}{L_1} \right)^2 (2-v) \lambda_1 e^{\lambda_1 L_2} \quad (5.40)$$

$$b_{32} = \lambda_2^3 e^{\lambda_2 L_2} - \left(\frac{m\pi}{L_1} \right)^2 (2-v) \lambda_2 e^{\lambda_2 L_2} \quad (5.41)$$

$$b_{33} = \lambda_3^3 \sin(\lambda_3 L_2) + \left(\frac{m\pi}{L_1} \right)^2 (2-v) \lambda_3 \sin(\lambda_3 L_2) \quad (5.42)$$

$$b_{34} = -\lambda_4^3 \cos(\lambda_4 L_2) - \left(\frac{m\pi}{L_1} \right)^2 (2-v) \lambda_4 \sin(\lambda_4 L_2) \quad (5.43)$$

$$b_{41} = \lambda_1^2 e^{\lambda_1 L_2} - \left(\frac{m\pi}{L_1} \right)^2 v e^{\lambda_1 L_2} \quad (5.44)$$

$$b_{42} = \lambda_2^2 e^{\lambda_2 L_2} - \left(\frac{m\pi}{L_1} \right)^2 v e^{\lambda_2 L_2} \quad (5.45)$$

$$b_{43} = -\lambda_3^2 \cos(\lambda_3 L_2) - \left(\frac{m\pi}{L_1} \right)^2 v \cos(\lambda_3 L_2) \quad (5.46)$$

$$b_{44} = -\lambda_4^2 \sin(\lambda_4 L_2) - \left(\frac{m\pi}{L_1} \right)^2 v \sin(\lambda_4 L_2) \quad (5.47)$$

Dynamic stiffness matrix, $[K_L]$ of the plate can be formed combining Equations (5.23) and (5.29) as follows

$$\{F\} = [K]_L \{Y\} \quad (5.48)$$

Where

$$[K]_L = [B][A]^{-1} \quad (5.49)$$

The above stiffness matrix is defined based on the local coordinate system so that transformation matrix, $[T]$ is employed as follows to establish the stiffness matrix based in the global coordinate system.

$$[\bar{K}]_G = [T]^T [K]_L [T] \quad (5.50)$$

Where subscript G refers the global coordinate system

Modal parameters of the plate element can be calculated from Equation (5.51) presented below using the dynamic stiffness matrix $[K_L]$

$$[K_L]\{\phi\} = 0 \quad (5.51)$$

Where

$\{\phi\}$ - modal vector of the element

The dynamic stiffness matrix of the structure, $[\bar{K}]$, incorporating the influence of axial loads can be formed by assembling stiffness matrices of the elements considering compatibility of the nodes

With the use of the dynamic stiffness matrix, $[\bar{K}]$, the equation of free vibration of a structure with the influence of the axial forces of elements can be represented as

$$[\bar{K}]\{\bar{\phi}\} = 0 \quad (5.52)$$

Where $\{\bar{\phi}\}$ - modal vector of the structure

Equations (5.51) and (5.52) incorporate axial effects and hence capture the significant impact of the axial force on the modal parameters of the element and the entire structural framing system. However, it is not convenient to solve Equation (5.52) to examine the modal parameters with the influence of the axial forces of a complex structural framing system with shear walls as shown in Example 03 (discussed in the next section). The finite element software is thus employed for the proposed method as employed in Chapter 4.

It is examined in Chapter 4 the effects of axial compressive loads on column elements using the dynamic stiffness matrix of beam element and the Finite Element (FE) package, ANSYS (ANSYS Inc., 2007) was modified to capture the effects of the applied axial compressive loads of column elements and incorporated into the modal analysis. In this Chapter, this modified program is further enhanced based on the dynamic stiffness matrix of the plate element derived above in order to study capabilities of the vibration based parameter, Stiffness Index (SI) defined through Equation (4.34) in Chapter 4.

It is well known that when buildings are subjected to live loads, their column elements deform axially in the linear elastic region. The main objective of the methodology proposed herein is to develop a relationship between such axial deformations and vibration characteristics. This study is therefore limited to the linear elastic region.

5.3 Validation of the modified FE program and study the capabilities of Stiffness Index (SI)-Core shear wall element

In this section, three examples are presented. The first example is used to validate the proposed procedure using experimental data while the second example is used to study the impact of boundary conditions of the plate element on Stiffness Index (SI). The final example illustrates the application of the methodology to a geometrically complex structural framing system with shear walls.

5.3.1 Validation of the modified FE program-Core Shear wall element

It is necessary to study accuracy of the modified FE program which will be implemented in the other illustrative examples. This FE program was therefore used to develop a model of a plate element treated in an earlier experimental study on the influence of axial load on vibration characteristics of a plate by Ilankoi & Dickinson (1987). The properties of the plate element treated are tabulated in Table 5-1.

Table 5-1; Properties of the plate element

Property	Numerical value
Young' Modulus (GPa)	207
Poisson's ratio	0.3
Density (Kgm ⁻³)	7738
Length (mm)	250
Height (mm)	300
thickness(mm)	1

In the experimental study the vertical plate element had fixed boundary conditions at the bottom edge while only the vertical translation was allowed at the top. The other two edges were simply supported. The load was applied along the 250mm long top edge of the plate and was increased in several steps. The corresponding natural frequencies were measured at each load increment. The impact of incremental load on the frequency was then investigated from the experimental results. More information on the experimental testing can be found in the paper presented by Ilankoi & Dickinson (1987). The experimental testing was used to study both the linear and non-linear behavior of the plate element under the axial compressive loads. However, only the results in the linear range were selected to validate the modified FE program due to the fact that effects of axial deformation on this region is only investigated in this research as mentioned earlier.

A FE model for the plate element was developed using the modified FE program providing the appropriate boundary conditions. The axial (or in-plane) loads were applied in a manner similar to that in the experiment and the corresponding natural frequencies were extracted from the free vibration analysis while employing model updating techniques in order to improve the FE model. These techniques are used to

fine tune the boundary conditions and the plate parameters. The results for the natural frequencies are presented and compared in Table 5-2.

Table 5-2: Comparison of the frequencies from the experiment and the present study

P(N)	Experimental Study Frequency(Hz)	Present Study Frequency(Hz)	Difference (%)
309.4	66.65	66.89	0.36
618.8	64.27	65.3	1.60
928.2	62.52	63.37	1.36
1237.6	57.72	58.12	0.69
1547	54.96	55.52	1.02
1856.4	50.32	51.02	1.39
2165.8	49.43	49.2	-0.47

In the experiment, the top surface of the plate element was modified to facilitate the application of the in-plane or axial loads. As the dimensions of the modifications to the top surface had not been clearly stated, they could not be incorporated into the FE model. It was also difficult to simulate same the supported boundary conditions in the FE model as implemented in the experiment. Furthermore, mechanical systems used in the experimental setup to apply simply supported boundary conditions are difficult to simulate in the FE analysis due to friction. These may be reasons for the small difference between results of the experiment and the present study, even though the model updating techniques have been employed for the FE model. However, it is evident from Table 5-2 that the error is less than 2% highlighting the accuracy of the modified FE program used to capture the effects of axial loads and incorporate into the modal analysis.

5.3.2 Study the capabilities of Stiffness Index (SI) applied to core shear walls

5.3.2.1 Impact of the boundary conditions on SI

In this example, plate elements with different boundary conditions and subjected to axial compressive loads are selected to study the impact of their boundary conditions on the defined parameter, Stiffness Index (SI). Figure 5-3 shows the two plate elements labeled Case A and Case B with different boundary conditions while the properties of the elements are tabulated in Table 5-3. The main purpose of this study was to investigate the effects of boundary conditions at the base of the wall elements.

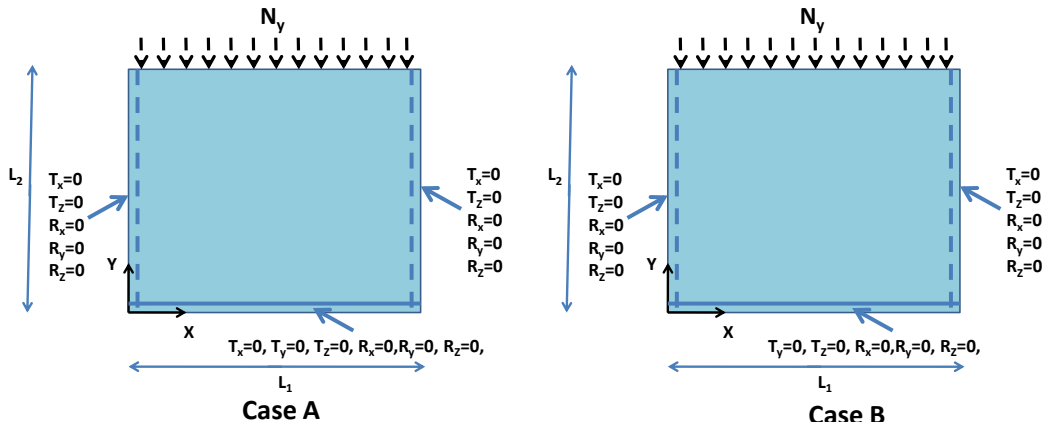
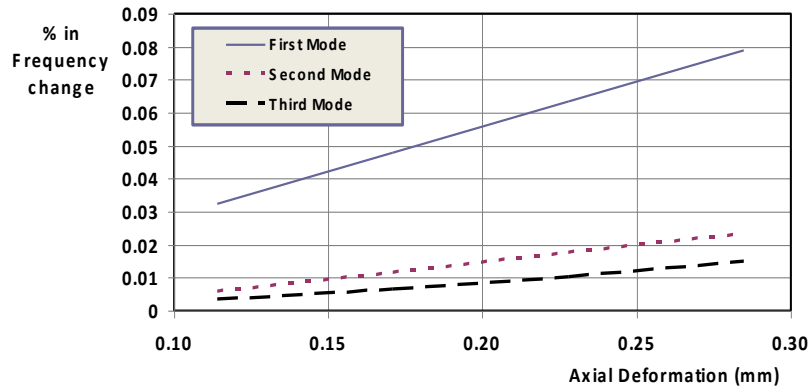


Figure 5-3: plate elements with different boundary conditions

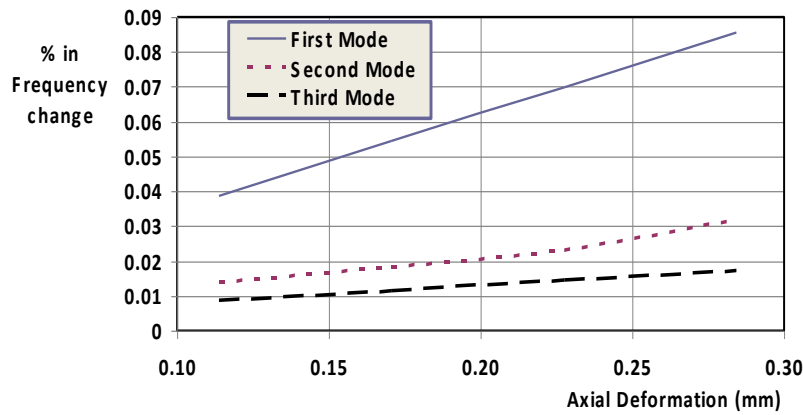
Table 5-3: properties of the plate elements

Property	Numerical value
Young's Modulus (GPa)	45
Poisson's ratio	0.2
Density (Kg m^{-3})	2300
L_1 (m)	6
L_2 (m)	4
Thickness(m)	0.5

The analysis was conducted using the modified FE program for Cases A and B while increasing the axial compressive force, N_y , from 4MN to 10 MN with several load increments. The frequencies and the corresponding modal vectors were extracted from the analysis while axial deformations were quantified from static analysis. Figures 5-4(a) and 5-4(b) illustrate percentage of the frequency change vs. the axial deformation for Cases A and B respectively while Figure 5-5 shows deformation contours of first three modes of the plate elements(Cases A and B) under the vibration.



(a)



(b)

Figure 5-4: percentage of frequency change vs. the axial deformation-(a) Case A and (b)-Case B

It is clear from Figure 5-4 that the percentage change of the frequency increases with axial deformations as a result of axial compressive forces and this is more pronounced in the first mode and reduces with the mode number. This highlights that stiffness change due to the axial compressive force can be captured using the first few modes. In each of the two cases A and B, it was also evident that the mode shape change due to the axial load was more pronounced for the first few modes. Figure 5-5 clearly indicates that mode shapes for Case A (see Figures 5-5(a) to 5-5(c)) are significantly different than those for Case B(see Figures 5-5(d) to 5-5(e)) indicating that the boundary conditions impact significantly on the mode shapes and result in the SIs.

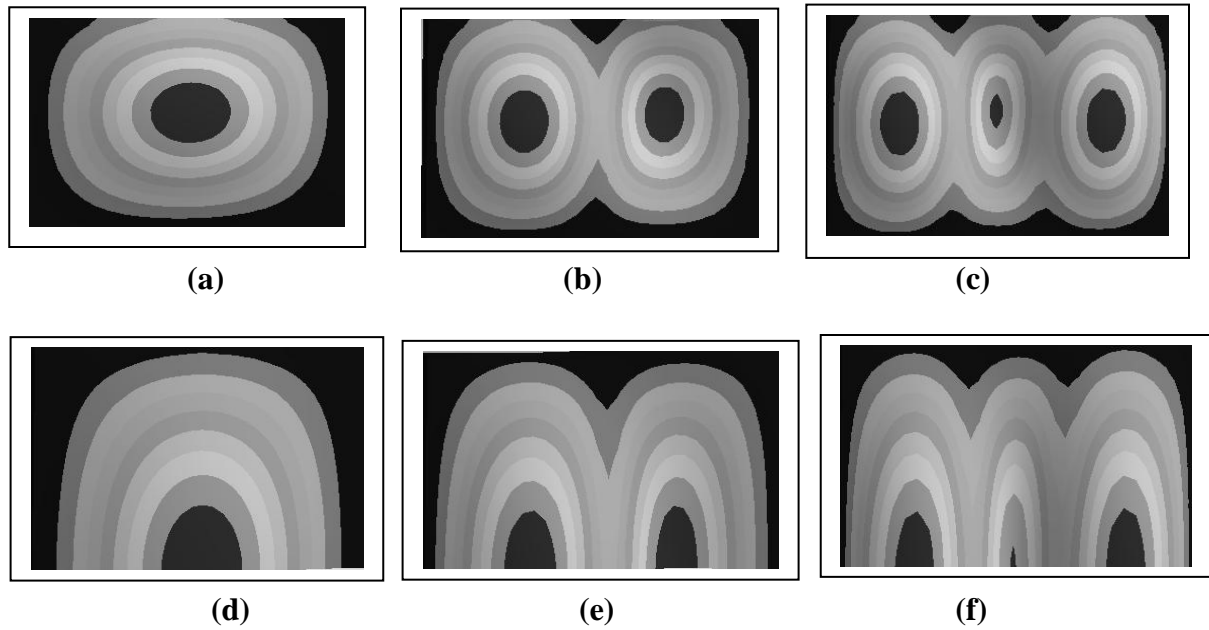
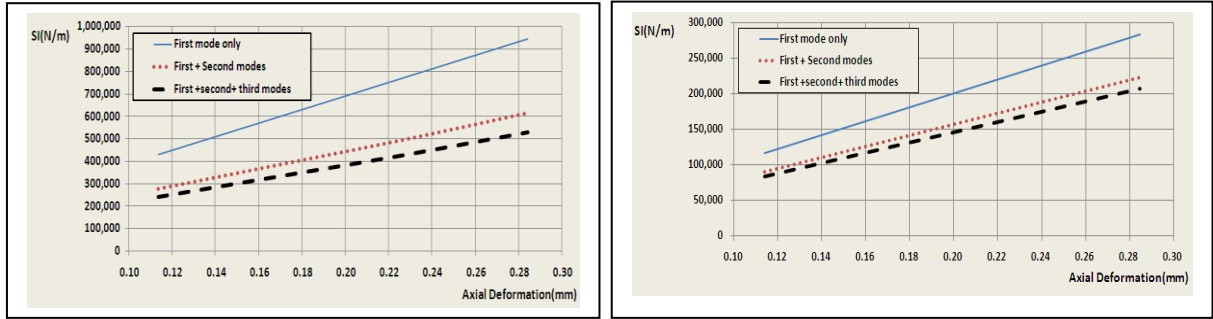


Figure 5-5; Deformation contours of the element (plan views): (a) –(c) first 3 modes for case A and (d) – (e) first three modes for case B

The defined parameter, Stiffness Index (SI) at each load increment is calculated using the modal parameters while the corresponding axial deformations are calculated using static analysis. Figure 5-6 presents the variation of SI with axial deformation for the both cases. It is evident from Figure 5-6 that SI does not change appreciably when more than two modes are incorporated into the calculation. This indicates that the first two modes are adequate to capture the effect of axial force and hence deformation. Variation of SIs of Case A (from 250,000 to 950,000) and Case B (from 80,000 to 275, 000) are also different confirming that SI has the ability to capture effect of different boundary conditions through the change of modal parameters as experienced by Chapter 4. As experienced by results of examples in Chapter 4, Figure 5-6 illustrates that the variation of SI with axial deformation is linear for the both cases.



(a) (b)

Figure 5-6: variation of SI with axial deformation- (a)-Case A and (b)-Case B

The next example will demonstrate more capabilities of SI, when it is applied to a geometrical complex structural framing system with cores/shear walls.

5.3.2.2 Capture the effects of the different tributary areas and the load migration

A three dimensional (3D) structural framing system with ten levels, shown in Figure 5-7, is selected to examine the capabilities of the proposed SI. This structure will not have a heavy computational demand for its analysis but will be adequate to explain the process so that it can be applied to more complex structural framing systems. Height of the floor is 4 m. Two cores with equal sizes named cores L and R are located in this structural system as depicted in Figure 5-7 so that impact of axial loads on the shear walls of these cores can be investigated through the defined parameter, Stiffness Index (SI). This framing system also comprises the stiff shear walls located at the 7th level (see Figure 5-7) so that load migration occurs as in a high rise building with outrigger and belt systems as experienced by Chapter 3. The material properties of the shear wall elements are tabulated in Table 5-4 while their sizes are tabulated in Table 5-5. In this example, the behavior of SIs of elements of the core walls L and R in levels 5, 7 and 9 are examined in order to capture the impact of the (stiff) shear wall at level 7 on the core wall elements at, below and above this level respectively.

Uniformly distributed loads are applied on slabs in different steps as tabulated in Table 5-6 to create different loading cases. These loading cases simulate the structure subjected to gradual load increments. The analysis was conducted for each loading case using the modified FE program and the corresponding modal parameters were extracted while the axial deformations were determined using static analysis. As in Example 2, these modal parameters were first used to determine the SIs plotted with respect to the axial deformations of walls of the cores L and R at the selected levels. For reasons discussed earlier only the first two modes (both bending) in the u and v directions shown in Figure 5-7(b) were used to calculate SIs of the elements.

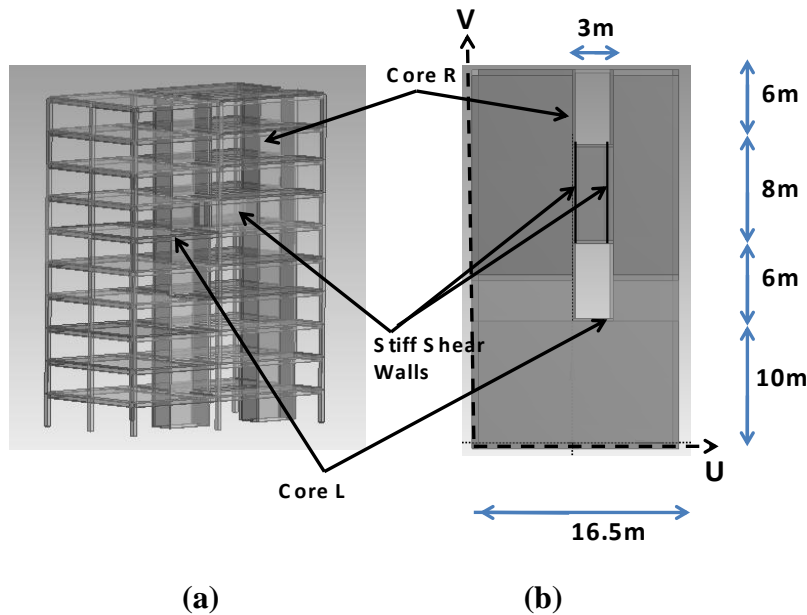


Figure 5-7: Structural framing system (a)- isometric view and (b)- plan view

Table 5-4: Material properties of elements

Structural Element	Material Property	Numerical Value
Shear walls of core	Density/(kgm^{-3})	2400
	Poisson Ratio	0.18
	Young's Modulus /(GPa)	30
stiff shear walls	Density/(kgm^{-3})	2400
	Poisson Ratio	0.18
	Young's Modulus /(GPa)	45

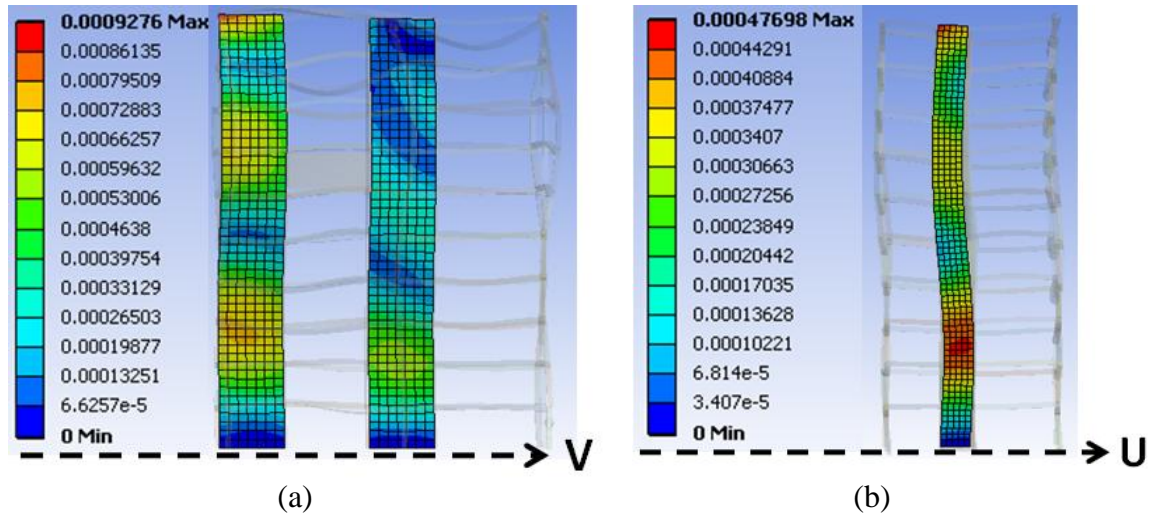
Table 5-5; Element sizes

Element	Thickness (m)
Core walls	0.25
(Stiff) shear walls located at 7 th level	1

Table 5-6: Applied loads on slabs

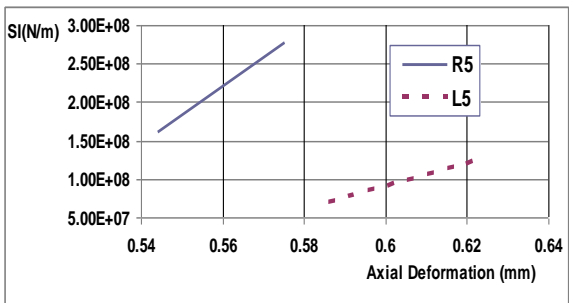
Levels	Loads on slabs(kPa)			
	Case 1	Case 2	Case 3	Case 4
1 to 6	2	2	2	2
7 and 8	0	2	2	2
9 and 10	0	0	1	2

Figure 5-8 presents contours of modal vectors of the first two modes of only the core wall elements. This is because the main objective of this paper is to develop a method to quantify axial deformations of the core walls/ plate elements in a structural framing system using modal parameters. It is evident from legends of Figure 5-8 that the behaviors of the modal vectors of the core walls at each level are different. This is due to the different tributary areas and the locations of the two cores. This difference can be used to capture the individual behavior of the elements using the proposed Stiffness Index (SI).

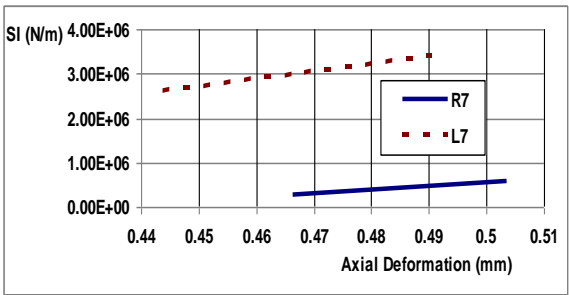


**Figure 5-8: Mode shapes (a) Mode 1 (Front View) and (b) -Mode 2 (End View)
(unit in meter)**

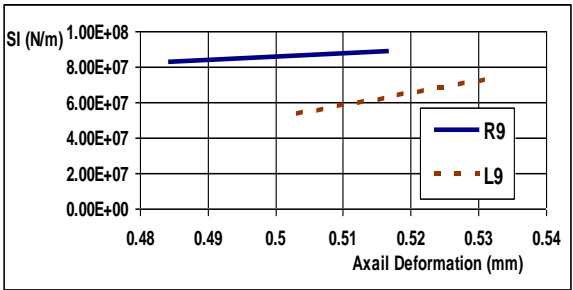
Figure 5-9 presents the variation between the SI and axial deformations of walls of cores L and R in the selected levels. The first and second letters of the legends refer to the particular core wall element and the level respectively. It is evident from this Figure that there are significant differences between the variations of SI(s) of the two selected elements at all 3 levels. This is mainly due to the variation of modal vectors used in the calculation of Modal Flexibility (MF). At the 5th level, element L5 is subjected to higher axial deformation than element R5 due to the larger tributary area of L5. As stiffness change is inversely proportional to axial deformation, the SI of element L5 is less than that of element R5 as shown in Figure 5-9(a). Similar comments apply to the elements L9 and R9 at level 9 as noticed from Figure 5-9(c).



(a)



(b)



(c)

Figure 5-9: variation of SI of elements of core with axial deformation-(a)- 5th level , (b)- 7th level and (c)-9th level.

Axial load of element L7 migrates to element R7 through the (stiff) shear walls connecting these two elements (see Figure 5-7) and this load migration controls the axial deformations notably. Due to this reason there are two important features (i) SIs of the elements at level 7 are lower than those at levels 5 and 9 and (ii) SI of L7 is higher than that of R7, a reverse in trends noticed at the other two levels. Figure 5-9 depicts that variation of SI vs. axial deformation is linear as experienced in the previous example.

Figure 5-9 demonstrates that the defined parameter, SI of an element in a structural framing system has an ability to capture the load migration and the effects of different tributary areas successfully. Chapter 3 highlighted that axial deformations of cores of high rise buildings are more pronounced due to the fact that they are subjected to huge loads from the upper floors even though these elements are mainly designed to carry lateral loads from natural sources such as wind. The findings discussed above confirm that SI proposed methodology can be implemented for core wall elements of high rise buildings. This is important as axial deformations and SI(s) of such elements are more pronounced than those in medium rise buildings.

5.4 Conclusion

Even though numerous methods have been developed to examine the axial effects of plate elements with different boundary conditions based on their natural frequencies, they cannot be discretely applied to the elements in a structural framing system since natural frequency used in those methods is a property of the entire structural system. Discrete capture of the dynamic properties of individual elements are required to accurately define the response of a diverse range of elements with many parametric variations that have been mentioned earlier.

Chapter 5 presents developments of dynamic stiffness matrices of a plate element and a structural framing system in order to examine the influence of the axial effects on the vibration characteristics. Capabilities of the vibration based parameter; Stiffness Index (SI) introduced in Chapter 4 is applied to plate elements in a structural framing system. Results highlighted that SI parameter can be used to identify the individual axial effects

of the elements capturing effects of boundary conditions, different tributary areas as well as the load migrations.

Outcomes of Chapters 4 and 5 conclude that Stiffness Index (SI), which uses Modal Flexibility (MF) phenomenon, can be applied to building structures comprising cores and column elements and capture the individual axial effects using the vibration characteristics.

6 DEVELOPMENT OF A VIBRATION BASED METHOD TO UPDATE AXIAL SHORTENING OF VERTICAL LOAD BEARING ELEMENTS IN REINFORCED CONCRETE BUILDINGS

Outcomes in Chapters 4 and 5 demonstrate that the axial deformation impacts on the vibration characteristics and this impact amplifies with building height and geometric complexity of structural framing systems. Chapters 4 and 5 highlighted a relationship between Stiffness Index (SI), which uses modal vectors and natural frequencies, and axial deformation and capabilities of SI presented through illustrative examples. In this chapter, SI is further enhanced in order to develop a novel vibration based parameter called Axial Shortening Index (ASI) to capture elastic deformation during construction and service stages of buildings. This novel parameter is applied to a geometrically complex tall structural framing system in order to examine its capabilities.

6.1 Introduction

Chapters 4 and 5 demonstrate the development of Stiffness Index (SI) parameter of a structural element, which depends on the vibration characteristics. Outcomes of these two chapters conclude that this parameter can be used to identify the individual axial effects of column and core shear wall elements of structural framing system. The main objective of Chapter 6 is to present development of a comprehensive procedure to update previous prediction of axial shortening of the structural elements based on the variation of vibration characteristics and thereby determine realistic differential axial shortening between various structural elements. Stiffness Index (SI) developed in Chapter 4 is further enhanced in order to propose a vibration based Axial Shortening Index (ASI) developed and presented in this chapter. The procedure incorporating ASI is proposed taking into account the time dependent effects of Young's modulus of reinforced concrete and construction sequence. This procedure can be used during the construction and service stages in order to verify and update previous predictions. A comprehensive example of a tall building with 64 storeys is treated in this chapter to illustrate the proposed procedure. The proposed procedure in this chapter can also be

used as a structural health monitoring tool during and after the construction to assess damage from extreme events such as earthquakes, hurricanes, or blasts.

This research uses the MF phenomenon to develop a relationship between elastic shortening and vibration characteristics. The effects of creep and shrinkage are then incorporated in order to quantify the total axial shortening in the elements and hence the differential axial shortening between any two vertical elements can be calculated. Gauges such as accelerometers and Pick-ups can be installed on structural elements so that vibration characteristics such as modal vectors and natural frequencies can be acquired (kanwar et al ,2008; Olmer, 1980). These gauges can be deployed when readings are necessary and they need not to be fixed permanently either during or after construction. As a result, these instruments do not require the same degree of protection as vibrating wire gauges, external mechanical gauges and electronic strain gauges resulting in lower cost of installation.

The model updating method described in this section uses time dependent load application to represent construction sequences, time dependent parameters for Young's modulus of reinforced concrete based on GL2000 as described in Chapter 3.

6.2 Load Application

According to the construction process in high rise buildings, the typical time varying load history of a concrete element in the building can be represented as in Figure 3-3 in Chapter 3. As assumed in section 3.1.5 in Chapter 3, the Young's Modulus in concrete at this incremental load application is assumed to be constant. However, the time varying value of Young's Modulus of concrete is used in the analysis as time increased from T_1 to T_2 , from T_2 to T_3 and so on and this Young's Modulus can be calculated through Equation 3.4 in Chapter 3. As described in Chapter 3, the stress developed in concrete elements due to the construction load has been found to be less than $0.5 f_c'$ (where f_c' = characteristic strength of concrete). This stress is in the linear elastic region enabling the principle of superposition to be applied.

6.3 Model Upgrading Methods

The main advantage of using FE methods in structural analysis is the ability to generate accurate numerical models to simulate the action effects, stresses and strains under variable conditions of stiffness and loads (Brownjohn, 2009; Wu & Li, 2004). As discussed earlier, the dynamic properties of structure can be represented by vibration characteristics such as modal flexibility in such analysis

This research defines the two model upgrading methods; micro and macro based on variation of the mass and stiffness of a structure during and after the construction. Micro-upgrading occurs when mass is added by the structural components without any significant contribution to the stiffness of the whole building, for example, when wet concrete and simply supported beams are included into the building. Macro-upgrading occurs when structural components added to the building contribute to the stiffness as well as mass of the whole structure, and includes matured concrete and moment resisting frames. Young's Modulus is assumed as a constant during micro upgrading stage as stated in Section 6.1. Figure 6-1 depicts micro and macro upgrading methods defined in a structure from construction to service stage. As shown in this figure stage 1, stage 2 etc, in which instantaneous loads from mass of materials used to fabricate the floor above (a certain level) are applied on the structure without any significant contribution to the stiffness of the whole structure are called Micro Upgrading. When added materials develop and contribute stiffness and mass to the structure is called Macro Upgrading, which occurs across stages 1-2, 2-3, etc with changes in the vibration characteristics. These are the only two realistic scenarios during the construction of a building. During the Micro-Upgrading process the effects of the added mass are realized both in free vibration analysis through the dynamic stiffness matrix (presented in chapters 4 and 5) and automatically in static analysis.

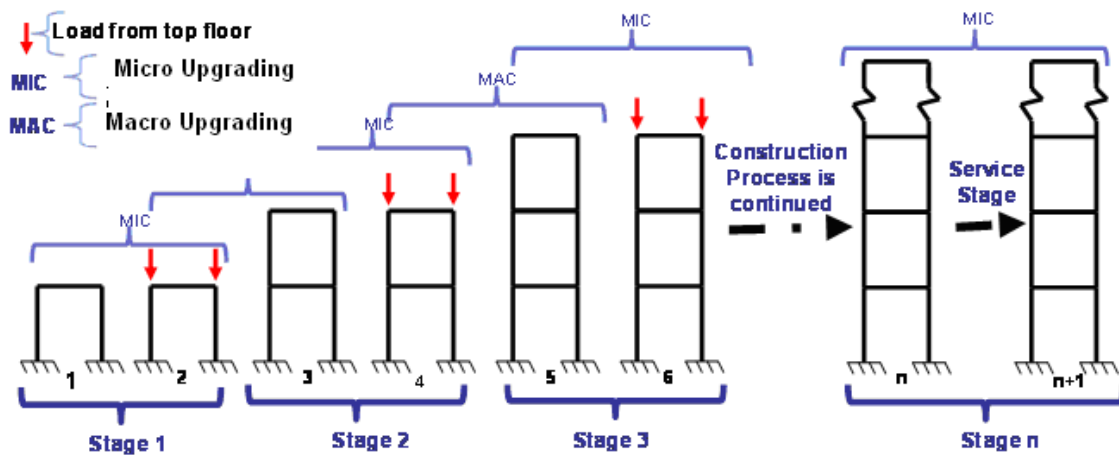


Figure 6-1: Model upgrading methods defined from the construction to service stages

It is necessary to calculate dead loads of the floors above a particular level and to incorporate these into the method at different stages. According to the geometric differences, sub FE models representing the floors are developed and analyzed separately to calculate the dead loads to be transferred to the building system as conducted in section 3.1.4 in Chapter 3. This approach is very important for high rise buildings with geometrically complex floors since the dead load of such floors can be estimated accurately as well as conveniently.

6.4 Vibration characteristics and Axial Shortening

6.4.1 Vibration characteristics

During construction, materials such as wet concrete used to fabricate structural elements in the floor above a certain level do not develop instantaneous stiffness and the ability to support external loads by the building system. Deformation of element in the floors below can occur due to the influence of mass of these materials. The stiffness of the structural elements in the floors below will be influenced by the maturing concrete (with time varying properties) resulting in the further deformation of these elements.

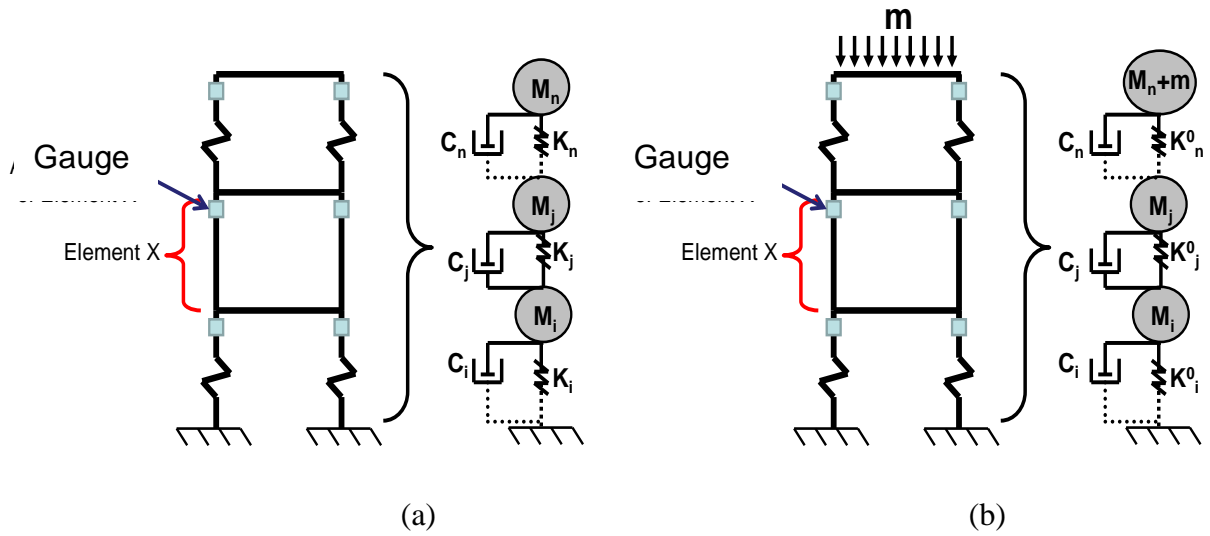


Figure 6-2: lump mass systems for a structure -3(a) - before upper floor construction and 3(b)-during upper floor construction

Figure 6-2 shows one of the construction stages. In this figure, “m” refers to mass of materials of the floor above (under construction) while M_x , K_x and C_x (where number of floors, $x = i, j$ and n) denote lump masses, stiffness and damping of each floor of the lump mass system. The superscript “o” indicates the new value of stiffness of the floors due to the mass “m” acting on the top of the structure. Locations of the instruments (accelerometers) are shown in this figure and they can be used to capture the vibration characteristics and to quantify the MF of the elements at any stage.

When a structure is subjected to free vibration during the construction stage, the mass of materials used to fabricate the upper floor contributes to the lump mass system as illustrated in Figure 6-2(b). The axial forces result in axial deformations in vertical structural elements, such as columns and cores, increase due to additional mass. Based on the outcomes of Chapters 4 and 5, it can be stated that the frequency of the structural elements and hence frequency of the whole structure decreases due to the increased axial forces. Vibration characteristics such as natural frequencies and modal vectors thus change with load increments. Moreover, the Young’s modulus of concrete changes with

time so that the stiffness of the structure and vibration characteristics change. Increasing mass reduces the natural frequency of the structure and increasing stiffness increases the frequency of the structure. The impact of additional mass from new construction is instantaneous while the increment of stiffness of the newly built components is time dependent. This results in continuous change of MF and hence Stiffness Index (SI) with time.

Equations 6.1 and 6.2 represent Modal Flexibility of element x depicted as in Figures 6-2(a) and 6-2(b) respectively

$$F_{XU} = \left[\sum_{r=1}^n \frac{1}{\omega_r^2} \phi_{xr} \phi_{xr}^T \right]_U \quad (6.1)$$

$$F_{XL} = \left[\sum_{r=1}^n \frac{1}{\omega_r^2} \phi_{xr} \phi_{xr}^T \right]_L \quad (6.2)$$

where subscript U and L denote the two load stages without and with mass “m” respectively.

When buildings are subjected to free vibration due to wind or traffic loads or both, the magnitudes of movement of the lower storeys are very low. Consequently, magnitudes of modal parameters and hence modal flexibilities are also very low. It is necessary to amplify these modal flexibilities in order to enhance the small time dependent incremental changes of these parameters in structural elements as the way to define Stiffness Index (SI) presented in Chapters 4 and 5. Hence, the reciprocals of Equations 6-1 and 6-2 are considered as follows

$$\frac{1}{F_{XU}} = \frac{1}{\left[\sum_{r=1}^n \frac{1}{\omega_r^2} \phi_{xr} \phi_{xr}^T \right]_U} \quad (6.3)$$

$$\frac{1}{F_{XL}} = \frac{1}{\left[\sum_{r=1}^n \frac{1}{\omega_r^2} \phi_{xr} \phi_{xr}^T \right]_L} \quad (6.4)$$

Equation 6-5 below captures the influence of the axial force in an element induced by mass of materials of the floor above in terms of model flexibility changes through the Stiffness Index (SI) parameter.

$$SI = \left(\frac{1}{F_{XU}} - \frac{1}{F_{XL}} \right) = \frac{1}{\left[\sum_{r=1}^n \frac{1}{\omega_r^2} \phi_{xr} \phi_{xr}^T \right]_U} - \frac{1}{\left[\sum_{r=1}^n \frac{1}{\omega_r^2} \phi_{xr} \phi_{xr}^T \right]_L} \quad (6.5)$$

Equation 6-6 can be written by considering log scale of Equation 6-5 to represent this influence in an amplified manner.

$$\log_{10}(SI) = \log_{10} \left(\frac{1}{\left[\sum_{r=1}^n \frac{1}{\omega_r^2} \phi_{xr} \phi_{xr}^T \right]_U} - \frac{1}{\left[\sum_{r=1}^n \frac{1}{\omega_r^2} \phi_{xr} \phi_{xr}^T \right]_L} \right) = \beta_x \quad (6.6)$$

Outcomes of Chapters 4 and 5 highlights that the resulting axial deformation (elastic deformation) influences the Modal Flexibility (MF) and hence SI and this can be captured by the Equation below.

$$\frac{\partial(\log_{10}(SI))}{\partial Z_x} = \frac{\partial \beta_x}{\partial Z_x} \quad (6.7)$$

where - Z_x is the axial elastic deformation of element x due to the axial force

To facilitate model updating (as described above) the parameter, ASI is introduced and defined as follows.

$$\frac{\partial \beta_x}{\partial Z_x} = \alpha_x = ASI \quad (6.8)$$

This parameter, ASI captures variations of flexibility and displacement (elastic shortening) of element x during and after the construction and is called the vibration based Axial Shortening Index (ASI). It can hence be used to quantify the progressive structural deformations both during and after construction. It is evident from Equation 6-8 that this parameter is directly proportional to stiffness and inversely proportional to elastic axial deformation.

6.4.2 Quantification of Elastic shortening

6.4.2.1 Design stage predictions

At the design stage predictions of elastic shortenings, Z of vertical members at different stages of construction are normally made using static analysis of finite element models of the building and based on the construction sequence. In addition, free vibration analyses of the appropriate Finite element models of the structure at different construction stages can be used to obtain the modal parameter β_x (Equation 6-6). Using these 2 parameters and Equation 6-8, the axial shortening index (ASI) Δ for each vertical member at the different construction stages can be calculated and retained for later use. The variation of axial shortening index (ASI) across the construction stages are normally plotted in a graph in which the vertical axis represents Axial Shortening Index (ASI) while the horizontal axis represents the number of the stage. Furthermore, four or five floors are usually considered at a time in the finite element modeling and analysis to plot the variations of ASI with time and the hence the ASI at intermediate stages can be found by interpolation.

6.4.2.2 Upgrading during construction

The natural frequencies and mode shapes extracted from the deployed accelerometers at the different construction stages can be used to obtain more accurate and realistic values of the modal parameter (β now updated to) β_x^p (where superscript , p denotes the practical measurements) for the vertical elements using Equation 6-7. These updated values β_x^p along with the previously obtained ASI can then be used to calculate the

updated values of the elastic shortenings Z_x^p (where superscript, p denotes the practical measurements) from Equation 6-9.

$$Z_x^p = \int \frac{1}{\alpha_x} \partial \beta_x^p \quad (6.9)$$

6.4.3 Quantification of axial shortening

The total axial shortening in consequence of a combination of elastic, creep and shrinkage shortenings can be calculated using the equation developed in Chapter 3 as follows.

$$H_x(t_n) = L \sum_{x=1}^n \left[\sum_{i=1}^n \left[\frac{Z_x^p(t_i)}{L} + \frac{E(t_i) Z_x^p(t_i)}{L} \frac{\phi_{28}}{E_{cm28}} \right] + \left(900K \left[\frac{30}{f_{cm28}} \right]^{1/2} \times 10^{-6} \right) \left(1 - 1.18h^4 \right) \left[\frac{t - t_c}{t - t_c + 0.12(v/s)^2} \right]^{0.5} \right] \quad (6.10)$$

Equation 6-10 represents the axial shortening $H_x(t_n)$ of element x at the considered time, t_n along the height of the building.

Equation 6-11 represents the total elastic shortening, $Z_x^o(t_n)$ of an element along the height of the building at time t_n subjected to the force history shown in Figure

$$Z_x^o(t_n) = \sum_{x=1}^n \sum_{i=1}^n Z_x^p(t_i) \quad (6.11)$$

Where i and x are defined as in the equations above.

At the design stage, results from the finite element analysis can be used to determine the parameter, vibration based Axial Shortening Index (ASI) □□ introduced above for each vertical structural element such as the core and columns in each of the stages 1, 2 to stage n (see Figure 6-2). From the numerical results, graphs of the variation of this Axial Shortening Index (ASI) □ with the stages, are plotted for each structural element.

During the construction of the real building, vibration characteristics such as modal vectors and natural frequencies at any stage of construction can be obtained using

strategically located accelerometers. The parameter, β_x^p , can then be calculated. Using the procedure mentioned in section 6.4.2.2, the elastic shortenings of element x can be estimated. From the volume to surface ratio of elements and humidity of the environment, the axial shortening of the structural element x due to shrinkage and creep can be determined using Equation 6-10 so that differential axial shortening between the elements can be calculated.

6.5 Illustrative example

A high rise building with 64 floors (floor height- 4m) as shown in Figures 6-3 and 6-4 is used to demonstrate the feasibility of the methodology described above. This building has two outrigger and belt systems constructed with 60 MPa concrete and spread over two floors; between floors 10 and 12 and between 42 and 44. Dotted lines in Figure 6-3(b) show locations of shear walls of the belt and outrigger systems. The columns and core are constructed with 80 MPa and 60 MPa concretes respectively, while the slabs are constructed with 40 MPa concrete. The reinforcement content of the structural elements is 3% in relation to the cross-sectional area. Tables 6-1 and 6-2 present the structural element sizes.

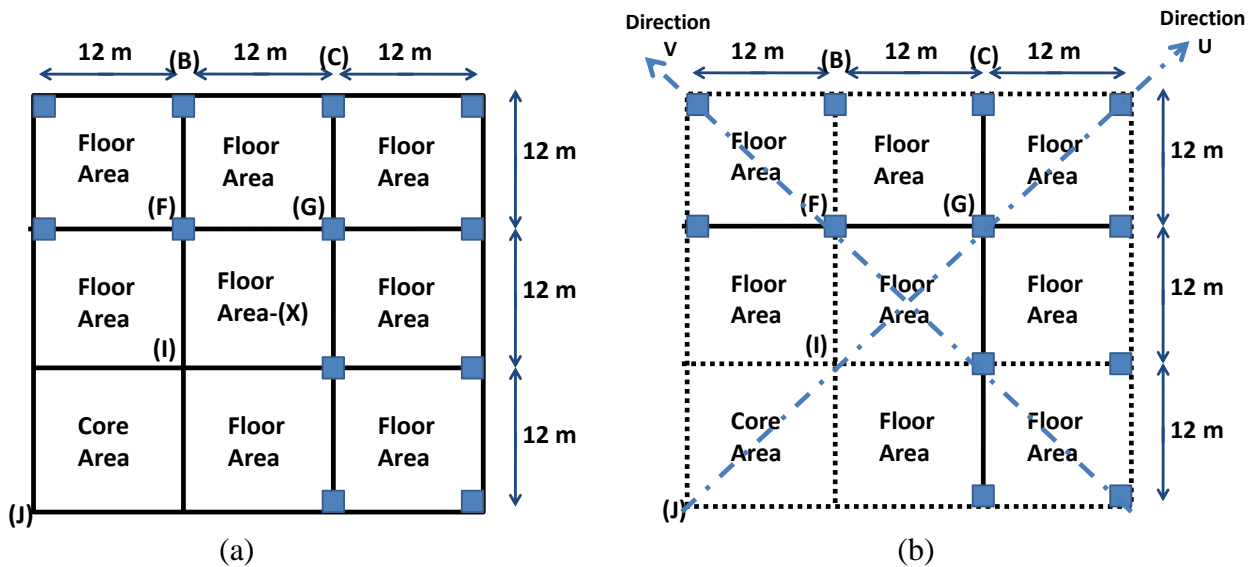


Figure 6-3: (a) typical plan view of the building and (b) locations of the shear walls in the outrigger and belt systems (dotted lines)

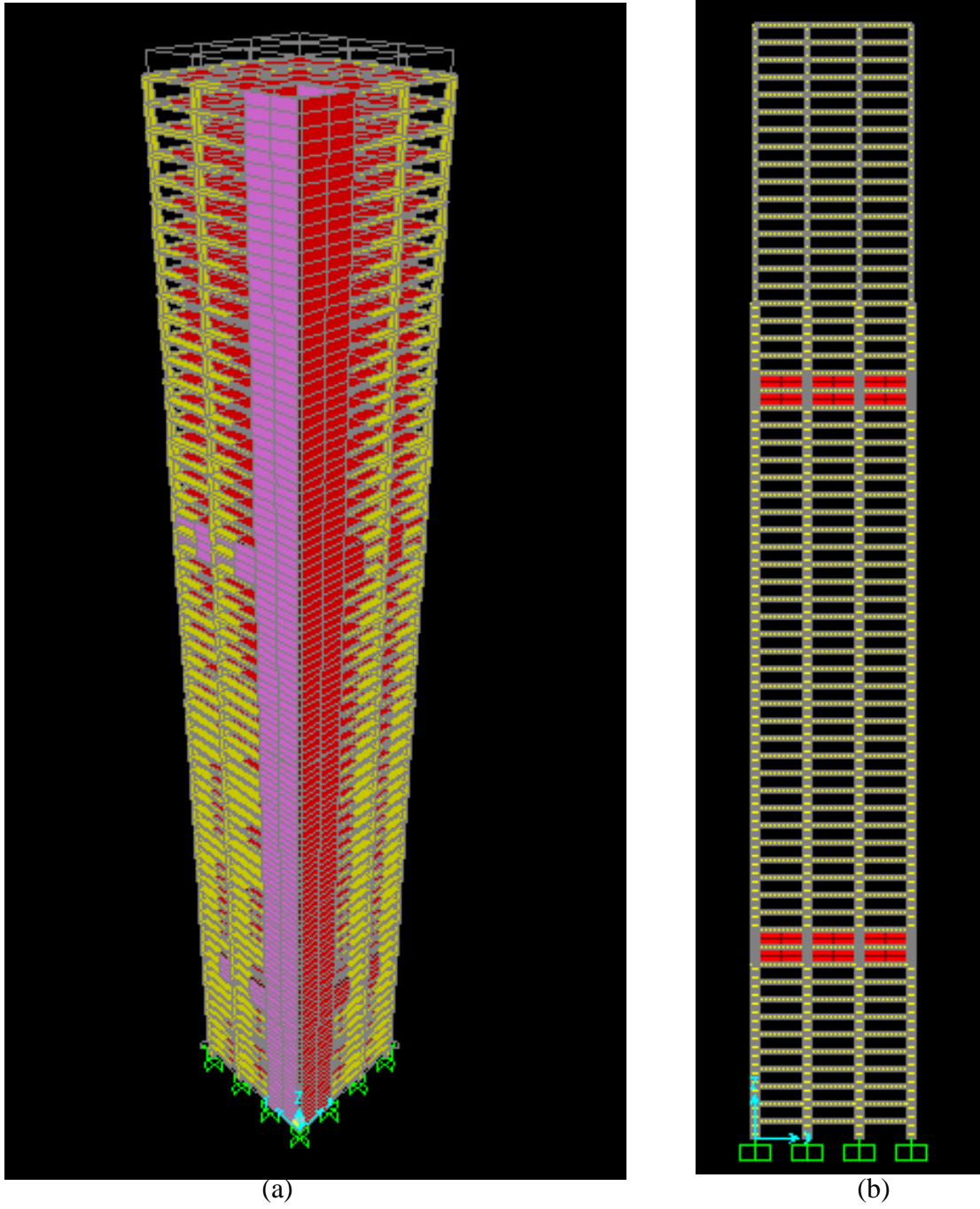


Figure 6-4: (a) isometric and (b) end view of the building

Table 6-1: Column sizes and core wall thicknesses

Location-(Floor Number)	Column size(m)	Core wall thickness(m)
0-16	2.0 x 2.0	1.2
17-32	1.8 x 1.8	1.0
33-48	1.6 x 1.6	0.8
49-64	1.4 x 1.4	0.6

Table 6-2: Thickness of shear walls of the outrigger and belt systems

Location	Shear wall thickness (m)
Lower (floors between 10-12)	1.0
Upper(floors between 42-44)	0.5

The analyses are carried out excluding weight of the form work and workers acting on the structure in the models which simulate the construction stages. A total of 32 different finite element models representing the different construction stages were developed to apply the methodology described above. Among these models, 16 were developed considering four floors at a time. This floor interval was selected because the American National Standard, (1990), ANSI S2 47-1990, recommends that when the height of a building is more than 4 floors (12m), subsequent measurement points should be added at every four floors and at the top of building. Additionally, it is assumed that the core is constructed one floor prior to other structural elements during the development of the models. The other 15 models were generated from the previously developed models to apply the axial loads, representing the mass of materials of the floor above, on the vertical elements such as columns and core at the different construction stages. The final model was developed by applying the live load of 2.5kPa for mechanical floor levels and 1 kPa for the remaining floor levels in order to study the behaviour of the structure during its service stage. These live loads were applied at a time of 700 days after commencement of the construction and it is assumed that these loads remain constant over the rest of time. Assuming 7 days per floor construction (construction sequence), the time dependent Young's Modulus of 40MPa, 60 MPa and 80 MPa concretes were incorporated into the analysis to formulate the actual behaviour of the structure.

Equation 3.1 in Chapter 3 is used to calculate the time dependent Young's Modulus of the reinforced concrete.

Columns B, C, F and G shown in Figure 6-3 were selected to study the influence of member location (and hence tributary area) and shear walls of the outrigger and belt systems on the axial shortenings. Two extreme locations I, J on the core are selected to examine the bending behaviour of the core due to the unsymmetrical nature of the building.

6.6 Results and Discussion

Results from the vibration analysis indicated that the 1st, 2nd, 4th and 5th modes of free vibration are bending and 3rd mode is torsional. The bending modes are about the two diagonal axes U and V indicated in Figure 6-3(b) of the plan view of the building. These five modes and their natural frequencies were examined since it is observed that the high frequencies and the corresponding modes do not impact significantly on the vibration based ASI. Periods of vibration associated with these modes and their variations during the construction stage are illustrated in Figure 6-5 which also indicates the micro and macro upgrading.

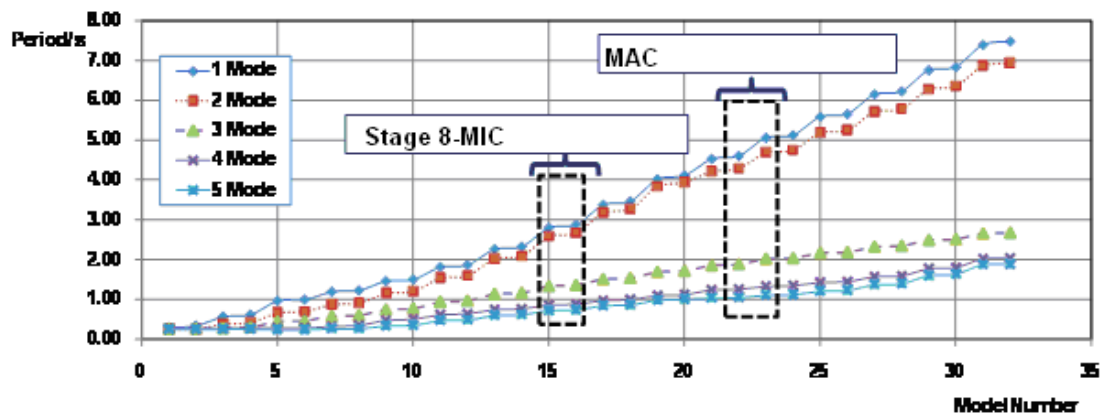


Figure 6-5: variation of the periods with model number from construction to service stage.

During micro upgrading there is an increase in the mass of the structural system due to the added low stiffness material such as wet concrete used to fabricate the floor above.

At the same time the stiffness of structural elements decreases slightly due to the increase in axial forces due from the added mass of the floor above. Despite these occurrences, there is no significant increase in the natural periods of the structure as evident from Figure 6-5, which illustrates that during micro upgrading, such as during stage 8 (corresponding to models 15 and 16), the periods increase only very slightly.

Figure 6-5 also shows one of the Macro Model Upgrading process incorporated into the simulation. When the Finite Element Model is subjected to such an upgrading, overall the periods increase somewhat significantly due to the increase in height of the structure. This increase in periods is more pronounced on first two modes (modes 1 and 2) than the others.

The structural elements at the different floor levels such as 4,12,32,42 and 52 are selected to evaluate the ASI using Equation 6-8 along with the values of Z and β extracted from the static and free vibration analyses of the different structural models. The floor levels 4, 32 and 52 are selected to study the behaviour of this index of the selected structural elements in the lower, middle and upper levels of the building respectively while the floor levels 12 and 42 are selected to study the behaviour of the index of the structural elements at the levels of the outrigger and belt systems. Furthermore, the locations of the core I and J are selected to study the bending behavior of the core which will be pronounced in this building due to its unsymmetrical nature.

During the construction of the building it may not be possible to monitor all five modes of vibration for upgrading. Hence, it is necessary to investigate the impact of number of modes used in evaluating ASI of elements and thus ASI of the selected elements are calculated incorporating one mode and five modes. The results indicate that the impact of number of modes is considerably low. Figure 6-6 illustrates variation of ASI(s) calculated including one mode as well as five modes for column B located at the 4th floor level with the construction stages. It is revealed clearly from this figure that impact of number of modes is very low, although it is preferable (if possible) to incorporate few

modes into the calculations in order to reduce minor variations and to improve the accuracy of results.

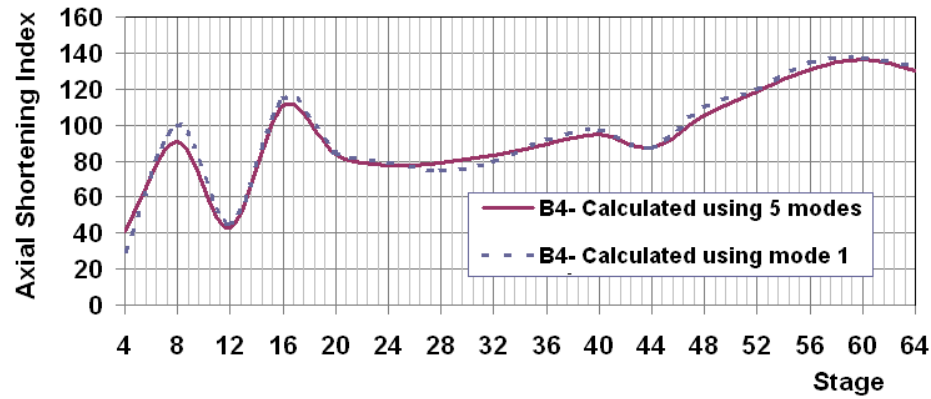
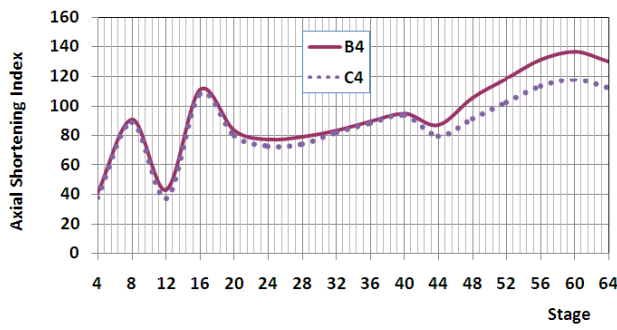
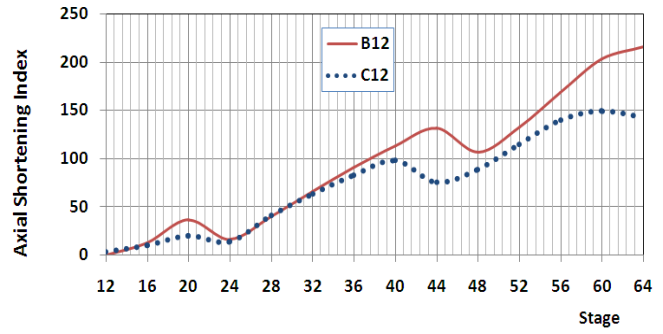


Figure 6-6: Comparison of axial shortening indexes of column B

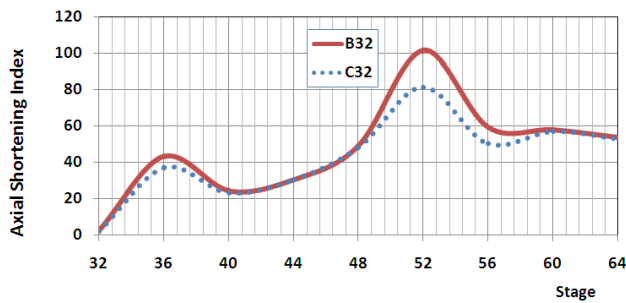
Figures 6-7 to 6-9 illustrate the variation of the axial shortening index of the selected structural elements (B, C, F and G) with the construction stages. In these figures, the vertical axis represents the ASI while the horizontal axis represents number of the stages. Figure 6-7 represents the variation of the ASI of columns B and C at the selected floor levels. As explained in the methodology above (and indicated in Equation 6.8), larger values of ASI indicate smaller values of elastic shortening and vice versa. Column B is connected with outrigger and belt systems whereas column C is only connected to the belt systems (see Figure 6-3(b)). Shear walls of these systems control the axial shortening of those columns and hence even though these two columns have equal tributary areas, elastic shortening of column B is lower than column C. Therefore, As shown in Figures 6-7(a) to 6-7(d), ASI of column B is higher than column C at most of the floor levels. However, the indexes of these elements are almost identical at the 52nd floor level (see Figure 6-7(e)) since impact of outrigger and belt systems on floors above from these systems is very low. This highlights that axial elastic deformation of the structural elements located above outrigger and belt systems are not subjected to the influence of these systems.



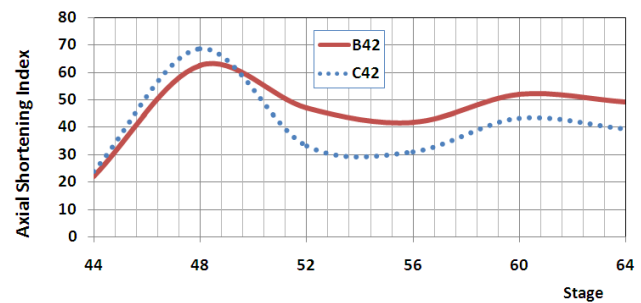
(a)



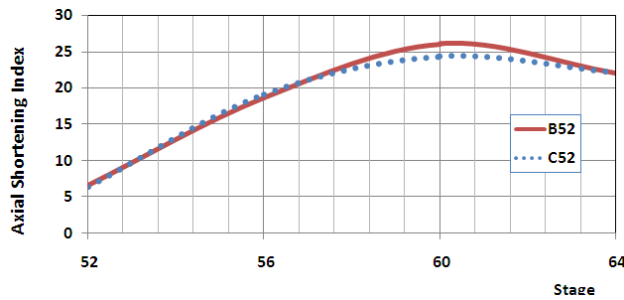
(b)



(c)



(d)

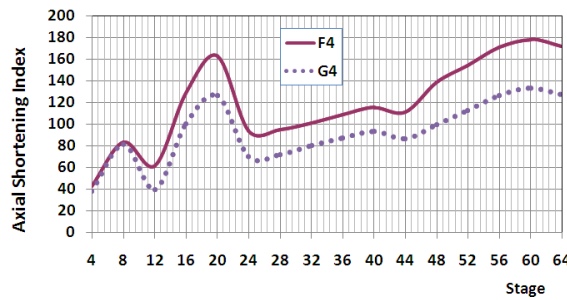


(e)

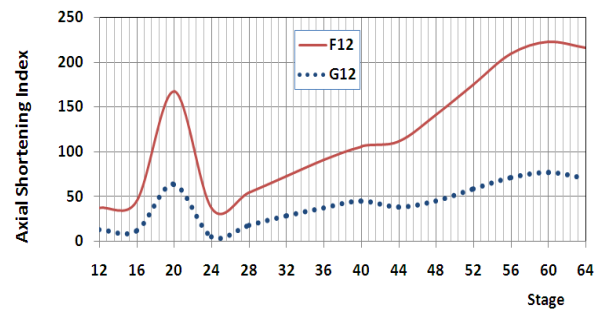
Figure 6-7: Variation of Axial Shortening Index of columns B and C at the different floor levels, (a)-Level 4, (b)-Level 12, (c)-Level 32, (d)-Level 42 and (e)-Level 52

Figure 6-8 shows the variation of ASI of columns G and F at the selected floor levels. These two columns have equal tributary areas, but column F is connected with shear walls of outrigger systems (at levels 10-12 and 42-44) whereas column G is not connected with such stiff structural elements (see Figure 6-3(b)). These shear walls control axial shortening of those members so that elastic shortenings of column G is

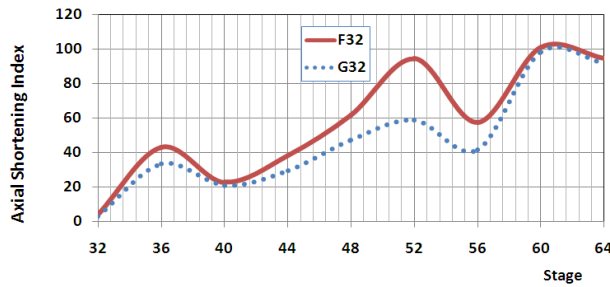
higher than column F at most of the floor levels. ASI of column F is therefore higher than column G at all levels including the 4th and 32nd floor levels (see Figures 6-8(a) and 6-8(c)), where there are no shear wall connections. The impact of these shear walls are more pronounced on these columns located at the 12th and 42nd floor levels since these shear walls are located in these levels. Figures 6-8(b) and 6-8(d) indicate that difference between ASI(s) of columns F and G are higher at levels 12 and 42 compared to those at other levels. Furthermore, ASI(s) of these two columns located at the 52nd floor level are almost identical (see Figure 6-8(e)) since influence of outrigger systems does not impact on the elements located above these systems.



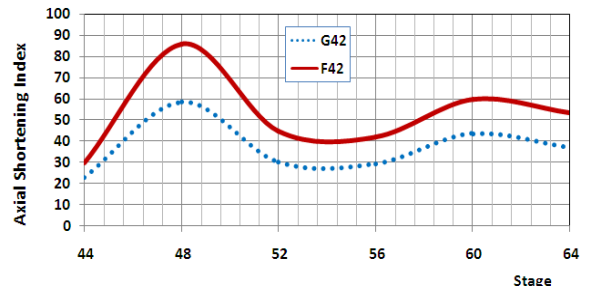
(a)



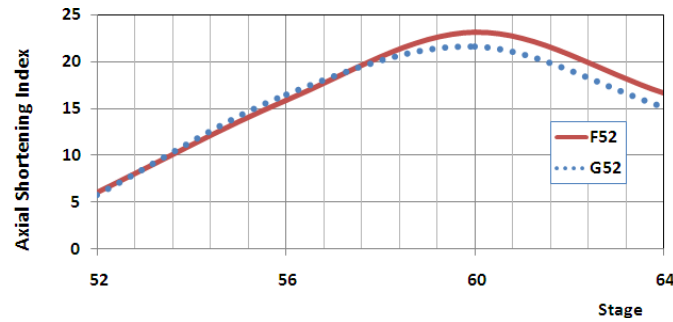
(b)



(c)



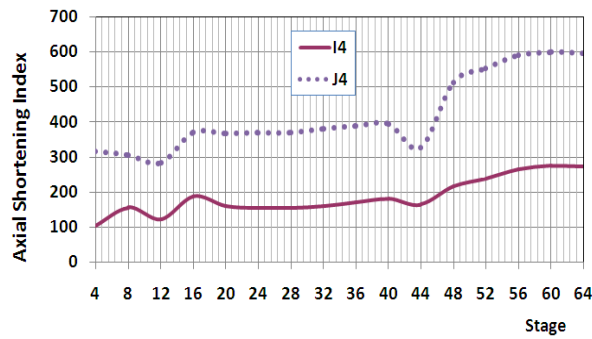
(d)



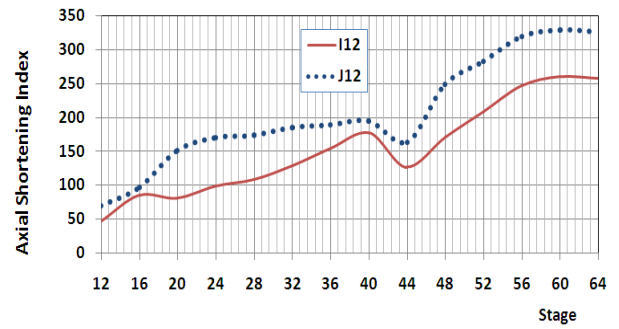
(e)

Figure 6-8: Variations of Axial Shortening Index of columns F and G at the different floor levels-(a)- level 4, (b)-level 12, (c)-level 32, (d)-level 42 and (e)-level 52

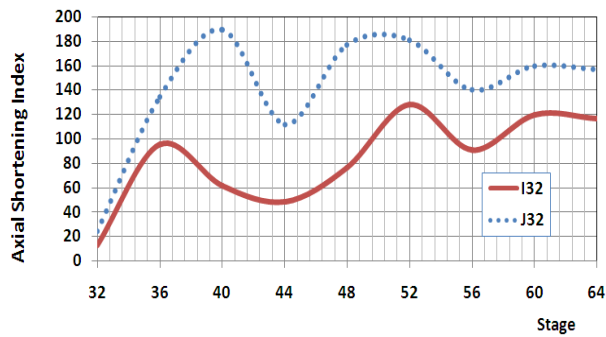
Figure 6-9 shows variation of ASI of locations I and J of the core at the selected floor levels. It can be seen from this figure that the index of location I is always low in comparison to that at location J since elastic shortening of location I is higher than location J due to the influence of different tributary areas. Because of this influence, the core also bends into the building. At stages 12, 42 and 44, Figure 6-9(b) shows reductions in the differences between the indexes as the outrigger and belt systems located at these floor levels control elastic shortenings of the selected locations of the core. However, this occurrence is not evident for I42 and J42 at the 42nd level in Figure 6-9(d) as the shear walls of the outrigger and belt systems have different sizes and Young's Modulus (see Table 6-2) and hence different stiffnesses at these locations. This confirms that the outrigger and belt systems at the lower levels have a larger impact on behaviour of the core at those levels and have less influence at the higher levels.



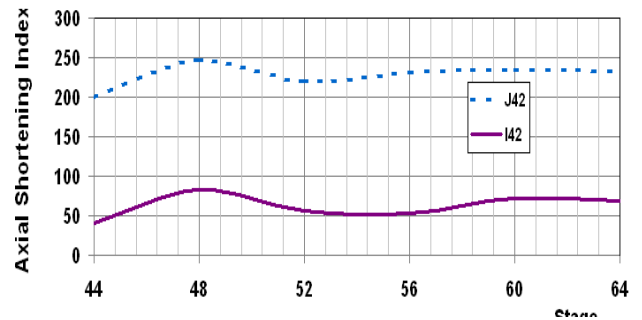
(a)



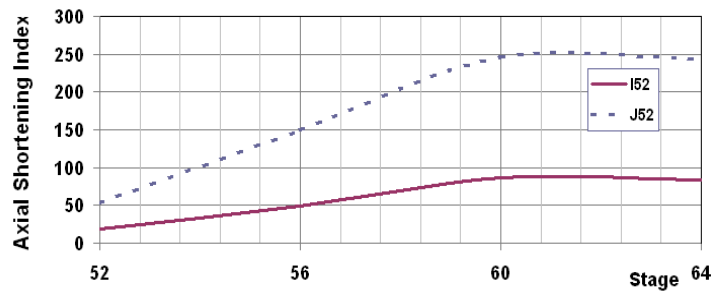
(b)



(c)



(d)



(e)

Figure 6-9: variations of Axial Shortening Index of the locations of the core at different floor levels-(a)- level 4, (b)-level 12, (c)-level 32, (d)-level 42 and (e)-level 52

At the 64th stage Figures 6-7 to 6-9 indicate that the axial shortening index can capture the elastic shortenings due to the axial load applied during the service stage of the building since the indexes of the structural elements tend to decrease gradually when the

service loads are applied. The reason for this is that elastic shortenings of such elements increase due to the applied service loads. This confirms that ASI proposed in this paper has an ability to capture such influences in the service stage as well.

Axial Shortening Index (ASI) of the selected structural elements at the intermediate stages such as the stages during the construction of the floor levels 7, 32 and 54 were calculated using (i) the proposed method and (ii) interpolation in the graphs shown above. Difference between both sets of results was less than 0.01% confirming that the intermediate stages can be calculated by applying the interpolation method.

6.7 Calculation -Elastic and Axial shortening

During and after the construction stages of the real building, vibration characteristics such as modal vectors and natural frequencies can be extracted from the deployed accelerometers and the defined parameter, $\beta_x (= \beta_x^p$ where superscript “p” denotes the physical measurement) can be calculated using Equation 6.6 for each element x. Axial elastic shortening, Z_x^p at the different stages can therefore be determined by substituting β_x^p and the existing ASI (which have been evaluated at design stage, as discussed earlier) into Equation 6.9. Elastic shortening of element x along the height of the building is obtained by substituting the calculated elastic shortening, Z_x^p into Equation 6.11. After acquiring humidity and volume to surface ratios of element x, axial shortening of element x along the height and at a certain time is evaluated through Equation 6.10.

Elastic shortenings of the selected elements are quantified numerically (using nodal displacements from static analysis) to explain the method presented above by substituting $Z_x(t)$ (in lieu of $Z_x^p(t)$) in Equations 6.10 and 6.11. Figure 6-10 reveals results from Equation 6.11 for the selected structural elements and the core at locations I and J. This Figure represents the elastic shortenings along the height of the structure. Moreover, the same elastic shortenings are then substituted into Equation 6-10 to quantify axial shortening of those elements. In the present case, 5340 days (around 15 years) after the commencement of the construction and 50% of humidity of the

environment are taken into account to calculate axial shortenings. Figure 6-11 shows axial shortening of the structural elements.

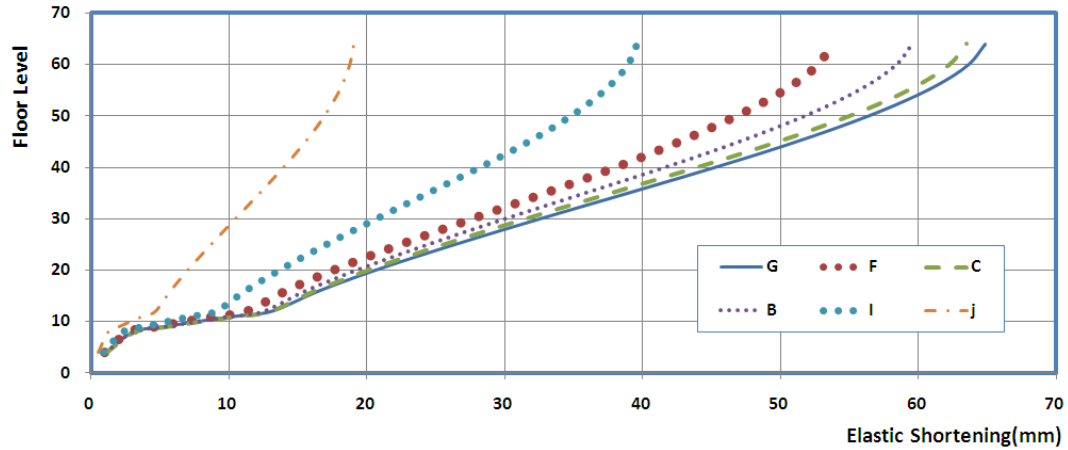


Figure 6-10: Elastic shortening of the structural elements

The core bends into the building due to influence of different tributary areas so that elastic shortening of location J is always less than location I. This is clearly revealed in Figure 6-10. Column F is connected with the shear walls of the outrigger systems so that the shear walls control the shortening of column F. Column G is not connected with such stiff structural elements so that column G shortens more than column F as shown in Figure 6-10. Column B is connected with the outrigger and belt systems whereas column C is connected with the belt systems. Both outrigger and belt systems control the shortening of column B while the belt systems control the shortening of column C. Therefore, the elastic shortening of column C is higher than column B as depicted in Figure 6-10. Behaviours of axial shortening of the structural elements are the same as their elastic shortening (see Figure 6-11). The magnitudes of the axial shortenings are higher than the elastic shortenings because of long term impact of creep, and shrinkage strains.

Axial shortening of location J is not included in Figure 6-11 due to the fact that the horizontal structural elements such as shear walls are not connected at this location. However, location I is connected with column F using shear walls of the outrigger

systems. Consequently, differential axial shortening between columns I and G is very important as it affects the capacity of the shear walls.

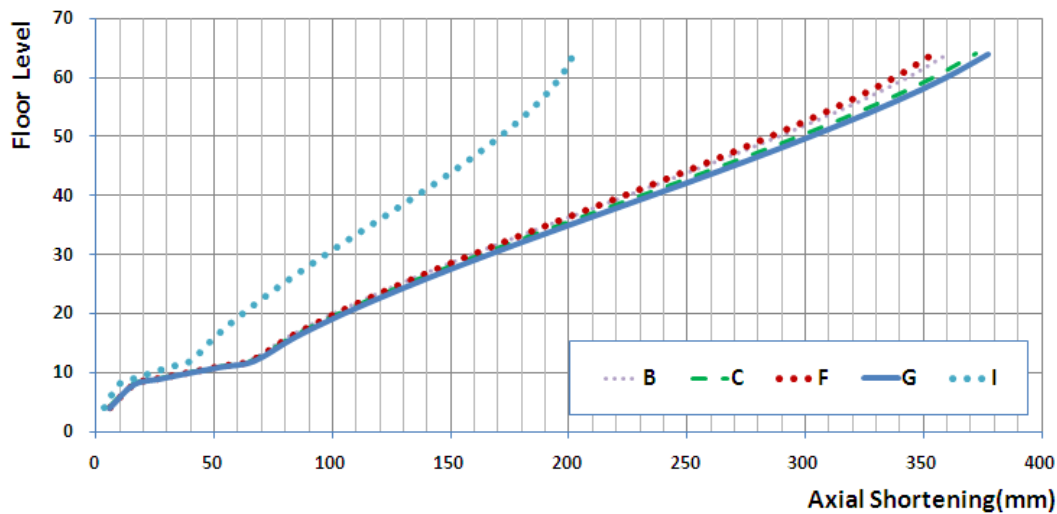


Figure 6-11: Axial shortening of the structural elements

The behaviour of slab X (across the locations I, F and G) shown in Figure 6-3(a) at the 64th floor level after the examined time frame (around 15 years) is revealed in Figure 6-12. This slab is subjected to warping action due to differential axial shortening of the vertical elements and it is possible that this might leads to unexpected deformation and probable damage, highlighting the detrimental effects of differential axial shortening. Additionally, the other services such as pipe lines and conduits associated with this slab may fail confirming that the influence of differential axial shortening is very important to measure during construction and service stages of the building structures to make adequate provision to mitigate the adverse effects.

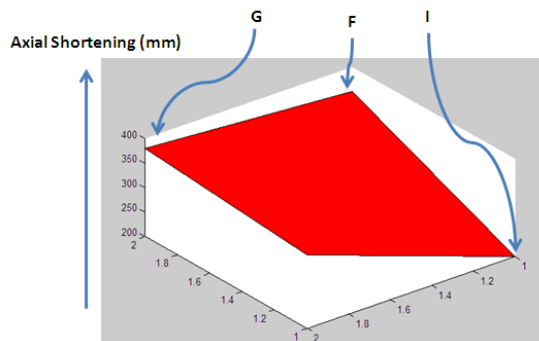


Figure 6-12: the behaviour of slab X

Results show that the (vibration based) ASI developed in this paper has the ability to capture flexibility (stiffness variation) and elastic deformation of vertical structural elements by taking into account influence of outrigger and belt systems, unsymmetrical nature of building and different tributary areas. This is an important feature since the elastic and creep shortenings, which give significant impact on long term shortening, depend on them. Therefore, it can be stated that ASI is a good indicator of progressive deformations occurring during and after construction of building structures.

6.8 Conclusion

Upgrading axial shortening during and after construction of a building provides valuable feedback to verify the actual performance in relation to the theoretical predictions. Using ambient vibration measurement for this purpose will avoid the practical drawbacks in present methods. With this in mind a comprehensive method based on variations in vibration characteristics has been developed to quantify the axial shortening of the structural elements. These vibration characteristics can be accessed through readings from accelerometers and or Pick-ups that are installed on structural elements during the construction process. The proposed method can be used to capture the variation of the flexibilities and axial deformations of the structural elements during and after construction. A numerical example which highlights the procedure and the main parameters involved is presented. Results in this example show that the axial shortening index has the ability to capture influence of shear walls of outrigger and belt systems, different tributary areas, and bending behaviour of the core (due to the asymmetric nature of the building) on axial shortening of vertical load bearing elements. It is hence evident that the proposed method can be used to update progressive structural deformations conveniently and efficiently.

7 CONCLUSION AND FUTURE WORKS

Global architectural trends have resulted in design and construction of geometrically complex high rise buildings using concrete as a primary construction material. Concrete is subject to instantaneous and long term axial shortening caused by “shrinkage”, “creep” and “elastic” deformations. Influences of differential axial shortening among columns and core shear walls in geometrically complex and irregular high rise buildings cause permanent distortion and deflection of the structural frame which impact significantly on building envelopes, building services, secondary systems and the life time serviceability and performance of a building.

The present practise to determine axial shortening in order to mitigate the adverse effects of differential axial shortening is as follows: (i) quantify axial shortening at design stage using numerical methods and (ii) use gauges to measure and verify predicted values at design stage and make adjustments during construction stage. However, existing numerical methods are based on elastic analytical techniques and simple laboratory experiments and they are unable to capture the complexity of true non-linear time dependent effects. Moreover, these techniques are not applicable to high rise buildings with outrigger and belt systems, Furthermore, it is impossible to conduct laboratory experiments to study the long term axial shortening of vertical members in a building incorporating time dependent load migration occurring among the structural components during and after the construction. This is due to the fact that axial shortening varies significantly over more than 15 years and the experiments cannot simulate the exact behavior of high rise buildings especially those with belt and outrigger systems and geometrically complex structural framing systems. Embedding the gauges permanently in or on the surface of concrete components to acquire continuous axial shortening measurements during and after construction with adequate protection is uneconomical, inconvenient and unreliable and hence measuring axial shortening in actual practice of building construction is gradually eliminated. This highlighted the need a comprehensive numerical method to predict axial shortening at

design stage and a procedure to monitor axial shortening during construction and service life.

This thesis addresses these needs and presents an innovative rigorous numerical procedure to quantify axial shortening at design stage and a vibration based procedure to monitor and update axial shortening during construction and service stages. These two developments are presented based on the well established material models of reinforced concrete (structural steel encased in concrete). However, the fundamental principles and computational techniques developed and incorporated in these two procedures can be applied to any concrete building without any limitation since all parameters are taken into account for these developments.

The numerical procedure developed in this research work incorporates time history analysis together with compression only elements and time varying Young's Modulus of reinforced concrete to formulate the actual construction process with time varying load application capturing the influences of load migration, outrigger and belt systems and variable axial loads. This numerical procedure is general enough to be applicable to all concrete high rise buildings to predict differential axial shortening between vertical elements and enable appropriate action to be undertaken at the planning and design stages to mitigate the adverse effects.

The vibration based procedure developed in this research work is based on concept of a dynamic stiffness matrix of a structural framing system with columns and walls which is developed and presented in this thesis to define the influence of the axial forces on the vibration characteristics. The analytical program using finite element technique is modified to incorporate the effects of axial forces on vibration characteristics. This modified technique can be used to examine the axial effects on the vibration characteristics of complex structural framing systems. Stiffness Index (SI), which uses Modal Flexibility (MF) phenomenon, was developed and used to investigate the individual axial effects of columns and core shear walls in a structural framing system using the vibration characteristics. SI has found to have the ability to capture the

individual axial effects successfully incorporating the influences of variable axial loads, the boundary conditions and load migration. The parameter, SI was then enhanced to develop a novel vibration based parameter called Axial Shortening Index (ASI) and a vibration based procedure to monitor axial shortening during construction and service life of a building that verify the actual performance in relation to the predictions. The vibration characteristics can be measured conveniently using accelerometers and or Pick-ups that are installed on structural components immediately after they are built. These two gauges require installing when the readings are necessary and hence the vibration based procedure will avoid the practical drawbacks. The procedure illustrates using a numerical example of a geometrically complex high rise building. Results showed that Axial Shortening Index (ASI) has the ability to capture influence of outrigger and belt systems, variable axial forces, and flexural behaviour on axial shortening of vertical load bearing members. It is hence evident that the proposed method with ASI can be used to measure axial shortening more accurately.

Outcomes of this thesis are highlighted that outrigger and belt systems impacts significantly on axial shortening of vertical structural components. These systems can be located strategically in order to reduce the differential axial shortening. Secondly, the rigorous numerical method developed and presented in thesis can also be improved in order to quantify axial shortening of concrete encased steel and steel encased concrete structural components in high rise construction which are becoming increasingly popular among present high-rise building constructions. Consequently, it is proposed as a future work of this thesis (i) refine the rigorous numerical method and the vibration based method developed and presented in this thesis using the ambient measurements and (ii) improve these methods in order to quantify the axial shortenings using ambient vibration measurements during construction and service stages of high rise buildings comprising concrete encased steel and steel encased concrete structural components and belt and outrigger systems.

8 REFERENCE

Abrate, S. 1993, *On the use of Levy's method for symmetrically laminated composite plates*, Journal of Composites, volume 24 (8), pp. 659-661

ACI Committee 209 ,1993, *Prediction of Creep, Shrinkage, and Temperature Effects in Concrete Structures (ACI 209R-92)*. ACI Manual of Concrete Practice, American Concrete Institute, Detroit, MI, Part 1

Adewuyi,A.P & Wu,Z.S 2010, *Modal macro-strain flexibility methods for damage localization in flexural structures using long-gage FBG sensors*, Journal of Structural Control and Health Monitoring, www.interscience.wiley.com. DOI: 10.1002/stc.377

Alexandar, S. 2001, *Axial shortening of concrete column in high rise buildings*, Magazine of Concrete Advice, No 33,pp. 36-38

American national standard, ANSI S2 47-1990, *Vibration of buildings- guidelines for the measurement of vibrations and evaluation of their effects on buildings*. Accredited Standards Committee S2, Mechanical Shock and Vibration, New York, USA

ANSYS Inc. (2007). ANSYS Workbench v.11.0 [Software] Canonsburg, PA: Ansys Inc. AS3600 , 2001, *Australian Standard for Concrete structures*, Committee BD-002, Concrete Structures.

Atkan. E ,Catbas, N., Grimmelsman & Pervizpour, K.2003. *Development of a Model Health Monitoring Guide for Major Bridges*, Drexel Intelligent Infrastructure and Transportation Safety Institute, <http://www.di3.drexel.edu> (visited on: 30-03-2008)

Bahra, A.S. and Greening, P.D. 2008, *Identifying axial load patterns using space frame FEMs and measured vibration data*, Journal of Mechanical Systems and Signal Processing, No 23 ,pp. 1282-1297

Baker,W.F., Korista, D.S. & Novak, L.C. 2007, *Burj Dubai: engineering the world's tallest building*, Structural Design of Tall and Special buildings, vol: 16, pp.361-375

Bakoss ,S.L,Burfitt, A.J & Cridland, I 1977, *Measurement of strain in concrete members with vibrating wire strain gauges*, Australian road research, vol 7 no 3, pp. 20-26

Banerjee,J.R 2000, *Explicit modal analysis of an axially loaded Timoshenko beam with bending-torsion coupling*, Journal of Applied Science, vol 67/307,pp. 307-313

Banerjee,J.R and Williams,F.W, 1994, *Coupled bending-torsional dynamic stiffness matrix of an axially loaded Timoshenko beam element*, International Journal of Solid and Structures, vol 31,No 6, pp. 749-762

Beresford F.D 1970, *Measurement of time dependent bahavior in concrete buildings*, forth Australian building research congress, Sydney, pp 23-26

Bokaian, A. 1988, *Natural frequencies of beams under compressive axial loads*, Journal of Sound and Vibration, vol: 126(1),pp. 49-65

Bokaian,A. 1990, *Natural frequencies of beams under tensile axial loads*, Journal of Sound and Vibration, vol:142 (5) ,pp. 481-498

Bontempi, F, 2003, *System-Based Vision for Strategic and Creative Design: Proceedings of the Second International Conference on Structural and Construction Engineering, Rome, Italy*, pp 107-115

Boonlualoah,S., Fragomeni,S. & Loo,Y.C 2005, *Aspects of axial shortening of high strength concrete vertical elements in a tall concrete building*, Developments in Mechanics of Structures and Materials-Deeks and Heo(eds),Taylor and Francis Group, London, pp. 737-742

Brownjohn, J.M.W, Pan, T.C, & Deng, X.Y. 2000. *Macro-updating of finite element modeling for core systems of tall buildings*, Proceedings of the 14th Engineering Mechanics Conference. Austin, TX: ASCE

Brownjohn, J.M.W. , Pan T.C., and Deng,X.Y 2009, *Macro-updating of finite element modeling for core systems of tall buildings*, www.ce.utexas.edu/em2000/papers/XYDeng.pdf, (viewed on 17 April 2009)

Bruj Tower official web site, 2008, <http://www.burj Khalifa.ae/> (visited on 10.15.2008)
Buyukozturk,O & Gunes,O 2008, *High-rise buildings: evolution and innovations*, web.mit.ed u/istgroup/ist/documents/CIB_Toronto_05-04.pdf, (viewed on 06 January 2008)

Carreira, D.J. & Poulos, T.D 2007,*Designing for effects of creep and shrinkage in high-rise concrete buildings*, ACI journal, SP-246-7, pp. 107-131

Catbas, F.N., Brown , D.L, & Aktan, E. 2006, *Use of modal flexibility for damage detection and condition assessment: case studies and demonstrations on large structures*, Journal of structural engineering, ASCE, Vol 132,No 11, pp. 1699-1711

CEB-FIP,1990, *Model Code for Concrete Structures*, first draft, Bulletin d' information No.195.Comité-Euro-International Du Béton-Fédération Internationale De La Précontrainte, Paris

Chang, T.P., Hu,C.Y. and Jane,K.C, 1998, *Vibration analysis of delaminated composite plates under axial load*, Journal of Mechanics Based Design of Structures and Machines, vol: 26(2),pp. 195-218

Chen, W.C and Liu, W.H 1990, *Deflections and free vibrations of laminated plates-Levy type solutions*, International Journal of Mechanical Science, vol 32, no 9,pp. 779-791

CNN tower official web site, 2010,<http://www.cntower.ca> (visited on 01.01.2010)

Cridland,L, Heiman,J.L, & Burfitt,A.J 1973, *Measurement of strain in a high rise reinforced concrete building*, Proceeding of Applied Mechanics Conference on Stress and Strain in Engineering, Institute of Engineers Australia, Pub. No. 73/5, Brsbane, pp.183-189

Cridland,L, Heiman,J.L, Bakoss,S.L & Burfitt,A.J 2007, *Measured and predicted axial strains and deformations in a column of a tall reinforced concrete building*, civil engineering monograph, No. C.E 79/1 ST.E, school of civil engineering, the New South Wales institute of technology, NSW, Australia

Della,C.N. & Shu, D. 2009. *Free vibration analysis of multiple delaminated beams under axial compressive loads*, journal of reinforced plastics and composites, Vol: 28 ,pp. 1365-1380

Donald,W.P,Donald,D.M, Henry,G.R & Corely,W.G,1980,*Time dependent deformations in a 70 story structure*, ACI journal (special publication), Vol: 27 , pp. 159-185

Dubai Future Projects, 2009 ,http://www.realtyna.com/dubai_real_estate/dubai-future-projects.html (visited on 01.01.2009)

Ellis, B.R., & Ji, T. 1996. *Dynamic testing and numerical modeling of the Cardington steel framed building from construction to completion*. The Structural Engineer, 74(11/4), pp. 86-192

Elnimeiri,M.M & Joglekar,M.R.1989,*Influence of column shortening in reinforced concrete and composite high rise structures*, ACI, special publication, SP 117-4, PP. 55-86

Fintal,M,Ghosh,S.K & Iyengar,H. 1987 ,*Column shortening in tall structures : prediction and compensation*,2nd edn, Skokie, Ill. : Portland Cement Association

Fintal,M. & Fazlur, R.K. 1987, *Effects of column creep and shrinkage in tall structures-analysis for differential shortening of columns and field observation of structures*, ACI journal, vol-1 (1971), pp. 95-12

Fintel,M., Ghosh, S.K & Iyengar, H.,1987, *Column shortening in tall structures-Prediction and Compensation*, Portland Cement Association in Skokie, pp 1-33

Friberg,P.O.1985, *Beam element matrices derived from vlasov's theory of open thin walled elastic beams*, International Journal for Numerical Methods in Engineering, vol 21,pp. 1205-1228

Gardner,N.J 2004, *Comparison of prediction provisions for drying shrinkage and creep of normal strength concretes*, Canadian Journal of Civil Engineering, Vol: 39,No 5,pp. 767-775

Ghosh, S. K. 1997, *Differential shortening in tall concrete buildings*, Proceedings of Structures Congress XV, Vol. 1, Portland, Oregon

Gibbons,C, Lee,A.C.C & MacArther,J.H 1998, *Design of the north east tower Hong Kong station*, Proceeding of the 5th international conference on tall buildings, Hong Kong, pp. 126-132

Gibbons,C, Lee,A.C.C, MacArther,J.H & Wan, C.H 2002, *The design and constructions of two international finance centre Hong Kong station*, Journal of advances in building technology, vol:1,pp. 703-712

Goel, R., Kumar, R. & Paul, D.K. 2007, *Comparative study of various creep and shrinkage prediction models for concrete*, Journal of Materials in Civil Engineering, ASCE, pp. 249-60

Hejll,A, 2007, *Civil Structural Health Monitoring -Strategies, Methods and Applications*, PhD thesis, Luleå University of Technology, Sweden

Ilankoi, S. and Dickinson, S.M, 1987, *The vibration and post buckling of geometrically imperfect simply supported rectangular plates under uni- axial loading part 11, experimental investigation*, Journal of Sound and Vibration, vol: 188(2),pp.337-351

Ivanovic, S.S, Trifunac, M.D, Novikova, E.I, Gadjakov, A.A. and Todorovsk, M.I 2000, *Ambient vibration tests of a seven story concrete building in Van Nuys, California, damaged by the 1994 Northridge earthquake*, Journal of Soil dynamics and Earthquake Engineering, pp. 391-411

Kanwar, V.S, Kwatra, N, Aggarwal, P. and Gambir 2008, *Health monitoring of RCC building model experimentally and its analytical validation*, International Journal of Computer Aided Engineering and Software, Vol 25, No 7,pp. 677-693

Kanwar, V.S, Kwatra, N, Aggarwal, P. and Sing, R,P 2010, *Use of vibration measurements in health monitoring of reinforced concrete buildings*, International Journal of Structural Integrity, Vol 1, No 3,pp. 209-232

Kapania, R.K. and Yang, T.Y.1986, *Buckling, post buckling and non linear vibrations of imperfect laminated plates*, Proceedings of the ASME Pressure Vessels and Piping Conference, Chicago,pp. 100-109

Kim, H and Cho, S, 2005, *Column shortening of concrete cores and composite columns in a tall building*, The Structural Design of Tall Buildings, vol:14, pp. 175-190

Li, Q.S., Wu, J.R., Liang, S.G. Xiao, Y.Q. and Wong, C.K 2004 b, *Full scale measurements and numerical evaluation of wind-induced vibration of a 63 story reinforced concrete tall building*, Journal of Engineering Structures, vol:26, pp. 1779-1794

Li, Q.S., Xiao, Y.Q. Wong, C.K and Jeary, 2004 a, *Field measurements of typhoon effects on a super tall building*, Journal of Engineering Structures, vol:26, pp. 233-244

Liu, Y. | 2007, *Strength, modulus of elasticity, shrinkage and creep of concrete*, PhD thesis, University of Florida, USA

Luong A. , Gibbons, C., Lee, A & MacArthur, J., 2004, *Two international financial center*, Proceedings of CTBUH 2004 conference, pp- 1160-1167

Subrahmanyam, M.B 1985 , *Basic functions for the buckling of plates*, Journal of Acta Mechanica, vol: 55, pp. 105-109

Neville, A.M 2005, *Properties of concrete*, 4th edn, Pearson Education Limited, England

Olmer, J. 1980, *Method of vibration measurement of tall structures*, Journal of Wind Engineering and Industrial Aerodynamics, vol:6, pp. 39-48

Pfeifer, D.W. , Magura, D. , Russell, H.G. & Corley, W.G. 1970, *Time dependent deformations in a 70 story structures*, ACI special publication, SP27-7, pp. 159-185

RILEM TC-107-GCS, 1995, *Errata: Creep and shrinkage prediction models for analysis and design of concrete structures—Mode B3*. Material Structures, vol:29, pp. 126

Russell, H.G & Corley, W.G 1978, *Time dependent behaviour of columns in Water Tower Place*, ACI journal (special publication), Vol:55, pp. 347-373

Russell, H.G. & Corley, W.D 1997, *Time dependent behavior of columns in Water Tower Place*, ACI special publication, SP 55-14, pp. 347-373

SAP2000 Inc, 2004. *SAP2000 ver .10 Integrated Finite Element Analysis and Design of Structures Analysis Reference [software]*, Computers and Structures, Berkeley, CA, USA

Shahdapuri, C, Mehrkar-Asl, S & Chandunni, R.E, 2010, *DMCC AL Mas Tower-structural design*, visited on line 01-02-2010

Shaker, F.J. 1975, *Effect of axial load on mode shape and frequencies of beams*, NASA (National Aeronautics And Space Administration) technical note, NASA TN-D-8109

Shibukumar,K.S, Leslie,R & Girija,K 2008, *Locating damages in cable stayed bridges using flexibility*, IE(I) Journal-CV,Vol:88, pp. 37-40

Shieh, S. S, Cang, C. C, Jong, J.H, 2010, *Structural design of composite super columns for the Taipei 101 tower*, , www.ncree.org.tw/iwscce/PDF/03%20-%20Shieh.pdf (visited on 01-01-2010)

Shih , H.W., Thambiratnam, D.P. & Chan,T.H.T. 2009, *Vibration based structural damage detection in flexural members using multi-criteria approach*, Journal of Sound and Vibration, vol: 323,pp. 645 – 661

Smith, B.S & Loull,A, 1991, *Tall building structures analysis and design*, John Wiley and son, inc, pp. 461-479

Sohn,H, Charles R. F, Francois, M. H, Devin D. S, Daniel W. S & Brett R. N, 2003, *A Review of Structural Health Monitoring Literature: 1996-2001*, Los Alamos National Laboratory Report, LA-13976-MS

Swaddiwudhipong, S, Lee,S.L and Zhou,Q. 2001, *The effects of axial deformation on vibration characteristics of tall buildings*, The Structural Design of Tall Buildings, vol: 10,pp. 79-91

Swaddiwudhipong, S., Sidji, S.S. and Lee, S. L 2002 , *The effects of axial deformation and axial force on vibration characteristics of tall buildings*, The Structural Design of Tall Buildings, vol: 11, pp. 309-328

Taipei 101,http://au.youtube.com/watch?v=-E_li-xCiLs, (viewed on 31 December 2008)
Tameroglu,S.S 1986, *General solution of the biharmonic Equation and generalized Levy's method for plates*, Journal of Structural Mechanics, vol:14(1),pp. 33-51

Tianyi, Y & Xiangdong,T 2007, *Differential column shortening effects in typical medium- to high-rise buildings*, structural congress, new Horizons and Better Practices, ASCE

Uy, B, 1998, *Concrete-filled fabricated steel box columns for multi storey buildings: behavior and design*, construction research communication limited, pp 150-158

Uy, B. , Das, S.,1997, *Time effects in concrete-filled steel box columns in tall buildings*, The structural design of tall buildings, Vol 6, pp 1-22

Ventsel, E. and Krauthammer T. 2001, *Thin Plates and Shells Theory: Analysis, and Applications*,Eduard and Theodor, CRC Press

Ventura, C.E. , Finn, W.D.L, Lord, J.F. and Fujita, N. 2003, *Dynamic characteristics of a base isolated building from ambient vibration measurements and low level earthquake shaking*, Journal of Soil Dynamics and Earthquake Engineering, Vol:23, pp. 313-323

Walter, D. and Kang, W. 1996. *Exact stiffness matrix for a beam element with axial force and shear deformation*, Journal of Finite Element in Analysis and Design, No 22 ,pp. 1-13

West, H.H and Geschwindner, LF 2002. *Fundamentals of Structural Analysis*, 2nd edition, John Wiley & Sons Ltd

Wu, J.R. and Li, Q.S. 2004, *Finite element model updating for high-rise structures based on ambient vibration measurements*, Journal of Engineering Structures, Vol:26, pp.979-990

Xiang, Y. Zhao, Y.B. and Wei, G.W 2002, *Levy solutions for vibration of multi-span rectangular plates*, International Journal of Mechanical Science, vol: 44,pp. 1195-1218

Xu, Y.L. & Chen,B.2008, *Integrated vibration control and health monitoring of building structures using semi-active friction dampers: part 1-methodology*, Journal of Engineering Structures, Vol: 30(3), pp. 573-587

Yesilce, Y. & Demirdag, O. 2008, *Effect of axial force on free vibration of Timoshenko multi-span beam carrying multiple spring mass systems*, International Journal of Mechanical Science, No 50, pp. 995-1003

Yesilce, Y. and Demirdag, O. 2008, *Effect of axial force on free vibration of Timoshenko multi-span beam carrying multiple spring mass systems*, International Journal of Mechanical Science, No 50, pp. 995-1003

Zhao, J. & Dewolf, J.T. 2006, *Sensitivity study for vibration parameters used in damage detection*, Journal of structural Engineering, Vol 25, No 4,pp. 410-416

Zhou,S.J 2002, *Load-induced stiffness matrix of plates* Canadian Journal Civil Engineering, vol: 29,pp. 181–184

Carroll, C., Gibbons, C., Ho,.G. ,Kwok, M., Lawson, R., Lee, A., Li, R., Luong, A., McGowan, R., Pope, C.,2009, *CCTV Headquarters, Beijing, China* ,www.arup.com/_.../D6E6AB4D-19BB-316E-4017A36ECEDCE0D6.pdf (visited on 10.10.2009)

Korista, D.S., Sarkisian, M.P.,Abdelrazaq, A.K.,1997,*Design and Construction of China's Tallest Building: The Jin Mao Tower*, www.chinamega09.groups.et.byu.net/reports/matthews.docx (visited on 05.01.2011)